5-2017

PROTEOMIC IDENTIFICATION OF HISTONE POST-TRANSLATIONAL MODIFICATIONS INDUCED BY DNA DOUBLE-STRAND BREAKS AND NOVEL PROTEINS INVOLVED IN THE DNA DAMAGE RESPONSE

Pingping Wang

PROTEOMIC IDENTIFICATION OF HISTONE POST-TRANSLATIONAL

MODIFICATIONS INDUCED BY DNA DOUBLE-STRAND BREAKS AND

NOVEL PROTEINS INVOLVED IN THE DNA DAMAGE RESPONSE

by

Pingping Wang, B.S.

APPROVED:

_____

Jessica K. Tyler, Ph.D., Advisory Professor

_____

Bin Wang, Ph.D.

_____

Xiaobing Shi, Ph.D.

_____

Grzegorz Ira, Ph.D.

_____

Nayun Kim, Ph.D.

APPROVED:

_____

Dean, The University of Texas MD Anderson Cancer Center UT Health

Graduate School of Biomedical Sciences

PROTEOMIC IDENTIFICATION OF HISTONE POST-TRANSLATIONAL

MODIFICATIONS INDUCED BY DNA DOUBLE-STRAND BREAKS AND

NOVEL PROTEINS INVOLVED IN THE DNA DAMAGE RESPONSE

A

DISSERTATION

Presented to the Faculty of

The University of Texas

MD Anderson Cancer Center UT Health

Graduate School of Biomedical Sciences

in Partial Fulfillment

of the Requirements

for the Degree of

DOCTOR OF PHILOSOPHY

by

Pingping Wang, B.S.

Houston, Texas

May, 2017

Dedication

This dissertation is dedicated to my parents and sisters for their unconditional love and continuous support, without which I would not have been able to achieve my dream of becoming a Doctor of Philosophy in a foreign country through a long fulfilling journey.

a lot whenever I had tough time. Thanks to Xuan, Ja-Hwan, Ryosuke, Myrriah, Liting and Zih-Jie for spending lots of fun time with me in and out of the lab. In particular, I want to thank my dearest classmates and labmates, Sangita and Richard, for generously sharing all kinds of useful information with me, listening to me and helping me become stronger during the journey. I hope we can maintain a lifetime friendship no matter where we go next. Also, thank Dr. Barry Sleckman and all the Weill Cornell labmates for their kind help and suggestions for my research.

I want to thank Drs. Stephanie Byrum and Alan Tackett from the University of Arkansas for the wonderful collaboration on the mass spectrometric analyses.

Thanks to my graduate school UT-GSBS at Houston for having the most considerate people work for students. Bill, Brenda, Elisabet, Lily, Joy, and Bunny all tried their best to answer my questions and seek solutions for my problems. Thank my graduate program of Genes and Development for supporting me. I want to specially thank Elisabeth for always being so helpful in any situation that I needed her. I appreciate the great resources and many good professional opportunities that UT MD Anderson Cancer Center provided me with.

Lastly, words cannot express my gratitude for my parents who gave me freedom to pursue my dreams wherever I wanted to go and unconditionally supported me as much as they could. I am grateful that my sisters are so encouraging, loving, trusting and supporting me. Also, I want to thank my kind brother-in laws and sweet nieces for giving me positive energies to go through this PhD journey.

PROTEOMIC IDENTIFICATION OF HISTONE POST-TRANSLATIONAL

MODIFICATIONS INDUCED BY DNA DOUBLE-STRAND BREAKS AND

NOVEL PROTEINS INVOLVED IN THE DNA DAMAGE RESPONSE

Pingping Wang, B.S.

Advisory Professor: Jessica K. Tyler, Ph.D.

Inaccurate repair of DNA double-strand breaks (DSBs) can lead to DNA mutation and chromosome rearrangements, causing human diseases such as cancer. Although we know the basic mechanisms of DSB repair, the added complexities in the chromatin context are unclear. This is partially due to the lack of unbiased systems for identifying proteins and post-translational modifications (PTMs) involved in DSB repair. In this work, we established a novel method, termed DSB-ChAP-MS (Double Strand Break-Chromatin Affinity Purification with Mass Spectrometry), for the affinity purification of a sequence-specific single copy endogenous chromosomal locus containing a DSB, followed by the proteomic identification of enriched proteins and histone PTMs. Providing validation of the DSB-ChAP-MS approach, we found many histone PTMs that had been previously implicated in the DNA damage response, as well as multiple new histone PTMs enriched on chromatin bearing a DSB from budding yeast. One of these, methylation of histone H3 on lysine 125, has not previously been reported. Among the novel proteins enriched at a DSB were the phosphatase Sit4, the RNA pol II degradation factor Def1, the mRNA export protein Yra1 and the HECT E3 ligase Tom1. Each of these proteins was required for resistance to

radiomimetics. Yra1 and Def1 were required for DSB repair *per se*, while Sit4 was required for rapid inactivation of the DNA damage checkpoint after DSB repair. Thus, our unbiased proteomics approach has led to the unexpected discovery of novel roles for these and other proteins in the DNA damage response.

Table of Contents

List of Figures

List of Tables

List of Appendices

Appendix 1: List of candidate proteins identified from the four rounds of DSB-ChAP-MS experiments.

Appendix 2: A commercial antibody to human histone H3 lysine 122 acetylation is non-specific *in vivo*.

Chapter 1

Introduction

1.1. General overview of the DNA double-strand break response

Genomic integrity is frequently threatened by DNA damaging factors, from either endogenous or exogenous sources. There are various types of DNA damage, including single-strand breaks (SSBs), double-strand breaks (DSBs), base lesion or loss, inter- or intra-strand crosslinks, and bulky adducts (Helleday et al., 2014). Among them, DSBs are arguably the most deleterious, since they create breaks on both strands of the DNA double helix and can cause chromosome rearrangements when misrepaired, and loss of chromosome arms or cell death if unrepaired (Mehta and Haber, 2014). In order to maintain genomic integrity, it is essential to accurately repair DSBs. The key importance of DSB repair is highlighted by the fact that its deregulation is at the heart of tumorigenesis and many other human disease syndromes (Jackson and Bartek, 2009).

In order to repair DSBs, cells have developed an elaborate DNA damage response. The DNA damage response involves a complex network of cellular pathways that sense, signal and repair DSBs (Ciccia and Elledge, 2010). It is initiated by surveillance proteins, which monitor DNA integrity and activate the DNA damage checkpoint response to avoid unfaithful transmission of genetic information to the progeny cells (Harrison and Haber, 2006; Zhou and Elledge, 2000). The DNA damage response also involves recruitment, to the DNA lesion, of the proteins that mediate the repair of the DNA molecule, followed by the subsequent inactivation of the DNA damage checkpoint. Several other processes including chromatin remodeling and transcription are also involved in the DNA

damage response (**Fig. 1**).

In addition to the dozens of proteins known to be involved in the DNA damage response, many post-translational modifications (PTMs) are induced to facilitate the DNA damage signaling and DSB repair (Oberle and Blattner, 2010; Rossetto et al., 2010; Schwertman et al., 2016).

1.2. The origins of DSBs

Both endogenous and exogenous factors can give rise to DSBs. The endogenous factors leading to the formation of DSBs include stalled DNA replication forks, free radicals and nucleases. DNA-binding proteins (Merrikh et al., 2012), abnormal DNA structure (Branzei and Foiani, 2010), and DNA replication errors, can cause stalled DNA replication forks that may convert into DSBs if they are left unresolved and collapsed (Labib and Hodgson, 2007). Free radicals, such as reactive oxygen species, can be produced during normal cellular metabolism, and they can generate DSBs by attacking the deoxyribose backbone of DNA (Valko et al., 2007). There are many kinds of endogenous nuclease-created DSBs that evoke certain important physiological or developmental activities in various organisms. One example is the RAG protein complex-generated DSBs for the initiation of V(D)J recombination that is of fundamental importance to lymphocyte development and maturation in mammals (Soulas-Sprauel et al., 2007). Another example is Spo11 endonuclease-generated DSBs that cause chromosome recombination during meiosis, which is a conserved process among many species (Lam and Keeney, 2014).

DSB formation

ku70 ku80

Dpb11

MRX

RPA

DSB sensors

DSB sensors

Rad24 RFC

9-1-1 clamp

Ddc2 Mec1

Transducer Kinases

Tel1

Rad9

Checkpoint Mediators

Rad53

Effector Kinases

Chk1

Dun1

Effectors

Pds1

DSB repair

Cell Cyle Arrest

Transcription

Chromatin Remodeling

Apoptosis
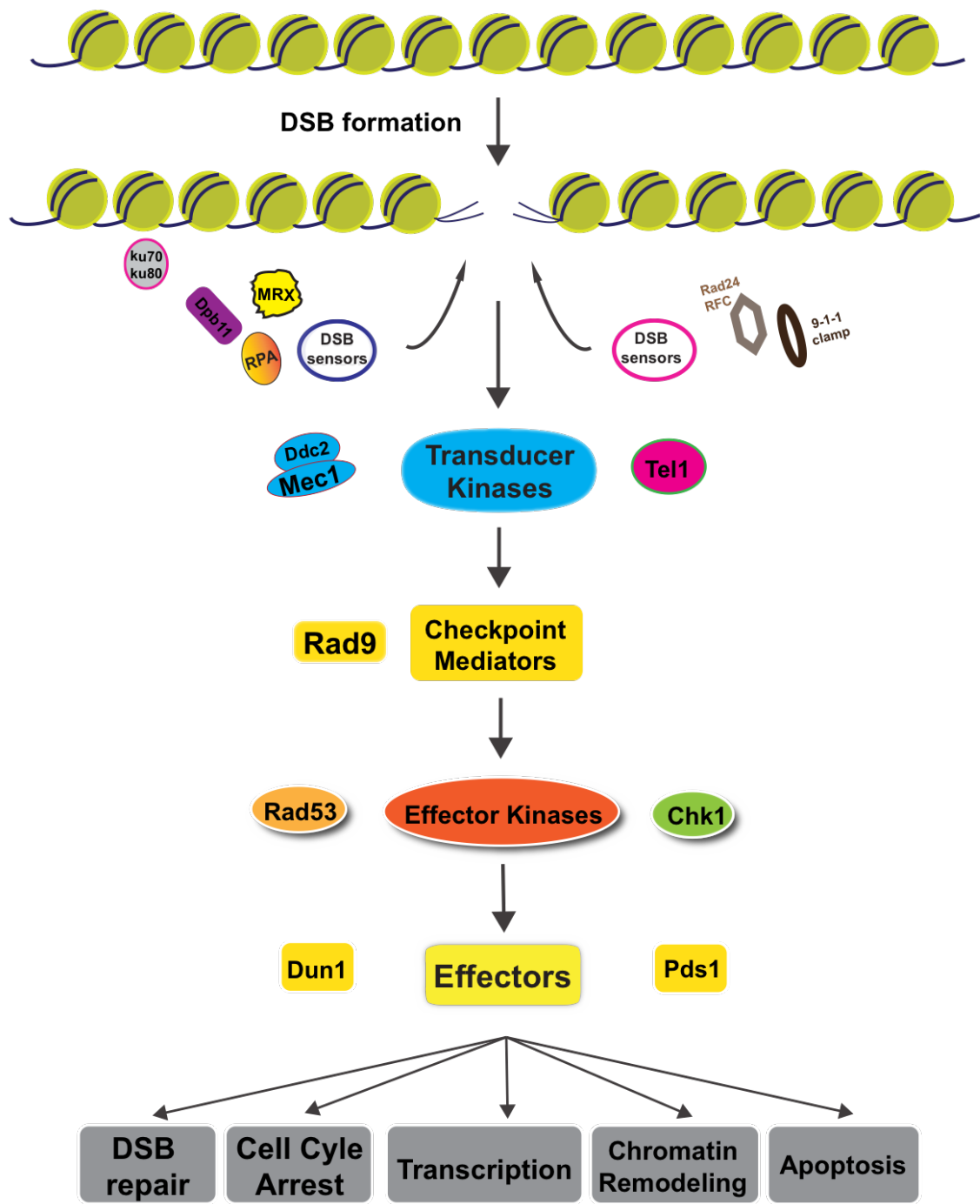
Figure 1. General overview of the DNA double-strand break (DSB) response in budding yeast. Upon induction of a DSB, the DNA repair factors and DNA damage sensors are recruited to the DSB. This is followed by the activation of the transducer kinases Mec1 and Tel1. With the help of checkpoint mediator Rad9, the transducer kinases activate the effector kinases Rad53 and Chk1 by phosphorylating them. The effector kinases in turn phosphorylate the effectors, which brings about cell cycle arrest, chromatin remodeling, transcriptional changes, increased repair efficiency and if the repair does not occur, apoptosis.

Exogenous factors, such as ionization radiation (IR) and chemical reagents can also create DSBs. IR creates SSBs and DSBs by attacking the deoxyribose of the DNA molecule through radicals produced by radiolysis. Two SSBs that are present on the opposite DNA strands but with no more than 10 bp distance from each other form a DSB (Hagen, 1994; Thompson, 2012). Although IR creates multiple other types of DNA damage such as base lesions, the major reason for IR-induced cell death is the formation of DSBs (Schipler and Iliakis, 2013). Among the wide variety of chemicals that can cause DNA damage, the radiomimetics like bleomycin, behave similarly to IR, and can directly create DSBs along with SSBs (Povirk, 1996).

1.3. The detection of DSBs

Shortly after the formation of a DSB in yeast, the broken DNA ends are bound by the Mre11-Rad50-Xrs2 (MRX) complex, which has a mammalian

counterpart of MRE11-RAD50-NBS1 (MRN) (**Fig. 1 and 2**). At the same time, the Ku complex (yKu70 and yKu80), another early DSB sensor, recognizes the DSB and competes with MRX for binding to the newly-generated DSB end (Clerici et al., 2008; Shim et al., 2010). There are two major DSB repair pathways, homologous recombination (HR) and non-homologous end joining (NHEJ) (details in Section 1.5). During DSB repair by NHEJ, the Ku complex binds to the DSB ends and holds the broken DNA ends together to ensure they can be properly rejoined through NHEJ (Walker et al., 2001; Wu et al., 2008). During NHEJ, MRX interacts with the DNA ligase IV (Dnl4) and its associated protein Lif1, thereby facilitating the Dnl4-mediated DSB end-rejoining (Chen et al., 2001). In the case of DSB repair by HR, the binding of MRX to the unprocessed DSB ends promotes initial DSB end resection (details in Section 1.5.1), which prevents the Ku complex from binding to the DSB ends and is an important step for HR repair (Nicolette et al., 2010).

1.4. DSB-induced checkpoint activation

Essentially, DSB-induced checkpoint activation is mediated by a series of protein phosphorylation events that occur after the detection of DSBs (**Fig. 1**). The two principle upstream checkpoint kinases Mec1 (ATR in mammals) and Tel1 (ATM in mammals) both contribute to the activation of DSB-induced checkpoint response (Gobbini et al., 2013; Harrison and Haber, 2006), which lead to cell cycle arrest through phosphorylation-dependent activation of the checkpoint effector kinases Rad53 (Chk2 in mammals) and Chk1 (Chk1 in mammals) (Gardner et al., 1999; Sanchez et al., 1999; Sanchez et al., 1996). In

6

mammals, in addition to ATR and ATM, another phosphoinositide 3-kinase-like (PI3K-like) kinase DNA-PK also contributes to checkpoint activation (Hill and Lee, 2010).

After DSB detection by MRX, Tel1 is recruited to the DSB site by interacting with Xrs2, the regulatory subunit of the MRX complex. This leads to checkpoint activation via Tel1, which is responsible for multiple phosphorylation events during the DSB response (Nakada et al., 2003). DSB end resection as an early step in HR creates 3' single-stranded DNA (ssDNA) overhangs that become bound by the single-stranded binding protein RPA (Alani et al., 1992) (**Fig. 2**). The extension of RPA-coated ssDNA recruits Ddc2 (ATRIP in mammals), which is in a complex with Mec1 and undergoes Mec1-dependent phosphorylation (Ball et al., 2005; Paciotti et al., 2000; Zou and Elledge, 2003). DSB end resection gives rise to a double-stranded (ds)-ssDNA junction that is recognized by the Rad24-RFC (RAD17-RFC in mammals) complex. The Rad24-RFC complex further helps load the 9-1-1 complex (or called 9-1-1 checkpoint clamp) consisting of Ddc1, Rad17 and Mec3 (RAD9, RAD1, and HUS1 in mammals) onto the ds-ssDNA junction (Kondo et al., 2001; Melo et al., 2001). The 9-1-1 complex, as an early DNA damage sensor, plays an important role in Mec1 activation during the checkpoint response. The Ddc1 subunit of the 9-1-1 complex directly activates Mec1, when the 9-1-1 complex and the Mec1-Ddc2 complex colocalize at a site of DNA damage (Bonilla et al., 2008; Majka et al., 2006; Navadgi-Patil and Burgers, 2009b). Also, Mec1-dependent phosphorylation of Ddc1 promotes the recruitment of Dpb11 (TopBP1 in

mammals), which is another activator for the Mec1 kinase (Navadgi-Patil and Burgers, 2009a).
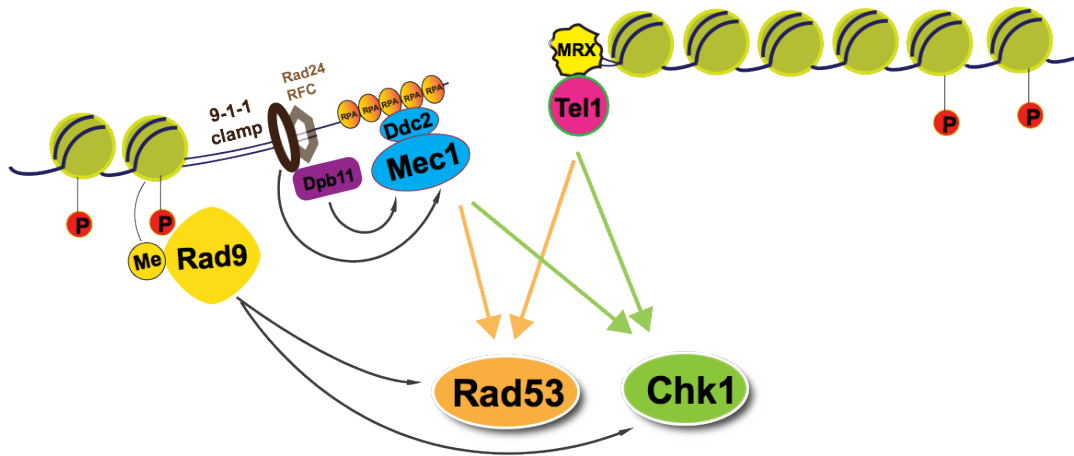
Figure 2. Mechanisms of DSB-induced checkpoint activation. Upon DNA resection, RPA coats the single-stranded (ss) DNA, and recruits Ddc2/Mec1. The 9-1-1 checkpoint clamp is loaded onto the double-stranded (ds)-ssDNA junction, with the help of the 9-1-1 clamp loader. The 9-1-1 clamp promotes Dpb11 recruitment to the broken DNA site. Both the 9-1-1 clamp and Dbp11 promotes Mec1 activation, which results in phosphorylation of Rad53 predominantly, aided by Rad9 and activation of Chk1. Unprocessed DSBs are recognized by the MRX complex, which recruits the kinase Tel1 resulting in activation of Chk1 and Rad53.

During the DSB response, chromatin undergoes various forms of modifications (details in Section 1.7) to facilitate the DNA damage-induced checkpoint activation and help DSB repair factors get access to the broken DNA ends (Su, 2006). An essential histone PTM during DSB signaling is phosphorylation of histone H2A on serine (S) 129 (γH2A) in yeast or phosphorylation of histone variant H2AX on serine (S) 139 (γH2AX) in mammals. In yeast, both Mec1 and Tel1 kinases mediate the formation of γH2A, which provides a platform for DSB signal amplification by recruiting other DSB response factors to the broken DNA site.

Among the various checkpoint proteins (**Table 1**) in yeast, Rad9 and Rad53 are central to DSB checkpoint regulation. Both Tel1 and Mec1 dependent checkpoint activation converges on Rad9 and Rad53, leading to phosphorylation of many downstream effector proteins including those that regulate cell cycle progression or transcription (Finn et al., 2012). Rad9 is a checkpoint adaptor protein, which is recruited to chromatin in the vicinity of a DSB through binding to γH2A and lysine (K) 79 methylated histone H3 (Grenon et al., 2007). Phosphorylation of Rad9 by Mec1/Tel1 after DSB detection facilitates the recruitment of Rad53 at sites of DNA damage and thus promotes Mec1/Tel1-dependent Rad53 phosphorylation (Schwartz et al., 2002; Sun et al., 1998; Toh and Lowndes, 2003). Also, phosphorylated Rad9 creates a scaffold for efficient Rad53 autophosphorylation (Gilbert et al., 2001). In addition, Rad9 after being phosphorylated, undergoes oligomerization, which is important for maintaining Rad53 activation and the checkpoint response (Usui et al., 2009). There is no

single mammalian homolog of Rad9, but 53BP1, BRCA1, and MDC1 are implicated as mammalian checkpoint adaptor proteins that are functionally equivalent to yeast Rad9 (Stewart et al., 2003; Venkitaraman, 2001; Wang et al., 2002).

Rad53 is an essential checkpoint effector kinase that becomes phosphorylated and activated in response to DNA damage. Rad53 is composed of a kinase domain and two Forkhead associated (FHA) domains located on each side of the kinase domain (Pike et al., 2003). Its FHA domains mediate the interaction of Rad53 with phosphorylated proteins (Durocher and Jackson, 2002), including Rad9 and Mec1/Tel1 (Sanchez et al., 1996). Mec1/Tel1-mediated phosphorylation of Rad53 plays a central role in the DSB-induced checkpoint response throughout the cell cycle (Pellicioli et al., 1999; Sanchez et al., 1996). As a serine (S) / threonine (T)-protein kinase, Rad53 targets multiple substrates during the checkpoint response. For example, Rad53 phosphorylates the protein kinase Dun1 (Chen et al., 2007), which is involved in DNA damage-induced transcriptional induction (Allen et al., 1994).

Another checkpoint effector protein in yeast is Chk1, which also plays an important role in the DNA damage checkpoint response. The activation of Chk1 also requires Rad9, but acts through distinct downstream mechanisms than Rad53. Chk1 is not essential for yeast viability, lack of which only confers mild sensitivity to DNA damage (Sanchez et al., 1999). However, Chk1 is important for the DNA damage checkpoint response because of its inhibitory effect on cell cycle entry into anaphase. Chk1 prevents the anaphase entry by stabilizing the

anaphase inhibitor Pds1 via phosphorylation and thereby preventing the degradation of Pds1 by the anaphase promoting complex (APC) (Ciosk et al., 1998; Sanchez et al., 1999).

	S. cerevisiae	Mammalian homolog	Function in S. cerevisiae
DNA damage sensors	Mre11-Rad50-Xrs2 (MRX)	MRE11-RAD50-NBS1 (MRN)	DSB detection, initial DSB end resection
	Ddc1-Rad17-Mec3 (9-1-1)	RAD9-RAD1-HUS1 (9-1-1)	Mec1/ATR activation
	Rad24-Rfc2-5	RAD17-RFC2-5	9-1-1 clamp loader
	RPA (Rfa1-Rfa2-Rfa3)	RPA (RPA1-RPA2-RPA3)	ssDNA binding
	Dpb11	TopBP1	Mec1/ATR activation
	Ku70-Ku80	KU70-KU80	DSB detection during NHEJ
	MRX	MRN	Initial DSB end resection
DSB end resection	Sae2	CtIP	Nuclease, initial DSB end resection
	Exo1	EXO1	Exonuclease, extensive DSB end resection
	Dna2	DNA2	Helicase/nuclease, extensive DSB end resection
	Sgs1	WRN, BLM	DNA helicase, promotes DNA unwinding
	Fun30	SMARCAD1	Chromatin remodeler, regulates DSB end resection
Checkpoint transducers	Tel 1	ATM	Upstream checkpoint kinase, checkpoint activation
	Mec1	ATR	Upstream checkpoint kinase, checkpoint activation
	Ddc2	ATRIP	Mec1/ATR partner/interacting protein
	Rad9	BRCA1, 53BP1 , MDC1	Checkpoint mediator, Rad53 and Chk1 activation
	Rad53	CHK2	Checkpoint effector kinase
	Chk1	CHK1	Checkpoint effector kinase
Checkpoint effectors	Pds1	PTTG	Anaphase entry inhibition
	Dun1	N/A	Protein kinase, DNA damage induced transcription
DSB repair	Rad51	RAD51, RAD51B, C, D	Recombinase in HR repair, strand invasion
	Rad52	RAD52	HR protein, helps Rad51 load onto ssDNA
	Rad54	RAD54	DNA translocase, promotes strand exchange
	Rad59	RAD52B	Rad52 paralog, promotes single strand annealing
	Ku70-Ku80	KU70-KU80	Repair by NHEJ
	Dnl4-Lif1-Nej1	LIG4-XRCC4	DSB end ligation during NHEJ repair
Chromatin remodeling	INO80	INO80	Checkpoint activation, affects both HR and NHEJ repair
	SWR1	SWR1	H2A.Z removal, checkpoint activation and DSB repair
	SWI/SNF	SWI/SNF	Promotes γH2A formation during DSB repair
	RSC	RSC	Multiple steps during HR repair
Checkpoint recovery	Ptc2	PP2C	Phosphatase, Rad53 dephosphorylation
	Ptc3	PP2C	Phosphatase, Rad53 dephosphorylation
	Pph3	PP4	Phosphatase, Rad53 and γH2A dephosphorylation
	Glc7	PP1	Phosphatase, Rad53 and γH2A dephosphorylation
	Asf1	ASF1a/b	Histone chaperone, dynamic interaction with H3 and Rad53
	Srs2	RTEL1	Helicase, Rad51 removal from ssDNA filament
	Sae2	CtIP	Nuclease, negative regulation of MRX

Table 1. A list of representative proteins involved in the DSB response. Detailed function of each individual protein as stated in the text of Chapter I.

1.5. DSB repair pathways

To counteract the deleterious effects caused by DSBs, cells have evolved several different repair pathways, the two most prominent being homologous recombination (HR) and non-homologous end-joining (NHEJ) (Mehta and Haber, 2014) (**Fig. 3**). HR requires the availability of a homologous template either on a sister chromatid or in an ectopic homologous region to guide repair, thus is usually error free. In contrast to homology directed repair, NHEJ occurs by directly re-joining the two DNA broken ends without the need for a homologous template, and often results in small deletions or insertions. Generally, the cell cycle stage at which DSBs are produced greatly influences the choice of DSB repair pathway (Jackson, 2002). In mammalian cells, NHEJ is mainly used in G_1 phase of the cell cycle, while HR is used during S and G_2/M cells due to the presence of the sister chromatid, which provides the sequence homology (Chapman et al., 2012). Although the use of the homologous template enables cells to accurately repair DSBs by HR, this repair process is a great deal more complex than NHEJ.

1.5.1. Homologous recombination

DSB end resection that occurs following the detection of a DSB is required for HR repair. The MRX complex and the DNA endonuclease Sae2 (CtIP in mammals) are responsible for the initial short-range DNA end resection after the formation of a DSB in yeast (Huertas et al., 2008; Moreau et al., 2001); and Exo1 or the Dna2-Sgs1 (Nuclease and DNA helicase, respectively) complex are involved in further DNA end resection following the production of short-range

ssDNA (Cejka et al., 2010; Huertas et al., 2008; Mimitou and Symington, 2008; Zhu et al., 2008). In addition to lack of sister chromatids in G_1 cells, another limitation for HR to occur in G_1 cells is the low activity of cyclin-dependent kinase 1 (Cdk1) / Cdc28 that promotes DSB end resection (Aylon et al., 2004; Ira et al., 2004). It has been shown that Cdk1/Cdc28 mediates phosphorylation of Sae2 and Dna2, both of which are important nucleases involved in end resection (Chen et al., 2011; Huertas et al., 2008).

After DSB end resection, the Rad51 protein replaces RPA to form a nucleofilament on the ssDNA, with the aid of the recombinase Rad52 (Lok and Powell, 2012). This nucleofilament searches for a DNA sequence with homology to the 3' overhang. Once found, the nucleofilament invades the identical donor DNA by a process called strand invasion, which requires the involvement of the evolutionarily conserved *RAD52* epistasis group proteins including Rad54, Rad55, Rad57, and Rad59 (Lisby et al., 2004). DNA synthesis occurs to extend the end of the invading 3' strands to restore the DNA sequence (Mehta and Haber, 2014). During this process, a hetero-duplexed DNA structure is produced, but in the end becomes resolved following DNA synthesis (**Fig. 3**). HR repair can be accomplished by a few related but distinct mechanisms, including gene conversion (Wang et al.), break-induced replication (Bird et al.), and single-strand annealing (SSA) (**Fig. 3**).

GC is the major HR repair pathway when the template shares homologous sequence with both ends of the DSB (Krogh and Symington, 2004; Mehta and Haber, 2014). There are two different mechanisms of GC: synthesis-dependent

strand-annealing (SDSA) pathway, and the double Holliday Junction (d-HJ) pathway (**Fig. 3D and 3E**). During SDSA, the newly synthesized ssDNA dissociates from the hetero-duplexed DNA structure and anneals with the ssDNA overhang on the other end of the DSB. Afterwards, DNA synthesis occurs to fill the DNA sequence between the two broken ends. As a result of HR repair by SDSA, non-crossover (NCO) repair products are generated (Ferguson and Holloman, 1996). In the d-HJ pathway, however, DNA synthesis at the 3' end of the invading strand causes extension of the hetero-duplexed DNA structure; and when the ssDNA on the other broken end anneals with the homologous template, a d-HJ structure is produced. The d-HJ structure can be resolved in two ways, either resolution or dissolution. For resolution, the dHJ structure is resolved by certain HJ resolvases such as Yen1 and Mus81 (Matos et al., 2011), leading to either NCO or crossover repair products. Alternatively, the dHJs can undergo helicase and topoisomerase (such as Sgs1 and Top3)-mediated dissolution to generate NCO products (Wu and Hickson, 2003).

BIR occurs when only one DSB end is present at the site of repair. For example, collapsed replication forks can lead to loss of one branch of the fork (McEachern and Haber, 2006). During BIR, DNA synthesis following DNA strand invasion allows long stretch DNA replication based on the donor template (**Fig. 3F**). The involvement of Rad51 is not required for BIR, although BIR does occur in a Rad51-dependent manner in many cases (Malkova et al., 1996). BIR plays an important role in the maintenance of telomeres (McEachern and Haber,

2006). However, BIR can be highly mutagenic, leading to loss of heterozygosity and non-reciprocal translocation (Llorente et al., 2008).

SSA involves DNA end resection between two homologous sequences in the same orientation on the same chromosome flanking a DSB (**Fig. 3G**). The homologous stretches of ssDNA on different DNA strands then anneal, leading to formation of the single-stranded tails that are subsequently removed by the Rad1-Rad10 complex through its endonuclease activity. As a result, the sequence between the two homologous regions is deleted (Mehta and Haber, 2014). During SSA, HR proteins such as Rad52 and Rad59 play an important role in strand annealing (Sugawara et al., 2000). However, SSA does not require the complete involvement of HR proteins such as Rad51, since it does not involve DNA strand invasion (Ivanov et al., 1996).
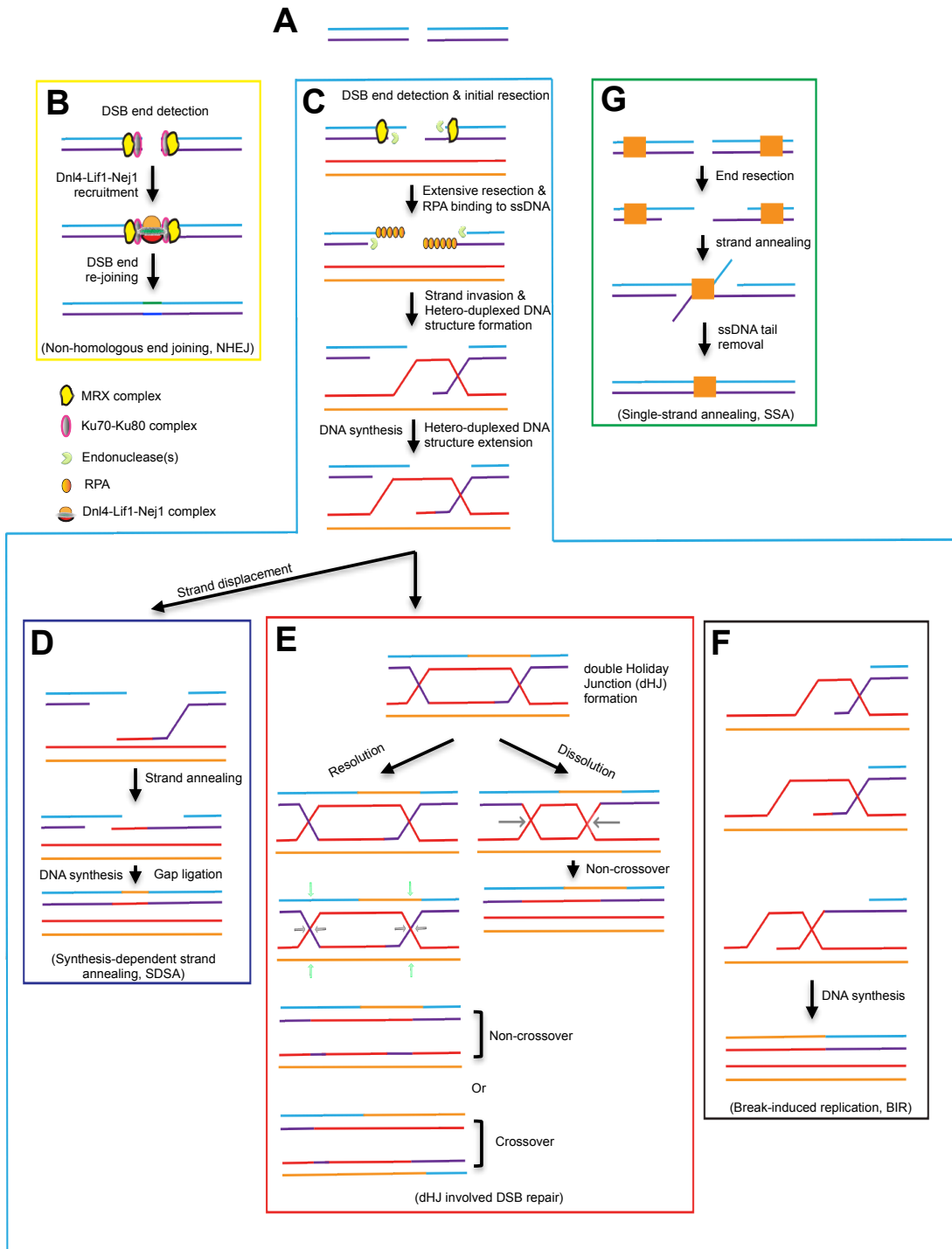
Figure 3. Schematic overview of distinct DSB repair pathways. (**A**) Formation of a DSB. (**B**) DSB repair by NHEJ. The broken DSB ends are tethered by the Ku70-Ku80 heterodimer and MRX. The end joining process is

mediated by the Dnl4-Lif1-Nej1 complex. (**C.G**) DSB repair by HR. (**C**) The distinct HR repair pathways when homologous template is on a different chromosome. After DSB generation, the broken DNA ends undergo resection to generate ssDNA overhangs, which are coated by RPA. Afterwards, Rad51 replaces RPA for binding to ssDNA and forms a nucleofilament, which then undergoes homology search and invades the undamaged homologous template. As a result, a hetero-duplexed DNA structure is produced. (**D**) HR repair through synthesis-dependent strand-annealing (SDSA). During SDSA, the invading strand is displaced and anneals with the ssDNA on the other end of the DSB. After DNA synthesis and gap ligation, non-crossover (NCO) repair products are generated. (**E**) HR repair through the double Holiday Junction (dHJ) pathway. In some cases, after DNA synthesis and extension of the hetero-duplexed DNA structure, the other end of the DSB gets involved in the formation of a dHJ structure, which can be resolved through either resolution or dissolution. Resolution results in either crossover or NCO products, while dissolution results in NCO products. (**F**) HR repair through break-induced replication (Bird et al.). BIR occurs when only one broken end is available for repair. After strand invasion, DNA synthesis proceeds until it reaches the other end of the homologous template. (**G**) HR repair through single-strand annealing (SSA). SSA occurs when a DSB is flanked by two direct homologous sequences. After extensive resection, the single-stranded homologous sequences anneal. The intervening ssDNA tails are subjected to removal. This figure was made based on the previous literature (Finn et al., 2012; Mehta and Haber, 2014).

1.5.2. Non-homologous end joining (NHEJ)

DSB repair by NHEJ essentially involves direct re-joining of the broken DNA ends, which usually undergo only limited processing. It does not require a homologous DNA template for repairing the DSB, and thus often causes small deletions or insertions (Lieber, 2010). NHEJ can take place at any cell cycle stage, but is of great importance to G_1 cells that lack sister chromatids and have limited Cdk1/Cdc28 activity (Aylon et al., 2004; Ira et al., 2004). In higher eukaryotes, NHEJ occurs more frequently than HR for DSB repair. The initial and essential step in the NHEJ pathway is binding of the Ku70-Ku80 heterodimeric complex to the unprocessed DSB ends (**Fig. 3B**). The Ku complex holds the broken DNA ends together and serves as a scaffold for recruiting other NHEJ factors to the break site, so as to ensure DSB repair by NHEJ. MRX, as a DNA end-bridging factor during NHEJ, interacts with the Dnl4-Lif1-Nej1 complex to facilitate Dnl4-mediated DSB end rejoining (Chen et al., 2001).

1.6. Checkpoint recovery after DSB repair

After DSB repair, the DNA damage induced checkpoint is turned off to resume cell cycle progression. This process is called checkpoint recovery (Lazzaro et al., 2009). Although the molecular mechanisms underlying DNA damage checkpoint activation have been extensively studied, relatively a lot is still unknown about how checkpoint recovery takes place in cells.

Various protein phosphatases have been implicated in the down-regulation of DNA damage-induced checkpoint (Hustedt et al., 2013). In yeast, PP2C protein phosphatases Ptc2 and Ptc3, PP4 phosphatase Pph3, and PP1

phosphatase Glc7 have been implicated in DNA damage checkpoint recovery after DSB repair. Ptc2, Ptc3, and Pph3 were found to be important for checkpoint recovery after repair of a HO endonuclease-induced DSB (Keogh et al., 2006; Leroy et al., 2003). Ptc2 and Ptc3 can specifically bind to and dephosphorylate Rad53 to inactivate the DNA damage checkpoint (Leroy et al., 2003). Pph3 regulates the phosphorylation status of γH2A in vivo and efficiently dephosphorylates γH2A in vitro (Keogh et al., 2006). Heideker J et al. (Heideker et al., 2007) proposed that Pph3-mediated γH2A and Rad53 dephosphorylation reply on different Pph3 adaptor proteins. In addition, Glc7 is important for checkpoint recovery after release from chemically induced DSBs, by dephosphorylating Rad53 (Bazzi et al., 2010). It is proposed that different Rad53 phosphorylation patterns induced by different types of DNA damage require distinct phosphatase(s) for Rad53 dephosphorylation during checkpoint recovery (Heideker et al., 2007).

In addition to protein phosphatase-dependent DNA damage checkpoint recovery, lots of other proteins appear to be involved in the inactivation of the DNA damage checkpoint. These proteins include but are not limited to the histone chaperone Asf1 (ASF1a/b in mammals), the DNA helicase Srs2 (RTEL1 in mammals), and the DNA endonuclease Sae2 (CtIP in mammals).

Asf1 is a highly conserved histone H3/H4 chaperone, involved in many processes, including chromatin assembly / disassembly, histone exchange, DNA replication, transcription, and chromatin silencing (Adkins et al., 2004; Donham et al., 2011; Sanematsu et al., 2006; Sharp et al., 2001). Intriguingly, Asf1 in

budding yeast also regulates DNA damage checkpoint recovery, due to its ability to dynamically interact with histone H3 and Rad53 (Tsabar et al., 2016). It has been shown that Asf1 binding to histone H3 promotes H3 acetylation on the lysine (K) 56 residue, which appears to be important for chromatin reassembly that is required for DNA damage checkpoint recovery (Chen et al., 2008). Also, Tsabar M et al. (Tsabar et al., 2016) showed that the Asf1 binding to Rad53, which only occurs once Asf1 releases histones, is required for complete dephosphorylation of Rad53 during DNA damage checkpoint recovery. The interaction between Asf1 and Rad53 may prevent Rad53 autophosphorylation in trans, so promoting checkpoint recovery.

The helicase Srs2 is also implicated in DNA damage checkpoint recovery. It was shown that srs2Δ exhibits a checkpoint recovery defect after DSB repair (Vaze et al., 2002). It was shown that Rad51 depletion can suppress the checkpoint recovery defect caused by SRS2 deletion by Vaze et al. (Vaze et al., 2002). Consistently, Yeung and Durocher (Yeung and Durocher, 2011) found that SRS2 deletion leads to Rad51-dependent ssDNA retention, which inhibits the down-regulation of the DNA damage checkpoint. Therefore, it has been suggested by Yeung and Durocher (Yeung and Durocher, 2011) that Srs2 allows checkpoint recovery by removing Rad51 from the ssDNA filament.

The nuclease Sae2 is involved in DSB end resection, as has been mentioned in Section 1.5.1. Another important function of Sae2 during the DNA damage response is to regulate checkpoint recovery. In the absence of Sae2, cells are defective in turning off Mec1/Tel1-dependent DNA damage checkpoint

(Clerici et al., 2006). It was suggested that the role of Sae2 in checkpoint recovery is associated with its negative regulation of the MRX complex during the DNA damage response (Clerici et al., 2006; Kim et al., 2008).

1.7. Chromatin remodeling during the DSB response

DSB repair has to occur in the chromosomal context of the genome within chromatin. During the DSB response, chromatin around the DSB is subjected to several remodeling processes, including histone post-translational modifications (PTMs), nucleosome repositioning and nucleosome disassembly / reassembly for the formation of an open chromatin structure to allow the DSB response machinery to access the DSB, properly transduce the DNA damage signaling and facilitate DSB repair (Price and D'Andrea, 2013; Seeber et al., 2013).

1.7.1. General overview of chromatin structure

In eukaryotes, genomic DNA and histones are packaged into a complex called chromatin, of which the fundamental subunits are the nucleosomes. Each nucleosome is composed of about 147 bp of DNA wrapped around a histone octamer, which consists of a tetramer of histone H3-H4 that contains two copies of each H3 and H4, and two dimers of H2A-H2B that flank the H3-H4 tetramer (Luger et al., 1997). Nucleosomes are linked by a segment of DNA termed the linker DNA that can be bound by linker histones such as histone H1. A chain of nucleosomes connected with linker DNAs forms the primary structure of chromatin of about 10 nm in diameter, and is described as the 10 nm fiber or "beads-on-a-string". The 10 nm chromatin fiber further coils into a super-helical structure of about 30 nm in diameter, and is therefore termed as "30 nm fiber" as

the secondary structure of chromatin. The 30 nm chromatin fiber can be subjected to further packaging to form more condensed chromatin structures (Maeshima et al., 2014).

During various cellular activities in eukaryotic cells, such as transcription, DNA replication, and DNA damage repair, regional chromatin structure needs to adopt an open state to allow the target DNA sequence to become accessible to the relevant machinery. DNA methylation, histone modifications, histone exchange or removal, and nucleosome repositioning, all can affect the chromatin structure.

1.7.2. Chromatin disassembly / reassembly during DSB response

A lot of evidence indicates that chromatin undergoes disassembly and reassembly during the DSB response and these processes are important for cell survival after DSB repair (Linger and Tyler, 2007). It was shown that histones are removed around a DSB site (Tsukuda et al., 2005), indicating nucleosomes are disassembled at a DSB. On the other hand, following DSB repair in yeast, chromatin is reassembled in a histone chaperone Asf1-dependent manner (Chen et al., 2008). Without chromatin reassembly, cells exhibit defects in turning off the DNA damage checkpoint and are subjected to cell death (Chen et al., 2008). It was suggested that the histone loss around a DSB site requires the MRX complex and the chromatin remodeling complex INO80 (Tsukuda et al., 2005), although this is likely reflecting a role for DNA resection in driving chromatin disassembly. Indeed, Chen et al. (Chen et al., 2008) suggested that histone loss around a DSB during HR depends on DNA end resection. Studies have showed

that transient incorporation of a histone H2A variant H2A.Z into chromatin is required for efficient DSB repair (Gursoy-Yuzugullu et al., 2015; Xu et al., 2012). It was suggested that the transient exchange of canonical H2A for H2A.Z after DSBs probably promotes chromatin disassembly to allow the onset of the DSB response, due to the fact that H2A.Z-containing chromatin is less stable (Xu et al., 2012). However, the mechanisms underlying chromatin disassembly and reassembly during the DSB response are poorly understood. For example, it is not clear which proteins and processes drive the chromatin disassembly and reassembly during DSB response, the spatial range of chromatin disassembly in response to a DSB, and differences in chromatin disassembly and reassembly between the DSB response and during other DNA activities such as DNA replication, etc.

1.7.3. Chromatin remodelers implicated in the DSB response

ATP-dependent chromatin remodeling complexes play a key role in altering chromatin structure in response to DSBs. They are large multi-subunit complexes that couple ATP hydrolysis to several chromatin altering activities, such as histones exchange, histone incorporation or removal, and nucleosome repositioning along the DNA (Price and D'Andrea, 2013; Seeber et al., 2013). In addition to the function of chromatin remodeling, certain chromatin remodelers have been shown to directly regulate the DNA damage checkpoint and / or DSB repair. Here, I summarize the functions of several chromatin remodelers during the DSB response, including Fun30, INO80, RSC, SWI/SNF and SWR1.

Fun30 (SMARCAD1 in mammals) is a chromatin remodeler involved in histone dimer exchange (Awad et al., 2010). Also, Fun30 is important for the rate and extent of DSB end resection (Chen et al., 2012; Costelloe et al., 2012; Eapen et al., 2012), possibly by removing from the DSB checkpoint mediator protein Rad9, which inhibits DSB end resection (Chen et al., 2012; Lazzaro et al., 2008).

The chromatin remodeling complex INO80 facilitates histone removal at a DSB site. It is recruited to DSBs by γH2A to promote DSB repair by either HR or NHEJ (Morrison et al., 2004; van Attikum et al., 2004). In addition, INO80 acts to regulate the DNA damage checkpoint response (Bao and Shen, 2011; Morrison et al., 2007; van Attikum et al., 2007).

The RSC complex has been shown to be important for DSB repair (Bao and Shen, 2007). The recruitment of RSC to a DSB site is mediated by its interaction with Mre11, and affects the level of γH2A (Liang et al., 2007). It is required for chromatin remodeling around an HO-induced DSB at the *MAT* locus (Kent et al., 2007). Also, RSC promotes strand invasion and the formation of holiday junctions during HR (Chai et al., 2005). It was also suggested that RSC promotes recombination between sister chromatids by recruiting cohesin, as RSC can interact with cohesin and is required for the formation of sister chromatid cohesion (Oum et al., 2011).

The SWI/SNF chromatin remodeling complex can be recruited to γH2A-containing nucleosomes around a DSB site by interacting with acetylated histone H3. On the other hand, SWI/SNF promotes γH2A formation, which in turn causes

more H3 acetylation, thus creating a feedback activation loop to facilitate DSB repair (Lee et al., 2010). In addition, it was suggested that the SWI/SNF complex plays a role in nucleosome removal on the homologous template during HR repair (Chai et al., 2005).

The chromatin remodeler SWR1 is involved in the removal of histone H2A.Z from chromatin during the DSB response (Mizuguchi et al., 2004). It is recruited to DSBs via direct interaction with γH2A (van Attikum et al., 2007). SWR1 depletion results in defects in both DNA damage checkpoint activation and DSB repair (Bao and Shen, 2011; van Attikum et al., 2007).

1.7.4. Histone chaperones implicated in chromatin remodeling

In addition to many chromatin remodeling complexes, multiple histone chaperones are of great importance to chromatin remodeling during the DSB response. While many studies have revealed that chromatin remodelers play a critical role in chromatin disassembly at DSBs, our knowledge of the histone chaperones that participate in chromatin disassembly during the DSB response is very limited.

The FACT complex as a chaperone for histone H2A-H2B dimers, facilitates the removal of H2A-H2B dimers from chromatin during transcription (Belotserkovskaya et al., 2003). It was shown that the FACT complex mediates the H2AX-H2B dimer exchange in chromatin, and therefore is implicated in DNA repair (Heo et al., 2008; Winkler et al., 2011).

As has been mentioned before (Section 1.7.2), transient incorporation of histone H2A variant H2A.Z into chromatin is required for DSB repair. In

mammals, it is the histone chaperone Anp32e that mediate the H2A.Z removal from chromatin bearing the DSB (Gursoy-Yuzugullu et al., 2015); while in yeast, the histone chaperone Chz1 together with the chromatin remodeler SWR1 are responsible for this process (Luk et al., 2007; Mizuguchi et al., 2004). As such, it is possible that these chaperones may also promote repair via their role in removing H2A.Z.

As for chromatin reassembly after DSB repair in yeast, the histone H3/H4 chaperones CAF-1 and Asf1 have been shown to be critical (Chen et al., 2008; Linger and Tyler, 2007). In humans, CAF-1 and Asf1 are both involved in chromatin reassembly during nucleotide excision repair (Mello et al., 2002). Thus, it is possible that CAF1-1 and Asf1 mediated chromatin reassembly after DSB repair is a conserved process. However, it is still under investigation with regard to which histone chaperones reassemble H2A-H2B dimers into chromatin after DSB repair. It is possible that H2A-H2B reassembly into chromatin occurs through a similar mechanism as during DNA replication, however that is also poorly understood. The members of the histone chaperone NAP1 family are evolutionary conserved, and mainly bind to H2A-H2B dimers (Dong et al., 2003; Park and Luger, 2006; Zhu et al., 2006). In *arabidopsis*, Nap1 depletion leads to defects in HR repair (Gao et al., 2012). Therefore, it is possible that Nap1 in yeast also plays a conserved role in chromatin remodeling during DSB repair by HR.

1.7.5. Histone post-translational modifications implicated in the DSB response

The DSB response involves many post-translational modifications (PTMs) on histones, including phosphorylation, ubiquitinylation, acetylation, methylation and SUMOylation (Polo and Jackson, 2011). The histone PTMs facilitate alterations in chromatin structure and recruitment of proteins that regulate the damage signaling or repair the broken DNA ends. In this section, I summarize the histone PTMs that are known to play a role during the DSB response (also see **Table 2**).

PTMs on histone H2A that are implicated in the DSB response include yeast γH2A (or mammalian γH2AX), mammalian H2A/H2AX ubiquitination on lysine (K) 13, K15 and K119 (H2A/H2AX K13ub, K15ub and K119ub), mammalian H2AX acetylation on K5 and K36 (H2AX K5ac and K36ac) and mammalian H2AX tyrosine (Y) 142 dephosphorylation (**Table 2**). As has been mentioned in Section 1.4, γH2A is very important for both DNA damage checkpoint activation and DSB repair, by recruiting DSB response proteins to the vicinity of a DSB. On the other hand, after DSB repair, dephosphorylation of γH2A is required for turning off the DNA damage checkpoint (Chowdhury et al., 2005; Keogh et al., 2006). In addition, γH2A facilitates the formation of other types of histone PTMs, for example, the acetylation of histone H3 on K9, K14, K18, and K23, which are also implicated in the DSB response (Lee et al., 2010). In mammals, the ubiquitination of histone H2A/H2AX on K13, K15 and K119 have been implicated in the DSB response. H2A/H2AX K13 / K15 ub was found

to be important for recruiting 53BP1 at a DSB site (Fradet-Turcotte et al., 2013; Mattiroli et al., 2012). H2A/H2AX K119ub can be induced by IR (Xie et al., 2010) and was shown to be required for DNA damage-induced histone turnover (Ikura et al., 2007). Also, H2A/H2AX K119ub is required for 53BP1 and BRCA1 recruitment at a DSB site (Doil et al., 2009; Huen et al., 2007; Kolas et al., 2007; Mailand et al., 2007). H2AX K5ac was shown to facilitate the formation of H2AX K119ub and the removal of γH2AX during the DSB response (Ikura et al., 2007). H2AX K36ac is involved in the recruitment of the Ku complex during DSB repair by NHEJ (Jiang et al., 2010). In addition, dephosphorylation of H2AX Y142 that occurs after the induction of γH2AX was suggested to maintain γH2AX and facilitate the recruitment of DSB response proteins such as MDC1 and ATM (Xiao et al., 2009). Since WSTF that catalyzes the phosphorylation of H2AX Y142 (H2AX Y142ph) is required for γH2AX foci formation, it was suggested that H2AX Y142ph that exists prior to the formation of a DSB may play a role in creating a chromatin environment around the DSB that facilitate the later induction of γH2AX (Xiao et al., 2009). As for the H2A variant H2A.Z, it was shown that H2A.Z SUMOylation plays a key role for DSBs relocating to the nuclear periphery (Kalocsay et al., 2009). Interestingly, it was shown that gene conversion is more efficient if the homologous donor template translocates to the nuclear periphery (Nagai et al., 2008).

Histone	*S. cerevisiae*	Mammals	Catalyzing enzyme
H2A/H2AX		K13ub	RNF168
H2A/H2AX		K15ub	RNF168
H2A/H2AX		K119ub	RNF8, RNF168
H2AX		K5ac	TIP60
H2AX		K36ac	CBP/p300
H2AX		S139ph	ATM, ATR, DNA-PKcs
H2AX		Y142ph	Phosphorylation by WSTF, dephosphorylation by EYA1
H2A	S129ph		Mec1, Tel1
H2B	K123ub		Bre1-Rad6
		K120ub	RNF20, RNF40
H3	K9ac	K9ac	Gcn5/GCN5 (yeast/mammals)
	K14ac	K14ac	Gcn5/GCN5 (yeast/mammals)
	K23ac	K23ac	Gcn5/GCN5 (yeast/mammals)
	K27ac	K27ac	Gcn5/GCN5 (yeast/mammals)
	K56ac	K56ac	Rtt109 in yeast, CBP/p300 in mammals
	K18ac	K18ac	Gcn5/GCN5, and CBP/p300 during NHEJ in mammals
		K4me3	SET1
		K9me3	Suv39h1
		K36me2	Metnase(or SETMAR)
		K36me3	SETD2
	K79me	K79me	Dot1/DOT1 (yeast/mammals)
H4	K5ac	K5ac	Esa1/Tip60 (yeast/mammals)
	K8ac	K8ac	Esa1/Tip60 (yeast/mammals)
	K12ac	K12ac	Esa1/Tip60 (yeast/mammals)
	K16ac	K16ac	Esa1/Tip60 (yeast/mammals), and MOF in mammals
	S1ph		CK2
		K20me2	Suv420H1/Suv420H2, MMSET
		K91ub	BBAP

Table 2. A list of known histone PTMs implicated in the DSB response.

Functions of each individual histone PTM as stated in the Section 1.7.5.

PTMs implicated in the DSB response on histone H2B include H2B mono-ubiquitination of H2B K123 (H2B K120 in mammals) (**Table 2**). Both yeast H2B K123ub and mammalian H2B K120ub stimulates the methylation of histone H3 on K79, which is important for DSB-induced checkpoint activation (Giannattasio

et al., 2005; Zhu et al., 2005). In addition, mammalian H2B K120ub was shown to be required for DSB repair *per se*, by recruiting either HR or NHEJ repair proteins to the DSB site (Moyal et al., 2011). Also, H2B mono-ubiquitination is suggested to promote chromatin decompaction to facilitate DSB repair (Moyal et al., 2011).

PTMs on histone H3 that are involved in the DSB response and are conserved from yeast to mammals include acetylation of H3 on K9, K14, K18, K23, K27, and K56, and methylation of H3 K79 (**Table 2**). In addition, mammalian methylations of H3 on K4, K9 and K36 have been implicated in the DSB response. Lots of evidence suggests that the acetylation of the N-terminal H3 K residues (i.e. K9, K14, K18, K23 and K27) is required for DSB response. In yeast, it was shown that mutations of these K residues of H3 or depletion of the corresponding histone acetyltransferase (HAT) Gcn5 result in defects in DSB repair (Tamburini and Tyler, 2005). Also, both Gcn5 and these N-terminal H3 lysine acetylation are enriched at the HO-induced DSB at the *MAT* locus (Tamburini and Tyler, 2005). In mammals, the H3 N-terminal lysine acetylation including K9ac, K14ac, K18ac, and K23ac (but not K27ac) was found to occur preferentially on γH2AX containing nucleosomes in a γH2AX-dependent manner, and recruits the chromatin remodeler SWI/SNF, which in turn facilitate the spreading of γH2AX around the DSB site (Lee et al., 2010), Ogiwara et al. (Ogiwara et al., 2011) found that mammalian H3 K18ac (but not H3 K9ac or K14ac) plays an important role in recruiting the Ku complex and SWI/SNF during DSB repair by NHEJ. Interestingly, the HAT proteins CBP and p300 catalyze the acetylation of H3 K18 during NHEJ (Ogiwara et al., 2011). H3 K56ac is a H3

globular domain PTM, and has been implicated in the DSB response in both yeast and mammals (Chen et al., 2008; Miller et al., 2010). In yeast, it was shown that H3 K56ac is important for chromatin reassembly after DSB repair (Chen et al., 2008). In mammals, H3 K56ac was shown to be DNA damage-inducible and H3 K56 mutants have increased sensitivity to DSBs-inducing agents (Yuan et al., 2009). Both yeast and mammalian H3 K79 methylation is important for the DSB response, since H3 K79 methylation helps recruit yeast Rad9 and mammalian 53BP1 to DSBs to facilitate DSB repair (Giannattasio et al., 2005; Huyen et al., 2004). In addition, studies in mammals have revealed three other H3 methylation that participate in the DSB response, including H3 K4me3, K9me3 and k36me (**Table 2**). H3 K4me3 was shown to facilitate V(D)J recombination (Stanlie et al., 2010). H3 K9me3 that is enriched at a DSB site by the methyltransferase Suv39h1, is critical for the activation of the HAT Tip60 and ATM during DSB repair (Ayrapetov et al., 2014; Sun et al., 2009). H3 K36me2 promotes the recruitment of NBS1 and Ku70 to a DSB site that is repaired by NHEJ (Fnu et al., 2011). Also another study found that H3 K36me3 is required for DSB repair by HR (Pfister et al., 2014).

PTMs on histone H4 that are implicated in the DSB response include acetylation of H4 on K5, K8, K12, and K16 in both yeast and mammals (**Table 2**). In yeast, mutants of these H4 K residues show increased sensitivity to an HO-induced DSB, and the HAT Esa1 that is specific for H4 lysine acetylation is enriched at the HO-induced DSB site (Tamburini and Tyler, 2005). In addition, Bird et al. (Bird et al., 2002) showed that mutants of these H4 K residues and a

temperature sensitive mutant of the essential gene *ESA1* are defective in DSB repair by NHEJ. In mammals, these four H4 acetylation that catalyzed by CBP/p300 were shown to promote the recruitment of the Ku complex and SWI/SNF during DSB repair by NHEJ (Ogiwara et al., 2011). Murr et al. (Murr et al., 2006) suggested that H4 acetylation by the HAT Tip60 is important for chromatin relaxation and recruitment of the repair proteins at a DSB site that undergoes HR repair. In addition, the HAT MOF-dependent H4 K16ac in mammals plays a critical role in the DSB response by modulating MDC1 recruitment to DSBs (Li et al., 2010; Sharma et al., 2010). On the other hand, deacetylation of H4 at K16 was shown to be important for 53BP1 signaling during the DSB response (Hsiao and Mizzen, 2013). These studies suggest that the fine-tuned regulation of H4 K16 acetylation / deacetylation is important for the DSB response, and the HAT that is responsible for mammalian H4 K16ac appears to be different according to different DSB repair pathways. Additionally, yeast phosphorylation of H4 on S1 (H4 S1ph) is DSB-inducible and suggested to promote NHEJ repair (Cheung et al., 2005). In mammals, H4 K20me2 and H4 K91ub also participate in the DSB response (**Table 2**). H4 K20me2 can be induced by DSBs and facilitates 53BP1 recruitment in collaboration with H2A K15ub (Botuyan et al., 2006; Pei et al., 2011). Interestingly, H4 K91ub was shown to induce H4 K20me2 and promote NHEJ by recruiting 53BP1 to DSBs (Yan et al., 2009).

There is lots of cross-talk between the various DSB response related histone PTMs. The well-regulated order in which the histone PTMs occur is

presumably important for the proper DSB response. The dynamics of histone PTMs in the context of chromatin plays an essential role in chromatin remodeling during DSB repair (Price and D'Andrea, 2013). Although much has been studied, the full repertoire of histone PTMs that regulate DSB response is still under investigation.

Chapter 2

Methods and materials

2.1. Plasmid construction

Plasmid *pFA6a-2LEXA-His3MX6* was constructed by inserting DNA oligonucleotides containing 2 tandem copies of the *LEXA* DNA binding site (2*LEXA*) into the *pFA6a-His3MX6* plasmid (Longtine et al., 1998) at the *BglII* site, which was concomitantly disrupted upon ligation. The DNA oligonucleotides containing 2*LEXA* (2LEXA_delBglII forward and reverse oligo sequences are listed in **Table 3**) were phosphorylated and annealed, before being ligated with *pFA6a-His3MX6* vector that had been *BglII* digested and dephosphorylated. The ligation product was transformed into chemically competent *E.coli* cells (Invitrogen, Cat # C404003)*,* and *BglII* negative clones were selected for sequencing to screen for 2*LEXA* correctly inserted to generate the *pFA6a-2LEXA-His3MX6* plasmid.

2.2. Yeast strain construction

The yeast strains used in this study are listed in **Table 4**. To make yeast strain PWY001 that has 2*LEXA* sites integrated about 500 bp to the right of the HO cut site at the *MAT* locus on Chr III, DNA fragments spanning the 2*LEXA* and *His3MX* cassette were PCR amplified from the plasmid *pFA6a-2LEXA-His3MX6* using HOcs-2LEXA-HIS forward and reverse primers (**Table 3**). These primers include homology 500 bp distal to the HO cut site at the *MAT* locus on Chr III, and the PCR product was then transformed into strain JRY2334. Transformants were selected on synthetic media minus histidine agar plates, and screened for clones with positive 2*LEXA* insertion at the target region, as determined by PCR screening. Plasmid *pLexA-PrA-Trp* expressing the LexA-Protein A fusion protein

(Byrum et al., 2012) was transformed into strain PWY001 to make strain PWY011. Strain PWY002 with the galactose-inducible *HO* gene integrated at the *ADE3* locus was constructed by transforming the linearized plasmid *pYIPade3HO* (kindly provided by Dr. Virginia Zakian) into PWY001, following the procedures described previously (Sandell and Zakian, 1993).

The yeast strain PWY081 containing the HO cut site (HOcs) at the genomic *ADH1* gene was constructed by transforming into strain JCY004 DNA fragments that were PCR amplified from the HOcs-13Myc-KanMX cassette at the 3' end of the *ADH1* gene using genomic DNA extracted from strain PCY23 (Chaurasia et al., 2012) as the PCR template. ADH1-HOcs forward and reverse primers (**Table 3**) were used in the PCR reaction, which produced DNA fragments with about 200 bp homology to the 3' end of *ADH1* gene on each end. The positive transformants were selected on G418 plates. Screening PCR reactions were performed using Scr-ADH1 primers (**Table 3**), which produce about 750 bp products only on clones that contain HOcs inserted at the 3' end of *ADH1* gene.

Yeast strains with Flag or HA tagging at the C-terminal of a gene of interest were made by PCR-mediated DNA fragment integration. The *pFA6a-3XHA-TRP* plasmid was used as the PCR template for making C-terminal 3XHA tagged strains, with primers designed based on F2 and R1 primers as described previously (Longtine et al., 1998). The *pFA6a-6XGly-3XFlag-HphMX4* plasmid was used as the PCR template for making C-terminal 3XFlag tagged strains (Funakoshi and Hochstrasser, 2009). Correct epitope tagging was confirmed by

36

PCR for positive insertion of the tag and selection marker at the end of the target

gene and by western blot analysis for epitope tag expression.

Primer	Forward Sequence	Reverse Sequence	Source
HOMAT	AGGTAAATTACAGCAAATAG	AACAACAACCTAGAGTAATG	(Chen et al., 2008)
RAD27	ACATCGCGCAAATGAAGGTT	TCAAGTTCCCAGAAAAACTG	(Chen et al., 2008)
YRA1-RTPCR	GCAGGATGCTGTAAGAGAATTT	TGTGATGTTAGCCATACCAGT	This study
ACT1-RTPCR	GTGATGGTGTTACTCACGTC	GTAGTCAGTCAAATCTCTACCGGC	This study
2LEXA_del BgIII	GATCGCGCTACTGTATATATATACAGTAGCGCCCTACTGTATATATATACATACGCG	GATCCGCGTACTGTATATATATACAGTAGGGCGCTACTGTATATATATACAGTAGCGC	This study
HOcs-2LEXA-HIS	ACCTTCGGCTTCACAATTTGTTTTTCCACTTTTCTAACAGCGGATCCCCGGGTTAATTAA	GGCGAATAAGATAAAGATAAGTTTGAAAGGTGATAAACGAATTCGAGCTCGTTTAAAC	This study
MATHO-ChIP	TTGGATCTTAACAAACCGTAAAGGT	GGTAACTAGCAAACAAAGGAAAGTCA	(Chen et al., 2008)
SMC2	GGTCCGGTAAGTCGAACATTTT	CTCGCACAGTGCTCATTGATG	(Chen et al., 2008)
ADH1-HOcs	TCTACCAGATACGTTAGAGCTAACG	CCGAGATTCATCAACTCATTGCTGG	This study
Scr-ADH1-HOcs	CTGGTTACACCCACGACGGT	CGTTAATTAACCCGGGGATC	This study
SIT4-3HA-TRP	CACGGCAAACCATAATAATCAAAGAGCCGGCTATTTCTTACGGATCCCCGGGTTAATTAA	GAATGCTCTTAGAATGTGCTTGTTGTGTATCGTATCGTAGGAATTCGAGCTCGTTTAAAC	This study
TOM1-3HA-TRP	ATTGGCAATCAATGAAGGGCATGAAGGGTTTGGTCTTGCCCGGATCCCCGGGTTAATTAA	TCTGTTCCTCTTCCTTGGGCAAGTGTTGTATGGTTAAAGGGAATTCGAGCTCGTTTAAAC	This study
EXO1-3FLAG-HPH	ATCTATCTCCTTGCTTTCCCAATTTGTTTATAAAGGTAAAGGGGGAGGCGGGGGTGGA	CTTACTCCAACCGTACCCTGTCCTACTTTACTGGGCATTGGAATTCGAGCTCGTTTTCGA	This study
YRA1-3FLAG-HPH	AGATCTGGACAAGGAAATGGCGGACTATTTCGAAAAGAAAGGGGGAGGCGGGGGTGGA	AATAAAACCAAATTAAATCAAACAAAAAATTGACAATTAAGAATTCGAGCTCGTTTTCGA	This study

Table 3. A list of yeast primers used in this study.

Yeast deletion mutants were made by homologous recombination-mediated gene replacement, i.e. replacing the open reading frame of the gene of interest with the indicated selective marker gene (**Table 4**).

Yeast transformation was performed using the lithium acetate method with ssDNA (single-stranded DNA from salmon sperm) as the DNA carrier (Gietz et al., 1992).

2.3. Western blot analysis of Rad53

For the transient zeocin time course experiments, cells were grown to mid-log phase, and treated with zeocin (10 mg/ml stock solution in H_2O) at a final concentration of 15 µg/ml (or 30 µg/ml for **Fig. 22C**) for 30 min. Cells were then washed three times in fresh YPD medium to remove zeocin, and harvested at the indicated time points by centrifugation. Yeast whole cell extracts were prepared using the Trichloroacetic Acid (TCA) method, as has been described before (Keogh et al., 2006) and separated on 7.5% SDS-PAGE gels. Anti-Rad53 antibody (EL7 clone) (Fiorani et al., 2008) was used to detect the Rad53 protein. Anti-G6PDH (Sigma) was used as a loading control.

Name	Genotype	Source
JRY2334	*MATa ade2-1 can1-100 his3-11,15 leu2-3,112 trp1-1 ura3-1*	(Thomas and Rothstein, 1989)
PWY001	JRY2334 *HOcs-2XLEXA-HIS*	This study
PWY002	PWY001 *ade3:GAL::HO*	This study
PWY003	PWY001 *rad52Δ::KanMX*	This study
PWY004	PWY002 *rad52Δ::KanMX*	This study
PWY015	PWY001 *rad54Δ::KanMX*	This study
PWY016	PWY002 *rad54Δ::KanMX*	This study
PWY011	PWY001 [*pLexA-PrA-TRP*]	This study
PWY012	PWY002 [*pLexA-PrA-TRP*]	This study
PWY013	PWY003 [*pLexA-PrA-TRP*]	This study

PWY014	PWY004 [*pLexA-PrA-TRP*]	This study
PWY017	PWY015 [*pLexA-PrA-TRP*]	This study
PWY018	PWY016 [*pLexA-PrA-TRP*]	This study
JKM179	*MATα hmlΔ::ADE1 hmrΔ::ADE1 hoΔ ade1–100 leu2–3,112 lys5 trp1::hisG ura3–52 ade3::GAL::HO*	(Lee et al., 1998)
PCY23	JKM179, with additional *HOcs-13Myc-KanMX* before the stop codon at genomic *ADH1* locus	(Chaurasia et al., 2012)
JCY004	JKM119 *MAT-HOinc*	This study, made by Josh Carson
PWY081	JCY004, with additional *HOcs-13Myc-KanMX* before the stop codon at genomic *ADH1* locus	This study
PWY099	PWY081 *def1Δ::URA3*	This study
YMV2	*MATaΔ::hisG hoΔ hmlΔ::ADE1 hmrΔ::ADE1 his4::URA3-leu2 (Xho1 to Asp718)-pBR322 leu2::HOcs ade3::GAL::HO ade1 lys5 ura3-52*	(Vaze et al., 2002)
YMV37	YMV2 *rad52Δ::HPH*	(Vaze et al., 2002)
PWY034	YMV2 *def1Δ::KanMX*	This study
PWY069	YMV2 *tom1Δ::KanMX*	This study
PWY061	YMV2 *ssa1Δ::kanMX ssa2Δ::LEU2*	This study
YMV45	*MATaΔ::hisG hoΔ hmlΔ::ADE1 hmrΔ::ADE1 leu2::leu2(Asp718-SalI)-URA3-pBR322-HOcs ade3::GAL::HO ade1 lys5 ura3-52*	(Vaze et al., 2002)
YMV46	YMV45 *rad52Δ::HPH*	(Vaze et al., 2002)
PWY062	YMV45 *ssa1Δ::kanMX ssa2Δ::LEU2*	This study
BAT009	*W303 MATa ade2-l canl-100 his3 -ll leu2-3,112 trpl-1 ura3-l GAL ade3::GAL::HO*	(Tamburini and Tyler, 2005)
BKD0665	BAT009 *rad52Δ::KanMX*	This study
PWY033	BAT009 *def1Δ::KanMX*	This study
PWY035	BAT009 *SIT4-3HA-TRP*	This study
PWY042	BAT009 *TOM1-3HA-TRP*	This study
PWY066	BAT009 *EXO1-3FLAG-HPH*	This study
PWY095	BAT009 *YRA1-3FLAG-HPH*	This study
JSY568	W303 MATa ade2-1 can1-100 leu2-3,112 his3-11,15 trp1-1 *def1Δ::URA3*	(Wilson et al., 2013)
JSY1198	JSY568, with additional *9xMyc-2xTEV-6xHis-DEF1* at genomic *DEF1* locus	(Wilson et al., 2013)

YCL003	*MATa ade2-1 can1-100 ura3-1 his3-11,15 leu2-3, 112 trp1-1 tor1-1 fpr1::NAT RPL13A-2xFKBP12::TRP1 bar1Δ::HPHMX4 YRA1-FRB::HIS3MX6*	Gift from Bing Li
W303-1A	*W303 MATa ade2-1 can1-100 leu2-3,112 his3-11,15 trp1-1 rad5-G35R*	(Thomas and Rothstein, 1989)
BY4741	*MATa his3Δ1 leu2Δ0 met15Δ0 ura3Δ0*	(Brachmann et al., 1998)
BY4742	*MATα his3Δ1 leu2Δ0 lys2Δ0 ura3Δ0*	(Brachmann et al., 1998)
ssa1/2Δ	BY4741 *ssa1Δ::KANMX ssa2Δ::LEU2*	Gift from Kevin Morano
Deletion mutants (BY4741 or BY4742)		(Giaever et al., 2002)
Yeast DAmP mutants (Haploid, *MATa*)		Thermo Scientific, Cat # YSC5090; (Schuldiner et al., 2005)
PWY109	*sit4Δ* (from BY4742 deletion library) [*pGAL1-HO-URA3*]	This study
PWY110	*sit4Δ* (from BY4742 deletion library) [*pRS316*]	This study
PWY111	*tom1Δ* (from BY4742 deletion library) [*pGAL1-HO-URA3*]	This study
PWY112	*tom1Δ* (from BY4742 deletion library) [*pRS316*]	This study
PWY113	YCL003 [*pGAL1-HO-URA3*]	This study
PWY114	JSY1198 [*pGAL1-HO-URA3*]	This study

Table 4. A list of yeast strains used in this study.

2.4. Alkaline-aided extraction of yeast proteins

This method was adapted from (Kushnirov, 2000), and was used to check tagged protein expression by western blot. For each sample, 1 OD_{600} cells were collected in a 1.5 ml tube by centrifugation. After washing the cell pellet in ice-cold ddH2O, the cells were resuspend in 50 μl of ice-cold ddH2O. 50 μl of 0.2 M

NaOH was added to the cell suspension and mixed well by vortexing. Cells were left in NaOH at room temperature for 5 min, and collected as a cell pellet by centrifugation at 13, 000 rpm x 1 min at 4°C. The cell pellet was resuspended in 200 μl of 1X SDS sample buffer (2% SDS, 10% glycerol, 0.1% bromophenol blue, 50 mM Tris-HCl pH 6.8, and 1% β-mercaptoethanol), and heated at 95°C for 5 min. After spinning down the protein sample at 13, 000 rpm for 3 min, 10 μl supernatant was loaded in each lane of a biorad SDS-PAGE gel. Antibodies used in the western blot analyses are listed in **Table 5.**

Antibody (animal source)	Amount used	Source	Cat #
G6PDH (rabbit)	1:100,000 (WB)	Sigma	A9521
α-Tubulin (rat)	1:1000 (WB)	AbDseroTEC	MCA78G
Flag (mouse)	1 ul per ChIP; 1:5000 (WB)	Sigma	F3165
HA (rabbit)	2 ul per ChIP ; 1:5000 (WB)	Abcam	9110
Protein A (mouse)	1:1000 (WB)	Sigma	P2921
Rad53 (mouse)	1:100 (WB)	(Fiorani et al., 2008)	
Myc (mouse)	2 ul per ChIP; 1:1000 (WB)	Sigma	M4439
Rad51 (rabbit)	1 ul per ChIP; 1:2500 (WB)	Abcam	63798
Rpb1 (mouse)	1:40, 000 (WB)	Cell Signaling	2629
Anti-mouse, HRP	1:5,000 (WB)	Promega	W4021
Anti-rabbit, HRP	1:5000 (WB)	Promega	W4011
Anti-rat, HRP	1:2500 (WB)	Sigma	A5795

Table 5. A list of antibodies used in this study

2.5. HO cutting and repair at *MAT* locus in liquid culture

For yeast strains derived from BAT009 (**Table 4**), efficient HO cutting and repair was achieved in either YEP (1% yeast extract + 2% peptone) + lactate (YEPL) or YEP + 2% raffinose (YEPR) media. In each case, yeast cells were grown up in YEP + 2% glucose (YPD) media from a single colony to reach, but not exceed, mid-log phase. Appropriate amounts of cells were washed in YEP three times before being resuspended in YEPL or YEPR, and grown to OD_{600} 0.4-0.5, at which point 2% galactose was added to the media to induce HO expression. Cells starting from 0.015 OD_{600}/ml required 12 hr growth in YEPL, while only 10 hr in YEPR was necessary to reach OD_{600} 0.4-0.5. To repress HO expression and allow repair of the HO-induced break, cells were treated with 2% glucose at 0.75 hr after galactose induction in YEPL, and at 2 hr after galactose induction in YEPR. Cells were harvested at the indicated time points.

For yeast strains bearing the *pGAL1-HO-URA3* plasmid (**Table 4**), cells were grown up in synthetic media lacking uracil (SC-uracil) + 2% glucose overnight. The appropriate amounts of cells were washed in SC-uracil (without glucose) three times before being resuspend cells in SC-uracil + 2% raffinose. Cells starting from 0.025 OD_{600}/ml in raffinose media needed about 14 hrs to reach OD_{600} 0.4-0.5, at which point 2% galactose was added to induce the expression of HO. 2 hrs after galactose induction, glucose was added to a final concentration of 2% to repress HO and allow repair. Cells were harvested at the indicated time points.

2.6. PCR analysis of HO cutting repair efficiency

For each time point, yeast cells were collected by centrifugation and genomic DNA was extracted. A multiplex PCR assay was performed as previously described (Tamburini and Tyler, 2005) using HOMAT and RAD27 (as a control) primers (**Table 3**). PCR products were separated by 1.5% agarose gel electrophoresis, stained with SYBR safe dye (Invitrogen, Cat # S33102) and visualized on a ProteinSimple Imager (FluorChem E system). The *RAD27* products are expected to be ~1.4 kb, while HOMAT primers are expected to amplify *MATa* products ~1.1 kb, and *MATα* ~1.2 kb. Quantifications of the relative amount of *MATa* or *MATα* during HO cutting and repair was performed using AlphaView software on a ProteinSimple gel documentation machine.

2.7. Chromatin immunoprecipitation at the *MAT* HO site

Yeast strains were cultured in liquid media as described (Section 2.5). For each ChIP time point, 6.5 OD_{600} cells were cross-linked by 1% formaldehyde with constant rotation at room temperature (RT) for 20 min, and then quenched by 136 mM glycine with constant rotation at RT for 5 min. Cell pellets were collected by centrifugation at 4000 rpm x 3 min at 4°C, and washed twice using ice-cold TBS (150 mM NaCl, 20 mM Tris-HCl pH 7.5) before being frozen in liquid nitrogen and stored at -80°C. Once cell pellets for all the time points were collected and frozen, they were thawed on ice, and resuspended in 400 µl ice-cold lysis buffer 1 (0.1% deoxycholic acid, 1 mM EDTA, 50 mM HEPES pH 7.5, 140 mM NaCl, 1% Triton X-100) supplemented with protease inhibitors. 400 µl glass beads (0.5 mm) were added to the cell suspension, which was then lysed

in 4°C by bead beating. Another 400 µl of lysis buffer 1 was added to the cell extract, which was then subjected to sonication (Branson sonifier 450: Timer Hold, Output 2, Duty cycle 100%) to yield chromatin fragments of about 500 bp in length. An aliquot (5%) of the chromatin extract was saved as the INPUT sample. Dynabeads Protein A (Invitrogen, Cat # 10002D) was incubated with the appropriate rabbit antibody for 2 hr at 4°C on a nutator. For mouse antibodies, Dynabeads Protein G (Invitrogen, Cat # 10003D) was used. The antibody coated dynabeads were added to, and incubated with, each cell extract overnight with constant rotation in 4°C. Dynabeads were collected using a magnet, and washed sequentially in ice-cold lysis buffers 1, 2 (same as buffer 1, except for NaCl with a final concentration of 500 mM) and 3 (0.5% deoxycholic acid, 1 mM EDTA, 250 mM LiCl, 0.5% NP-40, and 10 mM Tris pH 7.9), with two washes for each buffer. For each wash, dynabeads were incubated with the appropriate wash buffer on a rotator for 5 min at 4°C, and then applied to a magnet for bead collection. A final wash was carried out in 1X TE buffer. After the serial washes, the beads were spun down at 4000 rpm for 30 s, and collected using a magnet. The proteins were eluted from the beads with elution buffer (50 mM Tris pH7.5, 10 mM EDTA, and 1% SDS), and then treated in pronase (at a final concentration 4 mg/ml in elution buffer) at 42°C for 2 hr and 65°C for 8 hr to digest proteins and reverse cross-linking. DNA (ChIP and INPUT) was purified by MiniElute PCR purification kit (QIAGEN, Cat # 28006) following the manufacturer's instructions. The amount of DNA in either ChIP or INPUT was determined by SYBR Green based quantitative-PCR using the Roche LightCycler 480 system following the

manufacturer's instructions. Two sets of primers were used: one annealing at 500 bp to the right of the HO cut site at the *MAT* locus (MATHO-ChIP), and the other for amplifying *SMC2* as a control (**Table 3**). The protein enrichment at MATHO-ChIP (ChIP / INPUT) was normalized to *SMC2* (ChIP / INPUT). Finally, the fold enrichment of a protein at MATHO-ChIP / *SMC2* (ChIP / INPUT) was normalized to the time point before galactose induction, following a previously published data processing method (Chen et al., 2008).

2.8. Serial dilution assay

Yeast cells were grown in the appropriate media until they reached mid-log phase. Cells were collected by centrifugation, and resuspended in sterile Millipore H_2O. Cells were 10 fold serially diluted in sterile H_2O and cell suspensions were transferred onto the appropriate agar plates by a sterile spotter with 6 x 8 rows of pins. Yeast plates were incubated in 30°C for 3 days before being photographed. For yeast drug sensitivity tests, cells were grown in YPD media, and spotted onto YPD agar plates supplemented with the indicated amount of drug. For yeast HO sensitivity tests, yeast strains with *GAL1HO* integrated at the *ade3* locus were grown in YPD to mid-log phase before being washed with YEP to remove glucose. Cells were resuspended in YEPR and allowed to grow at least 6 hr before being subjected to serial dilution assays. The "glucose" and "galactose" plates are YPD and YEP + 2% raffinose + 2% galactose, respectively. As for yeast strains with the *pGAL1-HO-URA3* plasmid, cells were grown up in SC-ura + 2% glucose media. Mid-log phase cells were washed three times to remove glucose, and resuspended in SC-ura + 2%

raffinose and allowed to grow at least 6 hr before being subjected to serial dilution assays. The "glucose" and "galactose" plates are SC-ura + 2% glucose and SC-ura + 2% raffinose + 2% galactose, respectively.

2.9. RNA extraction and quantitative RT-PCR

Yeast RNA was extracted using the MasterPure™ Yeast RNA Purification Kit (Epicentre, Cat # MPY03100) following the manufacturer's protocol. cDNA was synthesized using Transcriptor First Strand cDNA Synthesis Kit (Roche, Cat # 04896866001). Before reverse transcriptase was added to the reaction, a mixture of RNA and the anchored-oligo (dT) 18 primer was denatured by heating at 65°C for 10 min and then cooled on ice. The cDNA synthesis reaction was performed at 55°C for 30 min, and then placed at 85°C for 5 min to inactive the reverse transcriptase. A reaction without the reverse transcriptase was performed as a negative control. Quantitative PCR was then performed using LightCycler 480 SYBR Green 1 Master (Roche) on a LightCycler 480 instrument. The *YRA1* transcript level was normalized to *ACT1*, which was a control transcript. Primer sequences are listed in **Table 3**.

2.10. SILAC-chromatin affinity purification and mass spectrometry

Yeast strains (**Table 4**) were grown at 30°C in synthetic medium lacking tryptophan, supplemented with either isotopically heavy lysine ($^{13}C_6$) for control strains that are lacking *GALHO* in the genome, or isotopically light lysine ($^{12}C_6$) for DSB-inducible strains at 70 mg/L. Cells were grown in media supplemented with 2% glucose until they reached mid-log phase, and then washed with media without glucose before being resuspended in media containing 2% raffinose.

Cells were allowed to grow 12 hr in raffinose media to reach 0.5 OD_{600}/ml, before 2% galactose was added to induce HO expression. 2 hr after galactose induction, cells were cross-linked with formaldehyde at 1.25% final concentration for 5 min, and quenched with 0.125 M glycine for 5 min at room temperature. Afterwards, cells were collected by centrifugation and washed once with cold Millipore H_2O. Cells were resuspended in suspension buffer (20 mM HEPES pH 7.4, 1.2% polyvinylpyrrolidone) at 100 µl per gram of cell pellet, and then frozen in liquid nitrogen in a drop-wise manner. The frozen cells were stored at -80°C before being further processed. For each chromatin affinity purification (ChAP) analysis, 6 L of control and 6 L of experimental cultures were prepared, respectively. Chromatin affinity purification using IgG beads and subsequent mass spectrometry (ChAP-MS) analysis was performed following the procedures described previously (Byrum et al., 2015). Briefly, the proteins were identified by MaxQuant with the following parameters: precursor ion tolerance of 10 ppm, fragment ion tolerance of 0.65 Da, false discovery rate of 1%, database search using the UniProtKB restricted to *S. cerevisiae* (7802 entries), Lys6 heavy label, fixed modification of carbamidomethyl (C), variable modifications of oxidation (M), acetyl (protein N-term), mono-, di-, tri-methylation (K), acetylation (K), phosphorylation (ST) and ubiquintination (K). Intensities for each identified peptide were manually extracted and the percent light ratio was calculated as L_{avg} / (L_{avg} + H_{avg}). The unspecific threshold for each ChAP experiment was determined according to the averaged light lysine percentage of ribosomal

proteins. The ChAP-MS was performed in collaboration with Dr. Stephanie Byrum in Dr. Alan Tackett's lab (University of Arkansas for Medical Sciences).

2.11. Pulsed field gel electrophoresis (PFGE)

Mid-log phase yeast cells were treated with zeocin (final concentration at 60 µg/ml for *sit4Δ* (from BY4741 deletion library) or *YRA1* DAmP (from the DAmP library) strains, or 45 µg/ml for *def1Δ* (JSY568)) for 90 min before being washed and then resuspended in fresh YPD media. Cells that had been harvested at the indicated time points were subjected to genomic DNA preparation and embedded in an agarose plug, as described in the manual for the CHEF Genomics DNA plug kit (Bio-Rad, Cat # 170-3593). The plugs and the yeast chromosome DNA size standard (Bio-Rad, Cat # 170-3605) were loaded into the wells of a 1% agarose gel (Bio-Rad, Cat # 162-0137), which was soaked in 0.5 X TBE buffer for electrophoresis at 14°C for 24 hr in a Bio-Rad CHEF-DR III System coupled to a cooling module. The setting was initial switch time 60 s, final switch time 120 s, ran at 6 volts / cm, and at a 120° angle. The agarose gels were stained with SYBR safe and visualized on a ProteinSimple Imager (FluorChem E system).

2.12. Yeast genomic DNA isolation

The yeast cell pellets were resuspended in 200 µl extraction buffer (2% Triton X-100, 1% SDS, 100 mM NaCl, 10 mM Tris-HCl pH 8.0 and 1 mM EDTA pH 8.0). Afterwards, 200 µl of glass beads and 200 µl of phenol:chloroform:isoamyl alcohol (Ambion, Cat # AM9732; pH adjusted to ~7.9 with the provided Tris Alkaline buffer) were added to the cell suspension. Cells were disrupted by being vortexed rigorously in a bead beater for 5 min at 4°C,

and then subjected to centrifugation at 13,000 rpm for 10 min at RT. The aqueous layer on the top was carefully transferred to a fresh tube, and 1/10 volume of 3 M sodium acetate (pH 5.2) and 2.5 volumes of absolute ethanol were added. The mixture was spun at 13,000 rpm for 10 min at RT. The pellet containing the genomic DNA was carefully washed with 70% ethanol twice, and precipitated by centrifugation at 13,000 rpm for 5 min at RT. After the pellet was air dried, it was dissolved in Millipore H_2O.

2.13. Flow cytometry analysis

0.5 OD_{600} of yeast cells at mid-log phase were harvested by centrifugation and resuspended in 300 μl of 50 mM Tris pH7.9. 70% ethanol was added to the suspension in a drop-wise manner and incubated with rotation at RT for 1 h. The fixed cells were spun and resuspended in 500 μl of 50 mM Tris pH 7.9, and then subjected to brief sonication (50% duty, 20% output, 5 s). The pelleted cells were resuspended in 90 μl of 50 mM Tris (pH 7.9) and 10 μL of 10 mg/ml RNase A (Sigma, Cat # R6513). After the cells were incubated at 37°C for 2 hr, they were washed once with 1X PBS and collected by centrifugation. The pelleted cells were mixed with 100 μl of propidium iodide at a final concentration of 50 μg/ml in 1X PBS, and incubated with constant rotation at 4°C overnight. Cells were sonicated under the same setting as above, and diluted by adding 2 ml of 1X PBS. The cells were analyzed by a Becton Dickinson LSRII flow cytometer.

2.14. Yeast medium

Synthetic medium lacking lysine and tryptophan: To make 900 ml synthetic medium lacking lysine, tryptophan (Sc-lys-trp), 1.85 g drop-out mix of

synthetic minus lysine, tryptophan (US Biological, Cat # D9537-12), 1.7 g yeast nitrogen base, and 5 g ammonium sulfate were dissolved in Millipore H_2O to make a final volume of 900 ml. pH was adjusted to 5.8 with sodium hydroxide.

Synthetic medium lacking uracil: To make 900 ml synthetic medium lacking uracil (Sc-ura), 0.77 g drop-out mix of synthetic minus uracil (Clontech, Cat # 630416), 1.7 g yeast nitrogen base, and 5 g ammonium sulfate were dissolved in Millipore H_2O to make a final volume of 900 ml. pH was adjusted to 5.8 with sodium hydroxide.

YEP medium: To make 900 ml YEP, 10 g of yeast extract and 20 g peptone were dissolved in 900 ml Millipore H_2O.

10 X lactic acid stock solution: To make 100 ml, 37 g of 85% lactic acid was added in 80 ml ddH2O. After being adjusted to pH 5.5 with sodium hydroxide, the solution was brought up to 100 ml with Millipore H_2O.

YEP + lactate (YEPL) medium: YEP was supplemented with lactic acid, which was 10 times diluted from the 10 X stock solution.

The above yeast medium was sterilized by autoclave at 120°C for 20 min. For yeast liquid culture, either glucose (20% w/v stock, sterilized by autoclave) or raffinose (20% w/v stock, sterilized by filter) was added to the appropriate medium to make a final concentration of 2%. For GAL-HO induction, the 20% galactose (w/v) stock solution was filter sterilized.

Chapter 3

Proteomic identification of novel proteins and histone PTMs enriched at a single-copy site-specific chromosomal DSB

3.1. Introduction and rationale

Given the complexity of the DNA damage response (outlined in **Chapter 1**), we postulated that novel proteins and histone PTMs that contribute to DSB repair or the DNA damage-induced checkpoint response remain to be discovered. An interesting but challenging question we wanted to address is how various proteins and histone PTMs collectively regulate repair and DNA damage signaling at a defined DSB site. In particular, since HR is such a complex repair mechanism intimately integrated with the chromatin structure, we sought to develop an unbiased approach to identify proteins and histone PTMs specifically localizing to a DSB undergoing HR repair.

A great deal of our knowledge of the mechanism of HR repair has come from studying the DSB within the *MAT* locus on chromosome III induced by the sequence-specific homothallic (HO) switching endonuclease in *Saccharomyces cerevisiae* (Haber, 2012). The HO lesion is repaired by homologous recombination using homology at the hidden *MAT* right (*HMR*) or hidden *MAT* left (*HML*) locus, resulting in mating type switching (Klar et al., 1982). Accordingly, we established a method to isolate chromatin fragments adjacent to the endogenous single copy *MAT* locus containing the HO lesion*,* based on the previously developed Chromatin Affinity Purification with Mass Spectrometry (ChAP-MS) method by Byrum et al. (Byrum et al., 2015), in order to identify proteins and histone PTMs enriched at a site-specific DSB. We termed this method DSB-ChAP-MS. Proof of concept of the ChAP-MS method has been provided previously by its ability to detect enrichment of proteins and histone

PTMs at the single copy chromosomal yeast *GAL1* gene that were known to be involved in its transcriptional activation (Byrum et al., 2012). Our DSB-ChAP-MS method is aimed to identify new proteins and histone PTMs occurring at DSBs and are important for the DSB response. Since the molecular mechanisms and protein components and histone PTMs involved in the DSB response are quite conserved from yeast to mammals (**Chapter 1**), our study in yeast is expected to provide new insights into the DSB response relevant to higher eukaryotes.

3.2. Results

3.2.1. Establishment of the DSB-ChAP-MS method

To establish the method of DSB-ChAP-MS that allows identification of novel proteins and histone PTMs involved in the DNA damage response during HR, I took advantage of the HO endonuclease-induced DSB at the *MAT* locus in budding yeast *Saccharomyces cerevisiae* (hereafter shortened to yeast) (**Fig. 4A**). Fusion of the *HO* gene to the *GAL1* promoter (p*GAL1*) enables temporal control of DSB induction upon addition of galactose (Herskowitz and Jensen, 1991) (**Fig. 4B**). To allow affinity purification of chromatin fragments from the endogenous *MAT* locus bearing the HO lesion, I integrated two *LEXA* DNA binding sites (shortened to 2*LEXA*) adjacent to the *MAT* HO site and constitutively expressed the LexA DNA binding domain fused to Protein A (LexA-PrA) using the *pLexA-PrA* plasmid (**Fig. 4B**). The 2*LEXA* were inserted approximately 500 bp to the right of the HO site, in order to avoid the loss of the double-stranded LexA DNA binding site and therefore loss of LexA-PrA binding,

which would occur upon DNA end resection if the *LEXA* sites were closer to the

HO lesion.
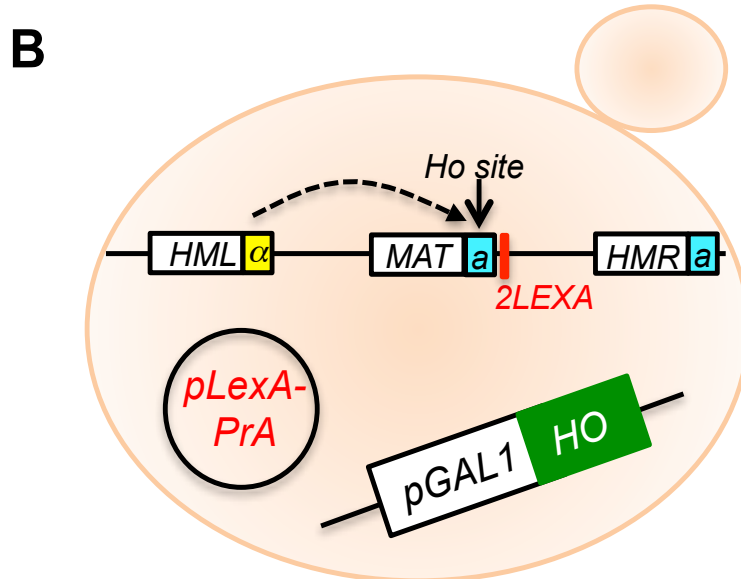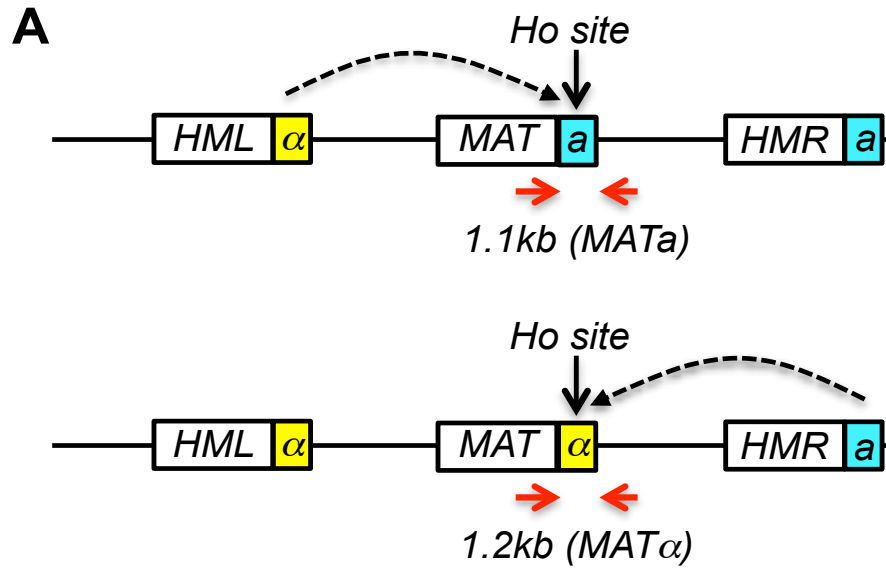
Figure 4. Construction of yeast strains used for the DSB-ChAP-MS method.

(A) Schematic of the yeast mating type loci. The HO endonuclease specifically creates a DSB at the HO site. Repair of the DSB is mediated by HR using the *HMR* or *HML* locus as the homologous donor. The primers shown in red can be used for PCR analysis for the dynamics of HO cutting/repair and the respective product sizes are indicated. **(B)** Schematic of the key elements in the yeast strains used for DSB-CHAP-MS. The HO gene is fused to a *GAL1* promoter that is galactose inducible. *2LEXA* DNA binding sites were integrated 500 bp downstream of the HO site, and a plasmid expressing LexA-Protein A fusion protein was introduced into the strains**.**

Using semi-quantitative multiplex PCR with the primers indicated in **Fig. 4A** to amplify over the HO site, an intact *MATa* locus yields a 1.1 kb PCR product, while repair using the homologous sequences from *HMLα* yields a 1.2 kb PCR product from the *MATα* locus. The control PCR product (*RAD27*) of about 1.4 kb is generated from another chromosome and serves for the purpose of normalization. Using this assay, we confirmed that the HO-induced DSB generation and repair in our DSB-ChAP-MS yeast strain (*MATa*) was very efficient (**Fig. 5A, B**). The reduction of the total relative *MAT* PCR product level below 100% reflects the presence of an HO-induced DSB at the *MAT* locus (**Fig. 5B**). The HO lesion was observed in approximately 80% of the cells 2 hr after galactose-mediated induction of the HO endonuclease. Glucose was added 2 hrs

after galactose addition to repress transcription of the HO gene to enable repair, and repair of approximately 90% of the *MAT* loci was apparent at the 7 hr time point (**Fig. 5B**). From the above analysis (**Fig. 5**), we selected the maximal time of DSB induction (2 hrs after galactose addition) for the DSB-ChAP-MS procedure.

A
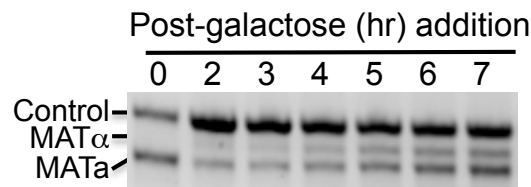
B
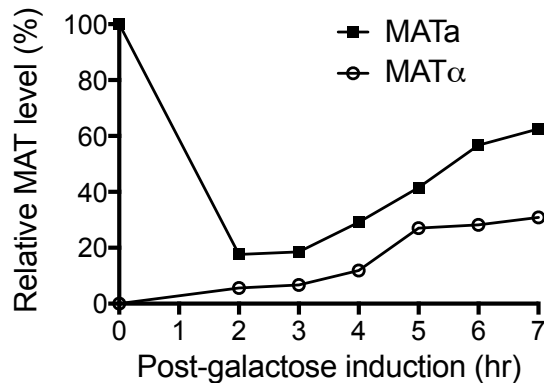
Figure 5. The HO cutting and repair is very efficient in the DSB-ChAP-MS yeast strain. (A) Analysis of HO cutting and repair in strain PWY012, using the primers shown in **Fig. 4A.** Galactose was added at time 0 and glucose at 2 hr. The control was a *RAD27* gene PCR product on a different chromosome. **(B)** Quantification of **A**, with *MAT* PCR products normalized to the control.

To measure enrichment of proteins and histone PTMs in the vicinity of the HO-induced DSB site by DSB-ChAP-MS, we used stable isotope labeling by amino acids in cell culture (SILAC)-based mass spectrometry (Byrum et al., 2012). Specificity of enrichment at the DSB was determined by purifying the same chromatin fragments from an isogenic yeast strain lacking the gene encoding HO endonuclease. In brief, we grew two yeast cultures: the culture with the inducible DSB undergoing repair (+DSB) was labeled with stable light lysine ($^{12}C_6$), and the culture with no HO endonuclease (-DSB) was labeled with stable heavy lysine ($^{13}C_6$) (**Fig. 6**). After formaldehyde cross-linking, the two populations of cells were mixed in a 1:1 ratio by weight. The chromatin was then sheared to approximately 1 kb fragments, and subjected to affinity purification of the LexA-PrA-bound chromatin fragments using IgG beads, as Byrum et al. performed previously (Byrum et al., 2012). The percentage of light lysine for each identified protein or histone PTM was determined by mass spectrometric analysis. An unspecific binding threshold was established based on the averaged percentage of light isotope of the ribosomal proteins that are considered to be contamination proteins during the purification. Proteins or histone PTMs enriched in the vicinity of a DSB are expected to have a percentage of light lysine above the unspecific threshold (**Fig. 6**).
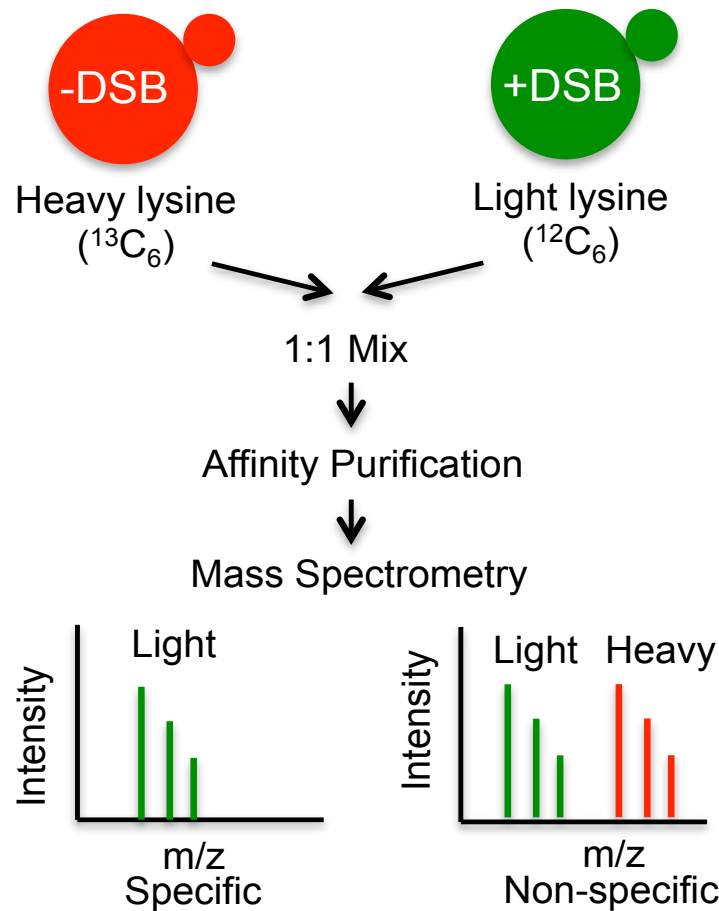
Figure 6. Schematic of SILAC based proteomic strategy for purifying proteins that specifically bind near the DSB. Two populations of cells were prepared: one without DSBs as a control was labeled with stable heavy lysine ($^{13}C_6$), and the other with the inducible DSB undergoing repair was labeled with stable light lysine ($^{12}C_6$). After formaldehyde cross-linking, the two cultures were mixed in a 1:1 ratio by weight, and further processed for affinity purification and mass spectrometric analysis. The strain lacking *pGAL1HO* is indicated by the red yeast cell "- DSB" while the green yeast cell "+ DSB" represents the isogenic yeast strain with *pGAL1HO*.

3.2.2. Proteomic identification of proteins enriched at a DSB undergoing repair using the DSB-ChAP-MS method

We performed DSB-ChAP-MS from cells that were wild type (WT) for DNA repair on two independent occasions, including more cells the second time (**Fig. 7**). We observed multiple protein bands upon coomassie staining of the ChAP samples (**Fig. 7**). The most prominent cellular protein in all ChAP samples was LexA-PrA (about 40 kDa), indicating the specificity of the purification procedure. In order to increase the proportion of cells that had the HO lesion at the time of the DSB-ChAP procedure, we also performed DSB-ChAP from strains that were deleted for the genes encoding the Rad52 and Rad54 homologous recombinational repair proteins (**Fig. 7**).

The non-specific threshold for each DSB-ChAP-MS experiment was established based on the averaged light lysine percentage of ribosomal proteins plus 1 standard deviation (SD), i.e., 53.86% + 4.23% (1 SD), 56.15% + 2.67% (1 SD), 46.38% + 1.54% (1 SD), and 50.74% + 1.86% (1 SD), for ChAP1, ChAP2, ChAP3 and ChAP4, respectively (**Table 6**).

We identified 18 proteins enriched at the HO lesion in our DSB-ChAP-MS analyses that were already known to function at DSB breaks (**Table 7**). Importantly, we did not find any known repair proteins to be depleted from the HO lesion in our DSB-ChAP-MS analyses, providing validation of our approach. In addition, we found 108 additional proteins enriched in the vicinity of the DSB that do not have clear roles in the DNA damage response to DSBs (**Appendix 1**).
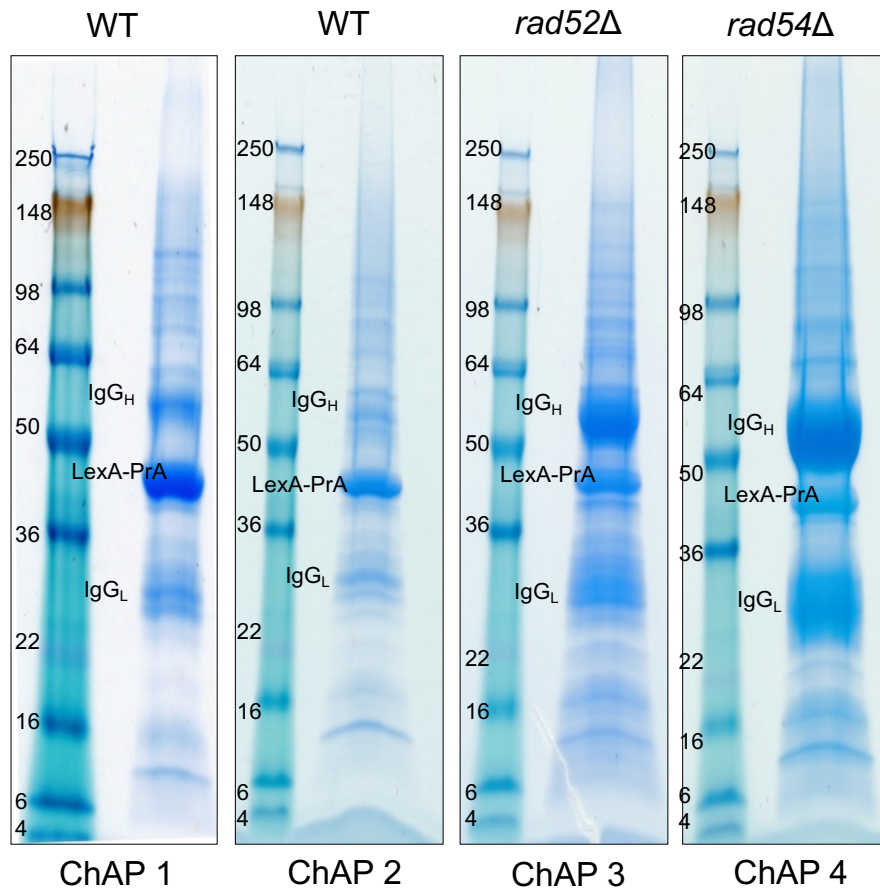
Figure 7. Coomassie-staining of the proteins from four different rounds of DSB-ChAP analysis resolved by SDS-PAGE. DSB-ChAP analyses labeled "WT" were performed from wild type yeast with strains PWY011 and PWY012. "*rad52Δ*" was performed from strains PWY013 and PWY014, and "*rad54Δ*" was performed from strains PWY017 and PWY018. The identities of the proteins were subsequently determined by mass spectrometric analyses of portions of the gels. This part of work was performed in collaboration with Drs. Stephanie Byrum and Alan Tackett from the University of Arkansas.

Among these 108 proteins, 81 were enriched at the DSB in the WT cells (**Fig. 8, Appendix 1**). Most of these proteins (77/81) were also enriched at the DSB in the *rad52Δ* cells while an additional 18 proteins were enriched at the DSB in the *rad52Δ* cells but not in the WT cells. Meanwhile only 55/81 proteins that were enriched at the DSB in the WT cells were also enriched at the DSB in the *rad54Δ* cells, while an additional 17 proteins were enriched at the DSB in the *rad54Δ* cells but not in WT cells. Meanwhile 8 proteins were enriched at the DSB in both the *rad52Δ* and *rad54Δ* cells, but not in the WT cells (**Fig. 8**). The proteins that were specifically enriched or depleted from the WT, *rad52Δ* or *rad54Δ* cells likely reflect their being recruited to the DSB at specific times in DSB repair.
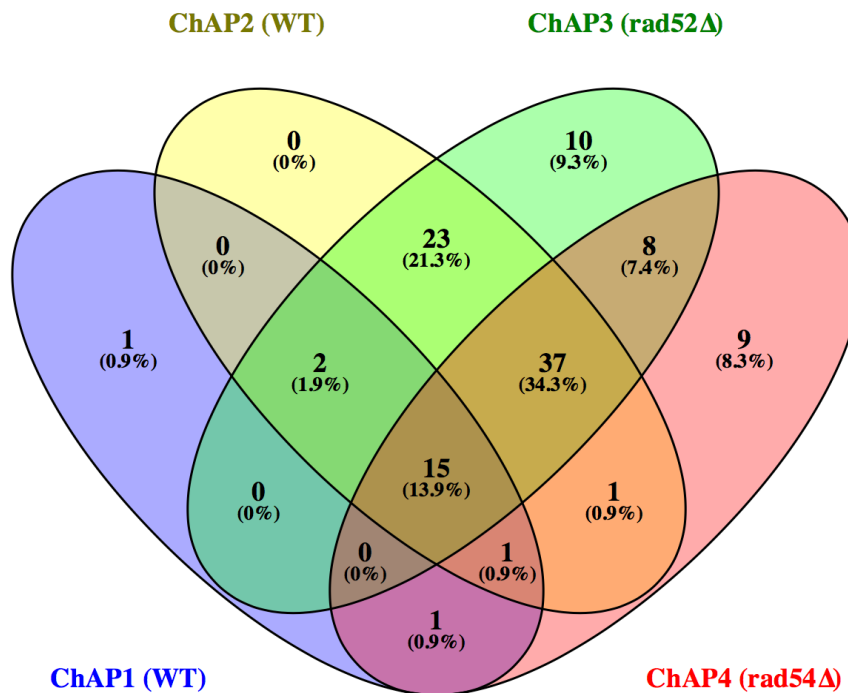
Figure 8. Venn diagram of the common proteins found to be enriched at the DSB for each DSB-ChAP-MS analysis, made using the Venny[2.1] software.

Each ChAP analysis identified 700-1200 total proteins as enriched, depleted or not changed at the DSB. Given that the yeast genome encodes over 3000 proteins, clearly our analysis is not able to detect all proteins, including some of the known DSB repair proteins. This may be because the undetectable proteins do not have lysine residues or are not abundant enough for detection.

ChAP #	Avg	SD	Avg - SD	Avg + SD	Avg - 2SD	Avg + 2SD
ChAP1	53.86%	4.23%	49.63%	58.09%	45.40%	62.32%
ChAP2	56.15%	2.67%	53.48%	58.82%	50.81%	61.49%
ChAP3	46.38%	1.54%	44.84%	47.92%	43.30%	49.46%
ChAP4	50.74%	1.86%	48.88%	52.60%	47.02%	54.46%

Table 6. The unspecific threshold for each DSB-ChAP-MS experiment. "Avg" indicates the averaged light lysine percentage of all the ribosomal proteins identified in the ChAP experiment. "SD" indicates standard deviation. The unspecific threshold stringency: Avg + 2SD > Avg + SD > Avg.

Gene	ChAP1	ChAP2	ChAP3	ChAP4
RFA1	47.20%	63.38%	51.80%	N.D
POL30	N.I	55.04%	48.67%	51.37%
BMH2	56.04%	57.46%	52.15%	60.61%
BMH1	52.69%	54.28%	51.40%	54.20%
PTC2	N.I	59.66%	N.I	N.I
PTC3	N.I	57.64%	N.D	N.I
POB3	N.I	N.D	67.52%	N.I
SPT16	N.D	67.97%	49.56%	51.15%
RVB1	N.D	66.95%	44.26%	N.I
RVB2	N.I	65.75%	58.61%	N.I
CDC28	N.I	60.58%	48.51%	N.I
GLC7	N.I	62.58%	50.05%	55.00%
IRC20	N.I	100.00%	98.00%	N.I
RAD10	N.I	N.D	N.I	N.I
MEC1	N.I	N.I	N.D	N.I
RSC8	N.I	N.D	N.D	N.I
RAD50	N.I	N.I	N.D	N.I
FUN30	N.I	N.I	N.I	N.D

Table 7. Summary of our identified proteins that have been previously implicated in the yeast DSB response. The light lysine percentage for each protein in each DSB-ChAP-MS experiment was listed. "N.I" indicates the protein was not Identified by our proteomic approach, "N.D" indicates the protein was identified by our proteomic approach but its light lysine percentage was not determined.

3.2.3. Proteomic identification of histone PTMs enriched at a DSB undergoing repair using the DSB-ChAP-MS method

Mass spectrometry of our four DSB-ChAP samples identified many histone PTMs with a high degree of enrichment at the DSB (**Table 8**). These included histone PTMs that were previously shown to be enriched upon DNA damage and / or functionally important for the DNA damage response (**Table 8**, Group 1), such as H3 K14, K18, K23 and K27 acetylation and H4 K5, K8, K12 and K16 acetylation (Tamburini and Tyler, 2005), H3 K56 acetylation (Maas et al., 2006; Masumoto et al., 2005) and H2B lysine 123 ubiquitination (Robzyk et al., 2000) . In addition to histone PTMs known to be involved in the DNA damage response, we also identified histone PTMs enriched in the vicinity of the DSB that have not previously been implicated in DSB repair (**Table 8**, Group 2). These included H2A K4ac K7ac, H2B K6ac K11ac, H2B K16ac, K17ac and H3 K122ac K125me. Given that these histone PTMs were enriched at DSBs with very high ratios of light lysine and given our success in identifying histone PTMs known to be involved in the DNA damage response (**Table 8**), we predict that these novel histone PTMs enriched at the DSB will also play roles during DSB repair.

Group #	Histone	PTM	ChAP1	ChAP2	ChAP3	ChAP4
Group 1	H3	K14ac	89.10%	55.60%	20.55%	86.28%
	H3	K18ac K23ac	57.70%	100.00%	88.87%	78.60%
	H3	K27ac	N.I	96.00%	N.I	95.70%
	H3	K56ac	N.I	60.20%	N.I	50.12%
	H4	K5ac K8ac	N.I	88.50%	N.I	N.I
	H4	K12ac k16ac	97.70%	100.00%	82.83%	92.27%
	H2B	K123ub	N.I	68.60%	N.I	42.19%
Group 2	H2A	K4ac K7ac	N.I	67.70%	N.I	45.45%
	H2B	K6ac K11ac	99.50%	N.I	N.I	N.I
	H2B	K16ac	100.00%	99.40%	82.47%	N.I
	H2B	K17ac	N.I	99.70%	N.I	N.I
	H3	K122ac K125me	95.80%	N.I	N.I	N.I

Table 8. List of histone PTMs identified as enriched at the HO-induced DSB site. The percentage of light lysine for a given histone PTM is shown (%). Group 1 includes histone PTMs known to be involved in the DSB response. Group 2 includes new histone PTMs identified as enriched at the HO-induced DSB site by our proteomic analyses. "N.I" indicates not identified.

3.2.4. Identification of novel DNA damage response proteins

From our DSB-ChAP-MS analyses, we selected 27 non-essential and 28 essential proteins for further characterization of their role in the DNA damage response. We focused on what we considered to be the most interesting proteins enriched in the vicinity of a DSB in at least one DSB-ChAP analysis that had nuclear localization and that had not clearly been implicated previously in DSB repair. First, we determined if the proteins enriched at DSBs were functionally important for the DNA damage response by measuring the contribution of the candidate genes to resistance to DSBs by serial dilution analysis on plates with and without the radiomimetic zeocin. We used isogenic yeast strains deleted for the non-essential candidate genes, or with hypomorphic DAmP (Decreased Abundance by mRNA Perturbation (Schuldiner et al., 2005) alleles of essential genes. Deletion of the non-essential candidate gene *CBF1, DEF1, NPL3, TOM1, PAT1, SIT4, GAS1, NPT1* or *PPZ1,* or bearing DAmP alleles of essential gene *SIS1, ACS2, YRA1, GUK1, PMI40* or *ERG13* conferred sensitivity to global DSBs induced by zeocin (**Fig. 9, Table 9**). As such, we characterize the proteins encoded by these genes as being novel DNA damage response proteins. The candidate proteins that were identified by the proteomic analyses as enriched at the DSBs, but whose mutation did not render sensitivity to DNA damage (**Fig. 9**), presumably perform non-essential and / or redundant functions during the DSB response.

A

YPD   10 µg/ml Zeocin

WT
rad52Δ
stm1Δ
glr1Δ
ymr226cΔ
kap123Δ
cbf1Δ
nap1Δ

WT
rad52Δ
def1Δ
sto1Δ
sod1Δ
apa1Δ
npl3Δ
rad23Δ

WT
rad52Δ
tom1Δ
pph21Δ
mlp1Δ

WT
rad52Δ
yhr127wΔ
ycr090cΔ
pat1Δ
sit4Δ
ufd2Δ

WT
rad52Δ
gas1Δ
fpr1Δ
npt1Δ
egd1Δ

WT
rad52Δ
cpr1Δ
mms2Δ
ppz1Δ

B

YPD   10 µg/ml Zeocin

WT
rad52Δ
cdc28
glc7
cdc48
top2
smt3
spt6

WT
rad52Δ
rsp5
yrb1
sis1
pwp1
acs2
cdc33

WT
rad52Δ
gna1
yra1
cdc39
cdc21
ncb2
hrt1

WT
rad52Δ
tub2
srp68
guk1
pmi40
arb1
dbp2

WT
rad52Δ
erg13
hem2
ret1
pse1
gln1
ess1

Figure 9. Mutants of multiple candidate genes whose protein products were enriched at the DSB show sensitivity to the radiomimetic zeocin. (A) Deletion mutants of non-essential candidate genes including *CBF1, DEF1, NPL3, TOM1, PAT1, SIT4, GAS1, NPT1* and *PPZ1* show sensitivity to zeocin. 10-fold serial dilutions on YPD or plates supplemented with zeocin. The *rad52Δ* mutant served as a positive control for DSB sensitivity. **(B)** DAmP mutants of essential candidate genes including *SIS1, ACS2, YRA1, GUK1, PMI40* and *ERG13* show sensitivity to zeocin. *CDC28* and *GLC7* DAmP mutant are positive controls for essential proteins identified adjacent to the HO lesion with known roles in the DNA damage response.

3.2.5. Some of the novel DNA damage response proteins are specific to the DSB response, while others are required for additional stress responses

To provide further mechanistic insight into the function of the novel DNA damage response proteins, we asked whether their role was specific to DSBs or general for multiple forms of stress. The other stresses tested include the ribonucleotide reductase inhibitor hydroxyurea (HU) that results in reduced DNA replication due to depleted nucleotide pools, the DNA alkylating agent methyl methane sulfonate (MMS), heat which activates the integrated stress response, the oxidative stress inducer hydrogen peroxide (H_2O_2), and the UV damage mimetic agent 4-Nitroquinoline 1-oxide (4-NQO).

We found that the candidate mutants exhibit distinct stress sensitivity profiles (**Fig. 10, Table 9**). For example, *def1Δ* is sensitive to all the stresses, whereas other mutants like *ACS2* DAmP, are only sensitive to the radiomimetic zeocin. These results indicate that while some of these novel DNA damage response proteins are involved specifically in the response to DSBs, others are part of a general DNA damage response, while others are more broadly involved in cellular stress responses.
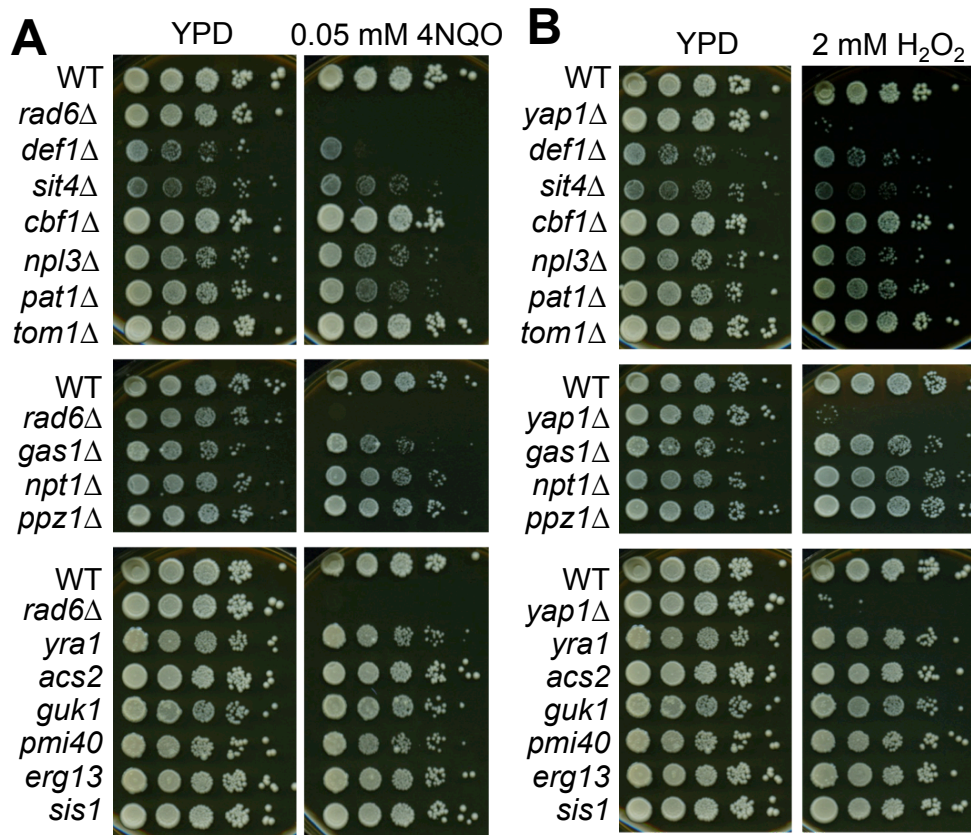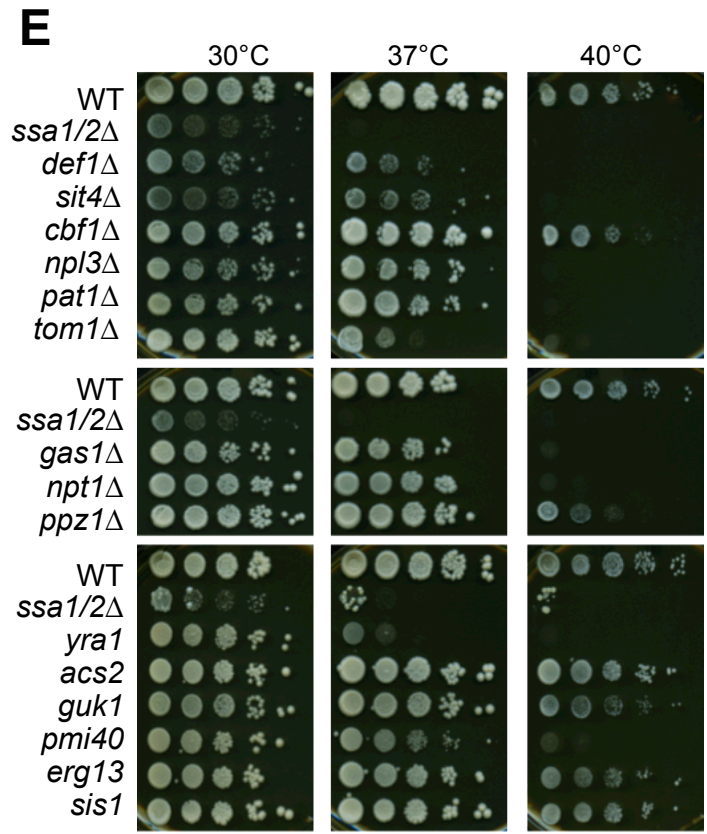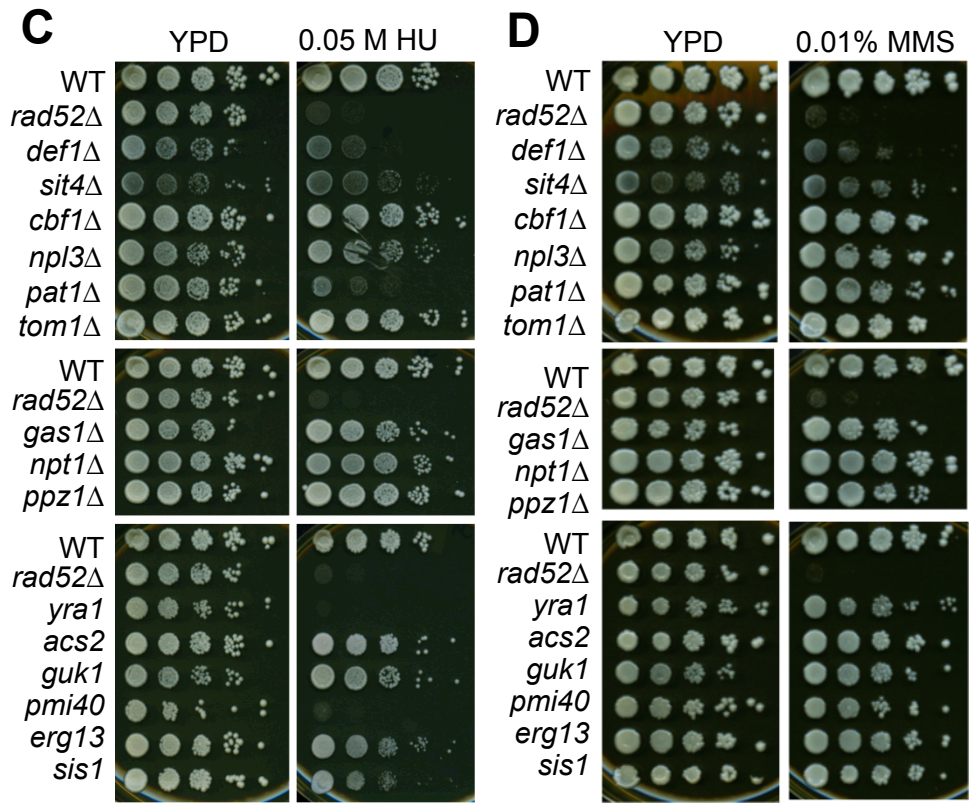
Figure 10. Profiling of the zeocin-sensitive candidate mutants' sensitivity to other types of stress. 10 fold serial dilution analyses of the indicated strains on plates with the indicated amounts of drugs or YPD as a control. **(A)** The *rad6Δ* mutant is a positive control for 4-NQO sensitivity. **(B)** The *yap1Δ* mutant is a positive control for H_2O_2 sensitivity. The *rad52Δ* is a positive control for **(C)** HU and **(D)** MMS sensitivity. **(E)** The *ssa1/2Δ* is a positive control for heat sensitivity.

To determine whether the novel DNA damage response proteins were sensitive to a single DSB in addition to global DNA damage, we induced a single DSB at the *MAT* locus. A *rad52Δ* mutant was included as a positive control for DNA damage sensitivity. Out of all the non-essential novel DNA damage response proteins, only Sit4 and Tom1 were required for resistance to the galactose-inducible HO endonuclease that cuts at the *MAT* locus (**Table 8, Fig. 11**). We were unable to measure the role of the essential novel DNA damage response proteins to repair of the HO lesion, since the available DAmP mutants are all derived from a *MATa* background that has a "*MAT-stuck*" mutation (Ray et al., 1991) preventing the HO endonuclease from cleaving the *MAT* locus.

71
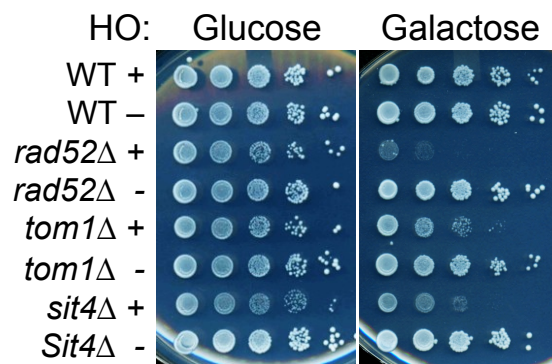
Figure 11. *SIT4* and *TOM1* **deletion mutants show sensitivity to constant induction of an HO-induced DSB at the** *MAT* **locus**. 10 fold serial dilution analysis of the indicated strains containing either an empty plasmid *pRS316* "-HO" or *pGAL-HO* "+ HO" on SC-uracil media containing either glucose or galactose. The strains were from the deletion library strains (MAT**α**).

Yeast Strain	Zeocin	4NQO	H_2O_2	HU	MMS	Heat	HO
def1Δ	++++	+++	+	++	++	++++	-
sit4Δ	+++	+	+++	-	-	++++	+
cbf1Δ	++	-	-	-	-	+	-
npl3Δ	++	+	+	-	-	++++	N.D.
pat1Δ	++	+	-	++	-	++++	-
tom1Δ	+	-	-	-	-	++++	+
gas1Δ	++++	++	-	-	-	++++	-
npt1Δ	+	-	-	-	-	++++	-
ppz1Δ	+	-	-	-	-	++	-
YRA1 DAmP	++++	-	-	++++	-	++++	N.D
ACS2 DAmP	++++	-	-	-	-	-	N.D
GUK1 DAmP	+++	-	-	-	-	-	N.D
PMI40 DAmP	+++	-	-	++++	-	+++	N.D
ERG13 DAmP	+++	-	-	-	-	-	N.D
SIS1 DAmP	+	-	-	+	-	-	N.D
Wild type	-	-	-	-	-	-	-

Table 9. **Summary of stress sensitivity of candidate yeast mutants.**

Sensitivity degree: ++++ > +++ > ++ > +; No sensitivity: -; N.D: not determined

3.2.6. The Ssa1/2 heat shock chaperones mediate the DNA damage response at elevated temperatures

We were surprised to find that so many of our mutants were sensitive to both zeocin and heat (**Table 9**). In mammals, hyperthermia causes defects in HR (Hunt et al., 2007; Kampinga and Konings, 1987; Pandita et al., 2009), but the molecular details are not clear and this has not been examined in yeast. Similarly, the mammalian Hsp70 proteins protect the genome against genomic instability after irradiation (Hunt et al., 2004), but their molecular role in DSB repair is unclear. Indeed, we found that resistance to zeocin is greatly reduced at elevated temperatures, suggesting that heat causes a defect in DSB repair. Furthermore, deletion of the genes encoding Hsp70 proteins in yeast, *SSA1/2*, greatly reduces yeast survival after exposure to radiomimetics, suggesting that they play an important role in the DNA damage response (**Fig. 12A**). Similarly, heat reduced viability about 100 fold upon induction of the HO endonuclease that generates a single break that is repaired by homologous recombination (**Fig. 12B, C**). This suggests that heat causes a defect in homologous recombination. Furthermore, in the single strand annealing strains, heat elevated the sensitivity to induction of an HO lesion that is repaired by single strand annealing, as did deletion of the *SSA1/2* genes (**Fig. 12C**). These results indicate that heat compromises an early stage in homologous recombination and that the heat shock chaperones Ssa1/2 promote early stages in homologous recombination prior to strand invasion.
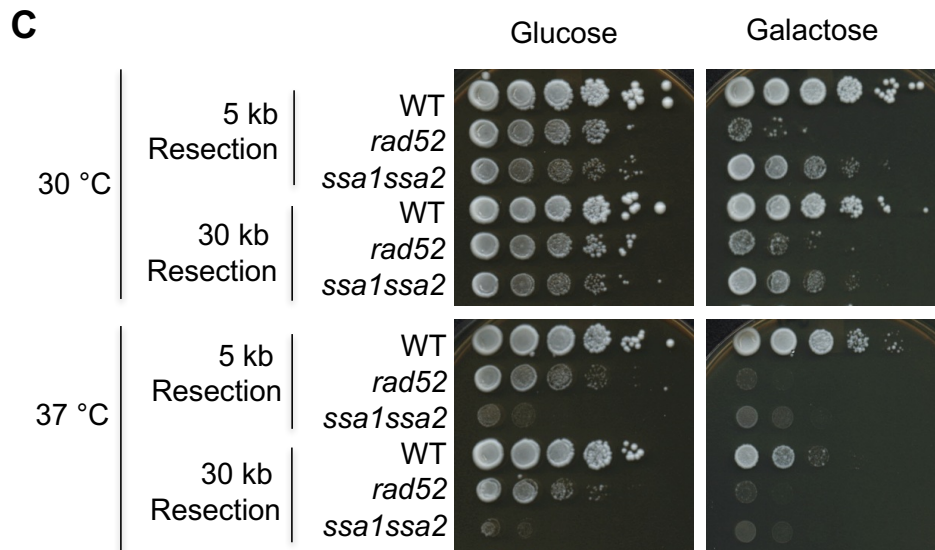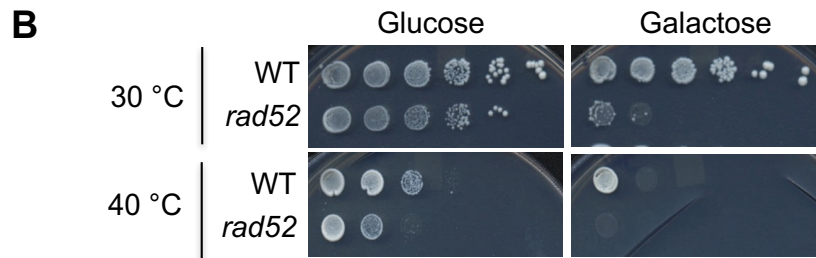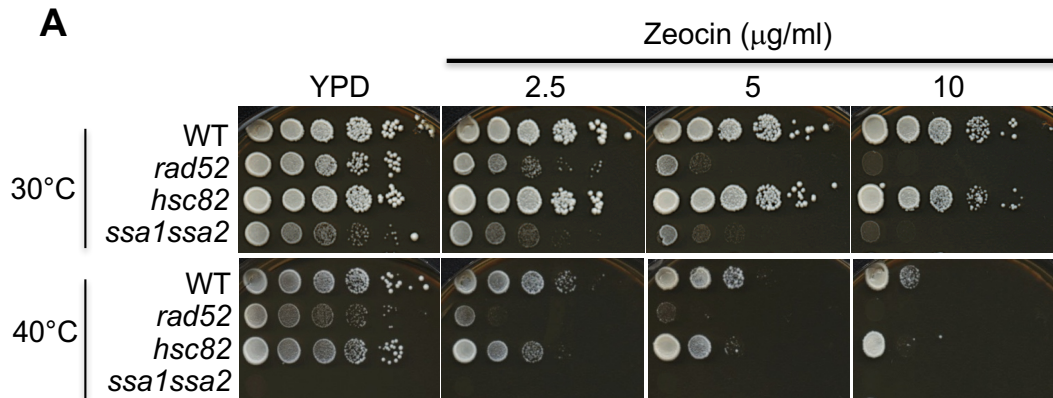
Figure 12. Hyperthermia or deletion of the yeast Hsp70 encoding genes (*SSA1/2*) leads to a defect in homologous recombination. (A) Yeast strains (BY4741) with the indicated gene deletions were 10 fold serially diluted and equal amounts plated onto control media (YPD) or media with the indicated amounts of zeocin. *HSC82* encodes the yeast Hsp90 protein, and appears to play little role in DSB repair. **(B)** Equal amounts of the WT (BY4742) or *rad52Δ* yeast strains carrying the *pGAL1-HO* gene, were 10 fold serially diluted onto media containing glucose or galactose at the indicated temperatures. **(C)** The 10 fold increased sensitivity of the *SSA1/2* deleted 30kb vs the 5kb resection strain to galactose indicates a defect in either resection or the DNA damage response. Similarly, there is a 100-fold increased sensitivity of the 30kb vs the 5kb strain to hyperthermia on galactose plates.

3.3. Discussion

Although the DSB repair pathways have been intensively studied, we still do not totally understand their interplay with transcription, the DNA damage checkpoint and their function in the chromatin context within the cell. Because the DSB response pathways are highly conserved from yeast to larger eukaryotes, dissecting the molecular mechanisms underlying the cellular response to DSBs in yeast facilitates our understanding of the complex regulatory events that occur in mammals. Accordingly, our DSB-ChAP-MS approach is the first method to enable proteomic analysis of histone modifications and proteins in the vicinity to a site-specific DSB. Using this approach, we have discovered several novel histone PTMs occurring at the site of DSB repair and novel proteins that are required for the different aspects of the DNA damage response.

We identified a few histone PTMs enriched around a yeast DSB that we are not aware of being previously implicated in the DSB response. These include H2A K4ac K7ac, H2B K6ac K11ac, H2B K16ac, K17ac and H3 K122ac K125me. Further validation of the roles of these histone PTMs during the DNA damage response awaits the development of specific antibodies. We also identified numerous histone PTMs enriched around DSBs that were previously known to impact the DSB repair process, including H3 K14ac, K18ac, K23ac, K27ac and K56ac, H4 K5ac, K8ac, K12ac and K16ac, and H2B K123ub. This validates our approach and indicates that these histone PTMs most likely function in a local manner to influence the DSB response. Interestingly, we did not identify H2A

phosphorylation on serine 129 (γH2A), a well-known DNA damage response, as either depleted, enriched or unchanged in our DSB-ChAP-MS procedure. i.e. it was not detectable. This is consistent with the reported very low levels of γH2A immediately 1-2 kb around a DSB (Shroff et al., 2004). We also identified a histone PTM that had not been reported before, to our knowledge. This was H3 K125 methylation. Given that ubiquitination of H3 K125 promotes chromatin assembly (Han et al., 2013), methylation of H3 K125 around a DSB would presumably block K125 ubiquitination, which would be desirable to promote chromatin disassembly during HR repair (Chen et al., 2008). It will be interesting to determine the function of this new histone PTM in general, and during the DSB response in the future.

Enriched at the DSB we found proteins known to be involved in the DNA damage response to DSBs (**Table 7**). Noteworthy, our analysis was far from saturating, as shown by the fact that identical sets of proteins were not identified by each DSB-ChAP-MS analysis and that some key DSB repair proteins (e.g. Rad52) were totally absent from the analysis. Additionally, the total number of detectable proteins in our DSB-ChAP-MS analyses was a fraction of the total number of cellular proteins.

We identified 108 proteins enriched around a DSB undergoing homologous recombination that have not been previously implicated in the DSB response (**Appendix 1**). Among the genes we tested, the non-essential *CBF1, DEF1, NPL3, TOM1, PAT1, SIT4, GAS1, NPT1* and *PPZ1* genes and the essential *SIS1, ACS2, YRA1, GUK1, PMI40* and *ERG13* genes promoted yeast

resistance to zeocin (**Fig. 9, Table 9**). Some of these genes have known functions in other molecular pathways that are not obviously related to DSB repair (**Table 10**). For example, *SIT4* encodes a protein phosphatase that is important for cell cycle regulation, and *YRA1* encodes an mRNA export protein. It would be interesting to determine how exactly these proteins impact the DNA damage response and why they localize to a DSB, as this may provide not only new insight into the repair process, but also may provide links between diverse pathways that were not previously appreciated.

It is noteworthy that some of the genes that we found to be important for resistance to zeocin have not been uncovered in previous screens for DNA damage resistance. The reason for this is unclear, but clearly indicates that our directed approach of performing the DSB-binding analysis to identify candidates for subsequent screening for DNA damage sensitivity was a more effective approach than just testing all 6000 yeast deletion strains.

It is interesting that many of the proteins that were localized to the DSB were not required for resistance to DNA damage. This may indicate that their function in DNA repair may be redundant with other proteins. Alternatively, these proteins may only play minor roles in DNA repair, or they may localize to breaks for reasons irrelevant to DNA repair. For example, the altered structure of DNA with released super-helical tension may provide a more favorable binding site for some proteins. It is also known that there are changes that occur around DSBs that are not required for repair *per se*. For example, transcription is completely inactivated and reactivated during DNA damage and repair respectively. It is

possible that some of the recruited proteins recruited to the DSB are involved in these responses to the break, but not for DNA repair *per se*. It is also possible that some of the proteins that were recruited to the break were background noise in the analysis.

Protein	Known Functions	Mammalian Homolog	References
Cbf1	A centromere-binding factor required for chromosome stability, regulates transcription	TBD	(Cai and Davis, 1990; Kuras et al., 1996; Mellor et al., 1990)
Def1	RNAPII and DNA polymerase δ degradation factor after UV irradiation, meiotic DNA processing, telomere maintenance	TBD	(Chen et al., 2005; Daraba et al., 2014; Jordan et al., 2007; Wilson et al., 2013)
Npl3	mRNA processing and export	SR family protein	(Bucheli and Buratowski, 2005; Dermody et al., 2008; Kress et al., 2008)
Tom1	E3 ubiquitin ligase, regulates transcription, involved in degradation of excess histones	Huwe1	(Saleh et al., 1998; Singh et al., 2009)
Pat1	mRNA processing, involved in maintenance of rDNA stability	PatL1/2	(Bonnerot et al., 2000; Scheller et al., 2007; Wang et al., 1999)
Sit4	A serine-threonine phosphatase, important for G1/S transition in cell cycle	PP6	(Angeles de la Torre-Ruiz et al., 2002; Sutton et al., 1991)
Gas1	Glucanosyltransferase, involved in transcriptional silencing	TBD	(Koch and Pillus, 2009)
Npt1	A NAD^+ synthesis enzyme, involved in chromatin silencing	NAPRT	(Smith et al., 2000)
Ppz1	Protein phosphatase Z, affects cell cycle	TBD	(Yenush et al., 2002)
Sis1	Hsp40 co-chaperone, regulates heat shock protein Hsp70 activity	Hsp40 family protein	(Lu and Cyr, 1998; Summers et al., 2013)

Acs2	Acetyl-coA synthetase, involved in histone acetylation, affects global transcription	ACS	(Takahashi et al., 2006)
Yra1	mRNA export factor, essential for viability	ALY	(Preker et al., 2002; Strasser and Hurt, 2000)
Guk1	Guanylate kinase, involved in nucleotide metabolism	GUK1	(Lecoq et al., 2000)
Pmi40	Phosphomannose isomerase, involved in protein glycosylation	PMI	(Smith et al., 1992)
Erg13	HMG-coA synthase, involved in sterol biosynthesis	HMGCS	(Parks et al., 1995)

Table 10. A list of known functions of the candidate proteins whose depletion lead to zeocin sensitivity.

Some of the gene products that were recruited to the DSB and promoted resistance to DSB-inducing agents, were additionally required for resistance to other forms of stress (**Fig. 10, Table 9**) indicating that they play general roles in the stress response. Further studies will be required to delineate their specific functions in the stress response in more detail.

Hyperthermia, the most efficient chemo- and radio-sensitizer known, is being used in clinical settings for inhibiting tumor growth (Bergs et al., 2007; Franken and Barendsen, 2014). Several laboratories have reported that hyperthermia inhibits DNA damage repair by homologous recombination in mammals (Hunt et al., 2007; Kampinga and Konings, 1987; Pandita et al., 2009). Driven by the finding that many of our novel DNA damage response proteins

were sensitive specifically to zeocin and heat, but not to other DNA damaging agents (**Table 9**), we investigated whether elevated temperature leads to defects in DSB repair, which would explain why our yeast mutants were hypersensitive to heat. Our data suggested this is also the case in yeast, since cells grown at elevated temperature are sensitive to zeocin and to induction of the HO lesion that is repaired by homologous recombination or single strand annealing (**Fig. 12**). Furthermore, cells lacking the yeast equivalents of human Hsp70 proteins, Ssa1 and Ssa2, were hypersensitive to the radiomimetic zeocin and induction of the HO lesion that is repaired by homologous recombination or single strand annealing (**Fig. 12**). Combined Ssa1/2 inactivation and heat caused an even greater increase in DNA damage sensitivity, suggesting that loss of Ssa1/2 and heat cause additive defects in homologous recombination. As such, we discovered a role for heat shock chaperones in homologous recombination, while elevated temperature reduces homologous recombination.

Chapter 4

Functional characterization of novel proteins

involved in the DSB response

4.1. Introduction and rationale

Given that we found by proteomic analyses that numerous candidate proteins localized to an HO-induced DSB (**Appendix 1**) and many of these candidate mutants were sensitive to the DSBs-inducing zeocin (**Fig. 9 and Table 9**), I sought to functionally characterize several of the candidate proteins of interest during the DSB response. Failure to grow following exposure to DNA damage can be for many reasons including failure to repair the DNA break or failure to inactivate the DNA damage checkpoint after DNA repair, via a process called checkpoint recovery (Lazzaro et al., 2009). Therefore, my strategy for functional characterization of novel proteins during the DSB response was to examine for a DSB repair defect and / or DNA damage-induced cell cycle checkpoint defect in yeast strains deleted for the candidate non-essential genes, or in a hypomorphic mutant, if the gene was essential. Also, I examined whether candidate proteins localized to a DSB site by Chromatin Immunoprecipitation (ChIP) assay. I prioritized the analysis on candidate gene products that showed the most significant enrichment at the DSB, had mammalian counterparts / homologs, had known protein modifying activity, or may provide novel links to other interesting processes such as transcription, DNA replication and cell cycle regulation. Accordingly, I selected four candidate proteins Tom1, Sit4, Def1 and Yra1 for further mechanistic studies during the DSB response.

TOM1 encodes a HECT E3 ligase that has a human homolog called Huwe1. It has been shown that *TOM1* is involved in transcriptional regulation through histone acetylation (Saleh et al., 1998) and degradation of excess

histone proteins (Singh et al., 2009). *SIT4* encodes a protein phosphatase with similarity to human PP6 (Stefansson and Brautigan, 2006), and is important for the G_1 to S phase transition during the cell cycle (Sutton et al., 1991). *DEF1* promotes transcription-coupled repair (TCR) via its role in degradation of RNA polymerase II (RNA pol II) at genes with single-strand DNA lesions (Woudstra et al., 2002). *YRA1* encodes an essential protein involved in mRNA export (Strasser and Hurt, 2000), which is homologus to human ALY. Intriguingly, Tom1, Sit4, Def1 and Yra1 were all identified by our DSB-ChAP-MS analyses as enriched at a DSB, and their mutants were all sensitive to chemically induced DSBs (**Fig. 9, Table 9**). In addition, *tom1Δ* and *sit4Δ* were sensitive to the induction of an HO lesion at the *MAT* locus (**Fig. 11, Table 9**). However, none of these four candidate proteins have been directly implicated in the DSB response previously.

4.2. Results

4.2.1. The DNA damage sensitivity of *tom1Δ* does not reflect a role of Tom1 in either DSB repair or checkpoint recovery

First, I asked whether the *tom1Δ* mutant strain could repair the HO lesion at *MAT* using the same PCR assay used in **Fig. 5**. As shown in **Fig. 13**, the HO cutting and repair in the *tom1Δ* mutant was identical to that occurring in its isogenic WT strain, indicating that Tom1 is not required for repair of the HO lesion at *MAT*.

Figure 13. *TOM1* is not required for repairing an HO-induced DSB at *MAT*. HO cutting and repair assay as described in **Fig. 5A.** The strains were the same as those used in **Fig. 11**.

To investigate whether Tom1 was involved in checkpoint recovery after DSB repair, I used another inducible HO system where the DSB is repaired by single-strand annealing (SSA). In the SSA system (Vaze et al., 2002), the HO lesion is induced between two repeated sequences spaced 30 kb apart on the same chromosome, in the YMV002 strain. Repair of this HO lesion occurs following 30 kb of resection and this temporal delay necessitates activation of the DNA damage checkpoint. As such, sensitivity to induction of the HO lesion that is repaired by SSA, in a strain that is otherwise proficient for DSB repair, is indicative of delayed DNA damage checkpoint recovery. I found that the *tom1Δ* mutant was not significantly more sensitive than the WT cells to induction of the HO lesion that is repaired by SSA (**Fig. 14**), suggesting that Tom1 does not play a role in checkpoint recovery.

SSA 30 kb resection strains
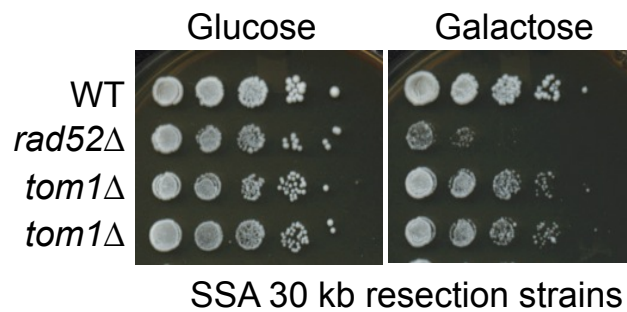
Figure 14. Deletion of *TOM1* does not confer yeast sensitivity to the induction of a single DSB that is repaired by SSA. The deletions were made in the YMV002 strain background with a single HO site that is repaired by SSA, requiring 30 kb of DNA resection.

In addition, the dephosphorylation kinetics of the effector checkpoint kinase Rad53 (Pellicioli et al., 2001), indicative of inactivation of the DNA damage checkpoint, was identical in the *tom1Δ* mutant and WT strain following transient treatment with zeocin (**Fig. 15**). Taken together, these data indicate that the sensitivity of *tom1* mutants to global DSBs and a DSB at the *MAT* locus does not reflect a role for Tom1 in either repair of DSBs or DNA damage checkpoint recovery.
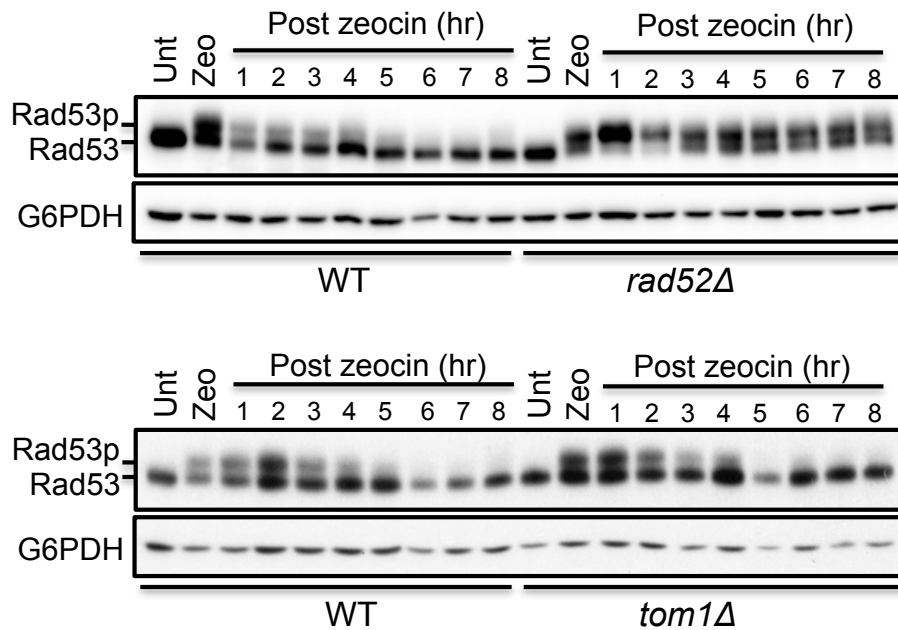
Figure 15. Deletion of *TOM1* does not affect dephosphorylation of Rad53 after removal of zeocin. The strains were from the deletion library strain (MATa). The *rad52Δ* served as a positive control for persistent Rad53 phosphorylation after release from a transient DSB-inducing treatment with zeocin. "Unt" and "Zeo" indicate untreated and zeocin-treated, respectively. "Post zeocin (hr)" indicates hours after washing out the zeocin. G6PDH served as a loading control.

4.2.2. Sit4 is required for recovery from the DNA damage checkpoint after DSB repair

To determine whether the sensitivity of the *sit4Δ* mutant to expression of the HO endonuclease (**Fig. 11**) was due to a defect in DSB repair, I examined repair of the HO lesion at *MAT* directly. While the *sit4Δ* mutant showed a delay in the appearance of DNA repair products, this was due to the delayed and reduced HO cutting observed in the *sit4Δ* mutant (**Fig. 16**).
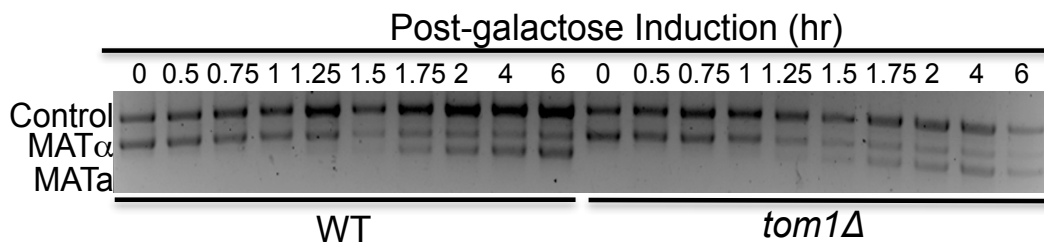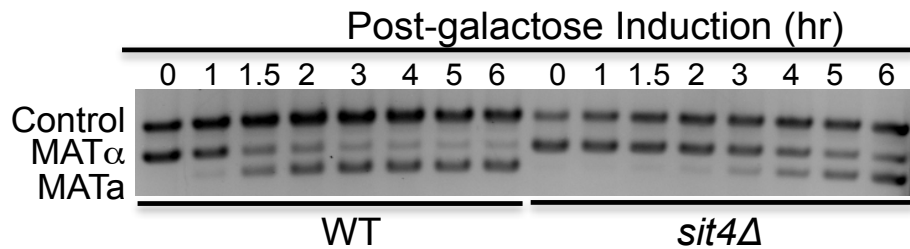

Figure 16. *SIT4* **is not required for repairing an HO-induced DSB at** *MAT* **locus.** HO cutting and repair assay as described in **Fig. 5A.** The strains were the same as used in **Fig. 11**.

Given that Sit4 was not required for DNA repair *per se*, I wanted to test if it played a role in checkpoint recovery. Unfortunately, I was unable to delete *SIT4* in the SSA strain background. This is probably because of the synthetic lethal interaction of *SIT4* with *SSD1* (Suppressor of *SIT4* deletion) (Sutton et al., 1991), which may bear mutation in the strain background used to create the SSA strain (Vaze et al., 2002). However, when we tested the kinetics of dephosphorylation of Rad53 following a transient zeocin treatment, it was apparent that dephosphorylation in the *sit4Δ* strain was approximately 4 hours slower than in the WT strain (**Fig. 17**).
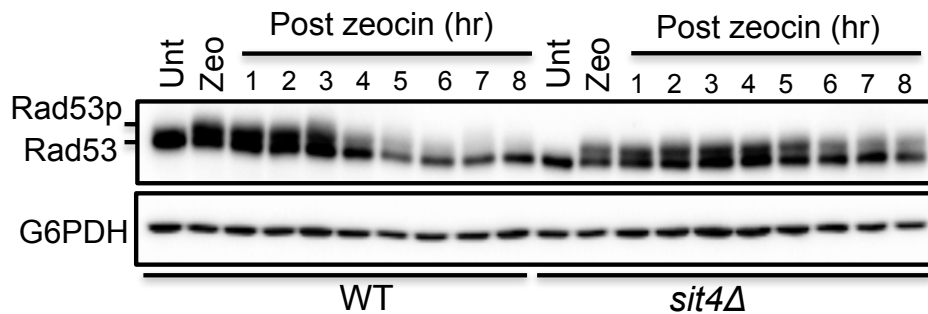
Figure 17. Deletion of *SIT4* delays dephosphorylation of Rad53 after removal of zeocin. The strains were from the deletion library strain (*MAT*a). "Unt" and "Zeo" indicate untreated and zeocin-treated, respectively. "Post zeocin (hr)" indicates hours after release from zeocin. G6PDH served as a loading control. The procedures were the same as described in **Fig. 15**.

Importantly, the *sit4Δ* mutant did not have a detectable defect in DSB repair following induction of global DNA damage with zeocin, as reflected in the smearing of the chromosomal bands resolved by pulsed field gel electrophoresis (PFGE) and their subsequent restoration after washing out zeocin (**Fig. 18).** Taken together, these data suggest that localization of Sit4 to DSBs reflects its role in checkpoint recovery after DSB repair.
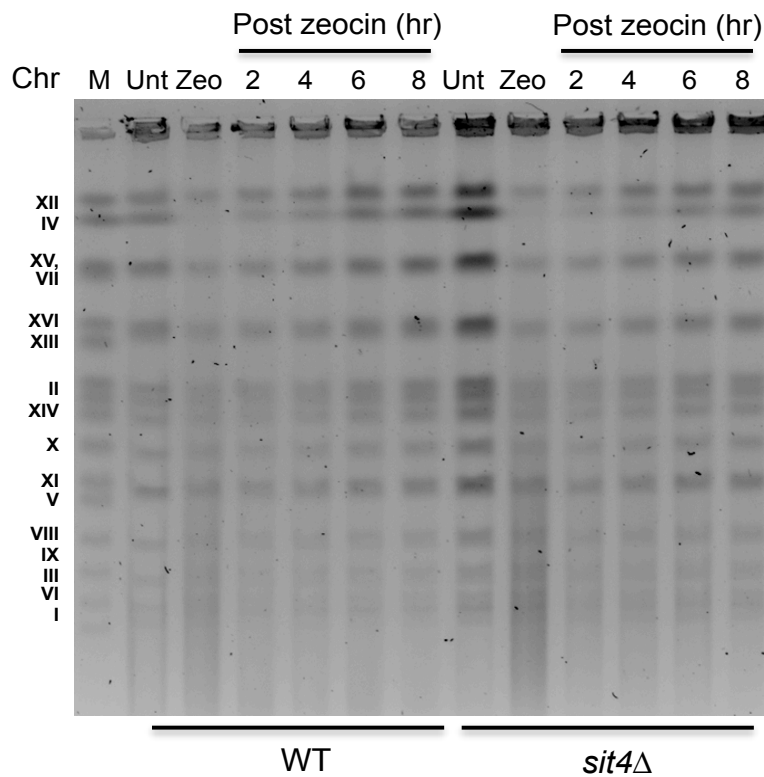
Figure 18. A *sitΔ* mutant is proficient for repairing chromosomal damage induced by zeocin. Chromosomal DNA was subjected to pulsed field gel electrophoresis (PFGE), from the indicated time points after removal of zeocin. "Unt" indicates untreated, "Zeo" indicates a sample before washing out zeocin, "M" indicates yeast chromosomal DNA marker, and "Post zeocin (hr)" indicates hours after release from zeocin.

4.2.3. Def1 promotes repair of global DSBs, independent of any putative role in degrading RNA polymerase II

Although *def1Δ* is sensitive to a broad range of DNA damaging agents (**Table 9**) and Def1 was found by our proteomic analyses as enriched at the HO lesion at *MAT*, I found deletion of *DEF1* did not particularly confer yeast sensitivity to induction of the HO lesion at *MAT* (**Fig. 19A**) beyond having slow growth, which was also seen on glucose plates. In agreement, there was no kinetic difference in the repair of the HO lesion at *MAT,* even though less DSBs were induced in the *def1Δ* mutant (**Fig. 19B, C**).

Given that Def1 promoted TCR via its role in degrading RNA pol II (Woudstra et al., 2002) and given that it has been reported that RNA pol II is degraded after DSB damage (Jha and Strahl, 2014), I asked whether Def1 specifically promotes DSB repair within highly-transcribed genes. To do this, I generated a strain (PWY081) where the HO site was inserted into the 3' end of the highly transcribed *ADH1* gene while the HO site at the *MAT* locus was deleted. I found that the *def1Δ* mutant version of this strain (PWY099) was not sensitive to induction of an HO lesion within the *ADH1* gene (**Fig. 19D**).

In addition, to determine whether Def1 plays any role in DSB repair by single-strand annealing (SSA) or DNA damage checkpoint recovery, I deleted *DEF1* in the 30 kb SSA strain YMV002. However, deletion of *DEF1* led to severe growth defects in YMV002 (**Fig. 19E, F**), thus preventing me from using this *def1Δ* mutant strain for further assays.

A Glucose Galactose

WT
rad52Δ
def1Δ

B Post-galactose (hr)   Post-galactose (hr)

0 0.5 1 2 3 4 5 6   0 0.5 1 2 3 4 5 6

Control
MATα
MATa

WT   *def1Δ*

C

WT MATa
WT MATα

def1Δ MATa
def1Δ MATα

Relative MAT level (%)
Post-galactose induction (hr)

D

HO site at:

Zeocin (μg/ml)

Glucose   Galactose   2.5   5

ADH1 WT
        def1Δ
        def1Δ

MAT   WT
        rad52Δ

92
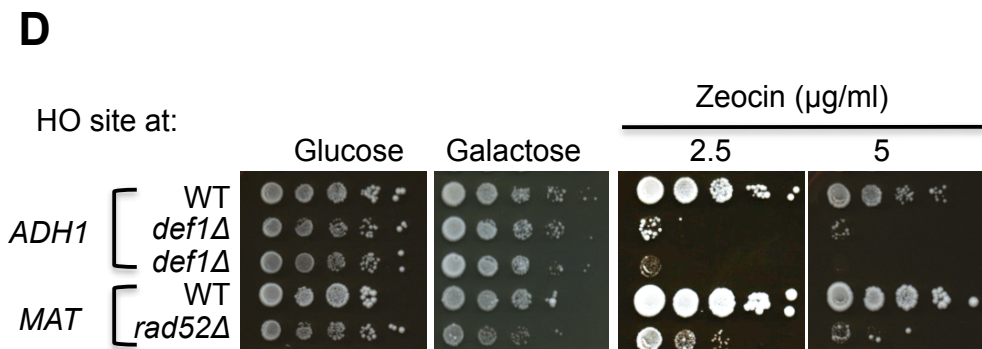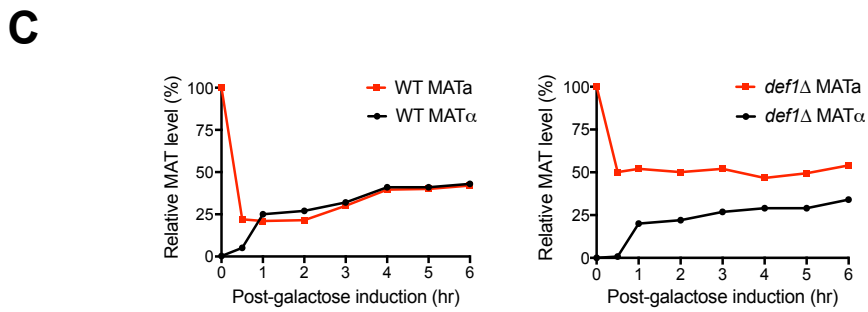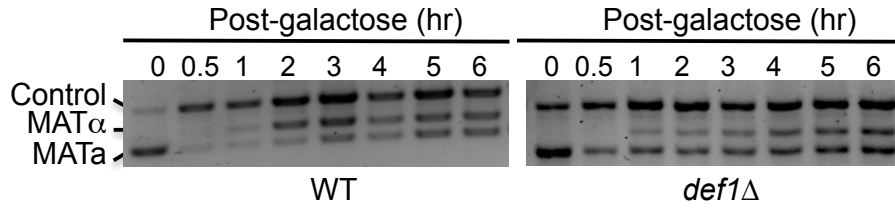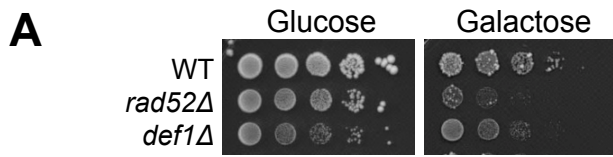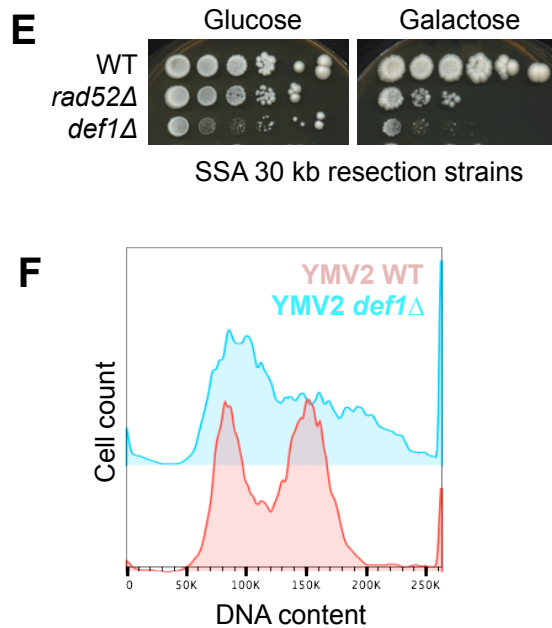
Figure 19. Deletion of *DEF1* confers yeast little (if any) sensitivity to site-specific HO lesions. (A) Deletion of *DEF1* confers yeast little (if any) sensitivity to an HO-induced DSB at *MAT*, measured using strain BAT009, BKD0665 and PWY033. **(B)** *DEF1* null mutant does not have a DSB repair defect at the *MAT* locus, using the assay shown in **Fig. 5A** and the strains used in **A**. **(C)** Quantification of **B**, with *MAT* PCR products normalized to the control *RAD27*. **(D)** Deletion of *DEF1* confers no sensitivity to an HO lesion within the *ADH1* gene, measured by 10 fold serial dilutions using strains PWY081, PWY099, BAT009 and BKD0665 onto plates containing the indicated supplements. The "*MAT rad52∆*" strain (BKD0665) served as a positive control for galactose and zeocin sensitivity. **(E, F)** *def1∆* in the 30 kb SSA strain YMV2 background shows growth defect. **(E)** The *def1∆* strain grows slowly on both glucose and galactose plates, and thus inconclusive for its HO sensitivity. **(F)** The *def1∆* strain without any treatment shows a severe G2/M defect detected by flow cytometry analysis.

Furthermore, in my hands, I found that deletion of *DEF1* had no effect on RNA pol II levels following treatment with global DSBs-generating agents (**Fig. 20**). As such, Def1 is not required for the repair of a unique HO lesion by HR, yet promotes resistance to global DSB induction.
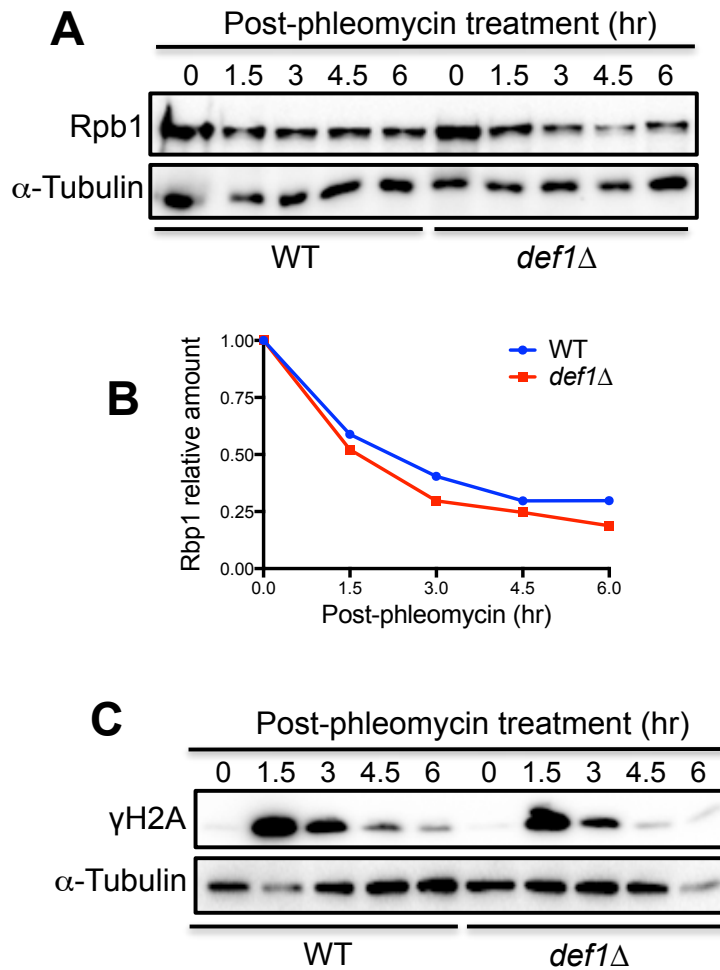
Figure 20. ***DEF1* null mutant is proficient for reducing Rpb1 levels in response to the radiomimetic phleomycin**. **(A)** The *def1Δ* (W303 background) strain reduces Rbp1 level similarly to its isogenic WT after constant phleomycin treatment. **(B)** Quantification of the gels in **A** shows that the *def1Δ* strain does not have a defect in reducing Rpb1 levels relative to the **α**-tubulin control after phleomycin treatment. **(C)** The *def1Δ* mutant shows the same H2A S129 phosphorylation dynamics as WT in response to phleomycin. Protein samples were the same as in **A**.

Given that we did not detect a role for Def1 in either repair or survival after induction of a single DSB made by the HO endonuclease (**Fig. 19**), we focused on its role in resistance to global DSBs. To be noted, I found that the *def1Δ* strain from the deletion library in the BY4741 strain background had four times as much DNA content as its isogenic WT strain by flow cytometry analysis (**Fig. 21A**). This result was confirmed by using another two isolates of *def1Δ* that I received from the deletion collection library from other labs. By comparison, a *def1Δ* strain (JSY568) in the W303 strain background has similar DNA content as the WT W303 strain (**Fig. 21A**). Although *DEF1* deleted mutants made from different parental strain backgrounds have unexpected different DNA content profiles, both of them are very sensitive to DNA damaging agents (**Fig. 21B**). Given that there may be additional unknown mutation(s) in the *def1Δ* from the *MATa* deletion library accounting for its increased DNA content, the strains I used for **Fig. 20** and **22** were all derived from W303.
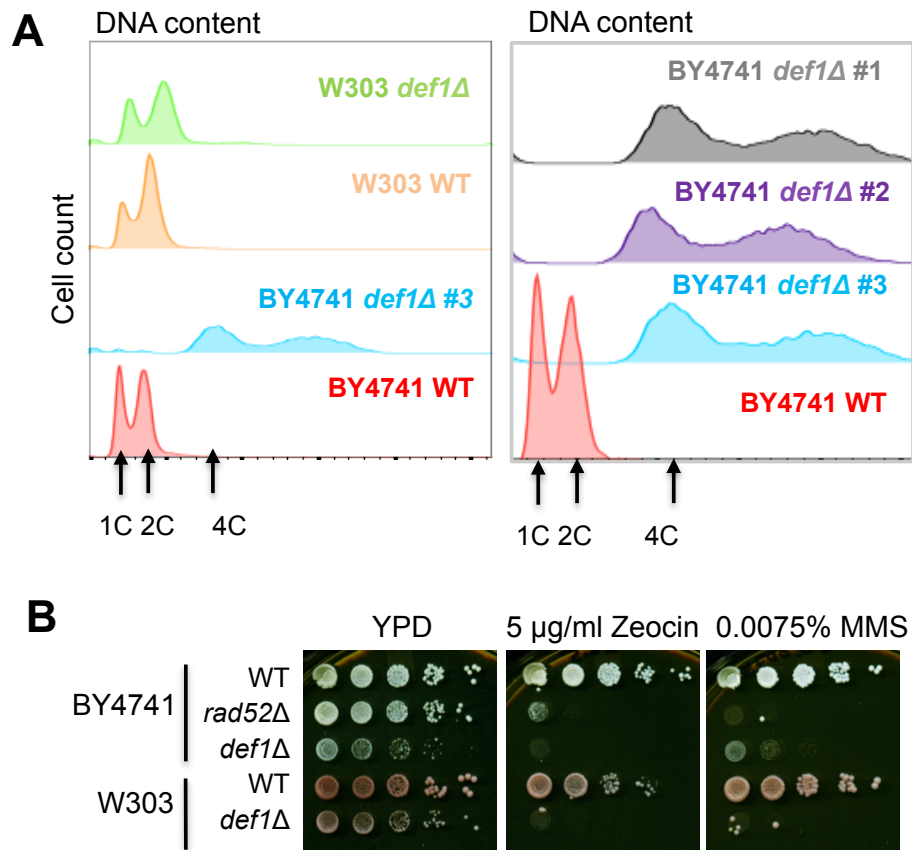
Figure 21. The *def1Δ* strain from the deletion library (*MATa*) has four times as much DNA content as its isogenic WT, while a W303 *def1Δ* strain has similar DNA content to W303 WT. (A) Flow cytometry analyses to determine the DNA content in exponentially growing yeast cells using strains W303, JSY568 (W303 *def1Δ*), BY4741 (WT), and three different isolates (from three labs, indicated by #1, #2 and #3) of the *def1Δ* from the yeast deletion library (BY4741) **(B)** Both W303 *def1Δ* and BY4741 *def1Δ* strains are sensitive to DNA damaging agents. 10 fold serial dilution analysis was performed using the same strains as in (**A**). The *rad52Δ* strain was a positive control for DNA damage sensitivity.

To determine whether Def1 is required for global DSB repair, I examined the ability of the *def1Δ* mutant yeast to repair global DNA damage by PFGE analysis of yeast chromosomes. As shown in **Fig. 22A**, while the chromosomes became intact in WT cells by about 5-6 hr after recovering from zeocin treatment, the restoration of the intact chromosomal profiles was delayed in *def1Δ* mutant cells. In agreement with the delayed repair of zeocin-induced DSBs in the *def1Δ* mutant cells (**Fig. 22A**), I found dephosphorylation of Rad53 was delayed several hours after removal of zeocin in the *def1Δ* mutant cells compared to wild type cells (**Fig. 22B, C**). Taken together, these data indicate that Def1 plays a role in global DSB repair.
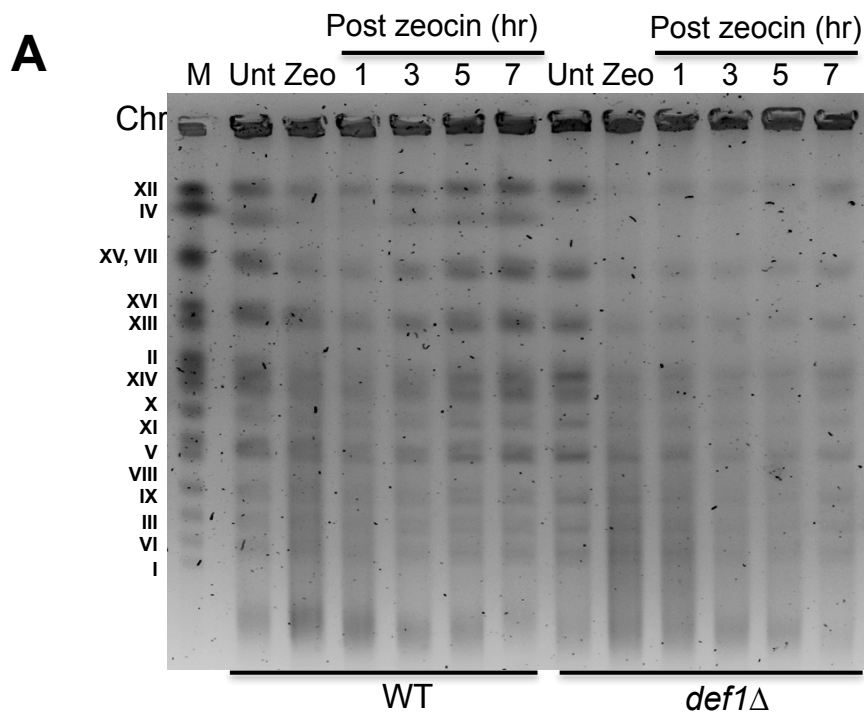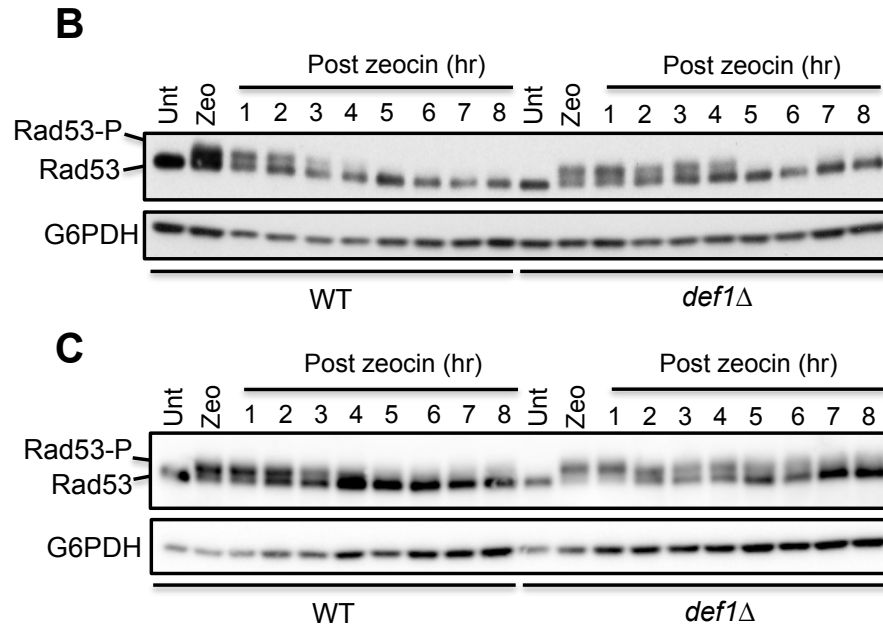
Figure 22. Def1 promotes DSB repair following radiomimetic treatment. **(A)** Deletion of *DEF1* leads to a defect in chromosomal repair after release from transient zeocin treatment. Chromosomal DNA was subjected to PFGE as in **Fig. 18**, from the indicated time points after removal of zeocin. (**B. C)** The *def1Δ* strain has a delay in dephosphorylating Rad53 after release from zeocin. Yeast cells were subjected to a 30 min zeocin treatment at a final concentration of **(B)** 15 µg/ml and **(C)** 30 µg/ml, and then washed to remove zeocin. The other procedures were the same as described in **Fig. 15**. All yeast strains were of W303 background. "Unt" indicates untreated, "Zeo" indicates a sample before washing out zeocin, "M" indicates yeast chromosomal DNA marker, and "Post zeocin (hr)" indicates hours after release from zeocin.

4.2.4. Yra1 plays a major role in DSB repair

As mentioned earlier, I found Yra1 localizing to DSBs by proteomic analyses and a DAmP hypomorph of *YRA1* was highly sensitive to zeocin (**Fig. 9**). Unfortunately, I was unable to generate an HO endonuclease-induced DSB at the *MAT* locus in the *YRA1* DAmP (*MATa*) mutant, due to the presence of HO uncuttable mutation at the *MATa* locus. Therefore, in order to determine whether Yra1 was required for repairing the HO-induced DSB at the *MAT* locus, I used an *YRA1* anchor-away (AA) mutant (Haruki et al., 2008). First of all, I confirmed that rapamycin-mediated Yra1 depletion from the nucleus confers the *YRA1* AA strain sensitivity to zeocin (**Fig. 23**). Interestingly, zeocin sensitivity of the *YRA1* AA mutant upon Yra1 depletion induced by rapamycin was apparent in asynchronous cultures, and was more apparent in cells synchronized in G_1 phase with alpha factor or in G_2/M phase with nocodazole (**Fig. 23**).
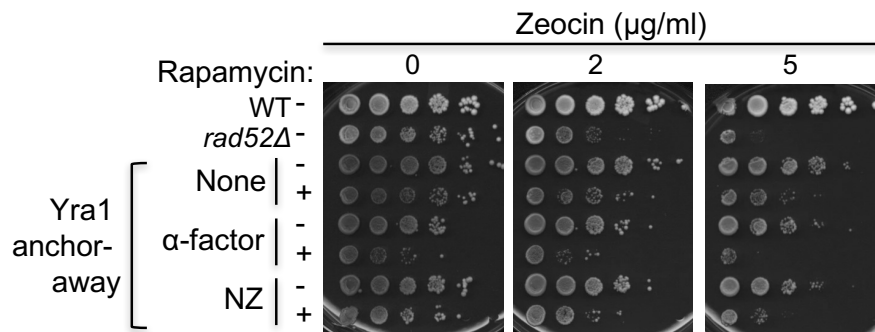
Figure 23. The *Yra1* anchor-away strain is sensitive to zeocin after rapamycin induction. Serial dilution analyses of yeast Yra1 anchor-away strain YCL003 on plates with the indicated amount of zeocin. The *rad52Δ* strain (from the MATa deletion library) is a positive control for zeocin sensitivity. "-" and "+" indicate whether rapamycin was added, and "NZ" indicates nocodazole.

Next, I examined the kinetics of the repair of the HO lesion at the *MAT* locus using a *YRA1* AA mutant. As shown in **Fig. 24**, I found no difference of HO cutting and repair dynamics upon depletion of Yra1.
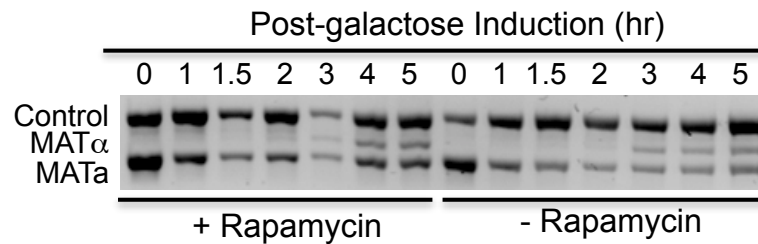
Figure 24. Depletion of Yra1 from the nucleus did not result in a defect in repairing the HO-induced DSB at the *MAT* locus. HO cutting and repair assay as described in **Fig. 5A,** using Yra1 anchor-away strain YCL003 transformed with *pGAL1HO* plasmids.

Given that there was no apparent role for Yra1 in repair of the HO lesion (**Fig. 24**), yet the *YRA1* DAmP hypomorph had striking sensitivity to zeocin (**Fig. 9**), I examined the global DSB repair using the *YRA1* DAmP mutant more closely. When examining the repair of global DSBs by PFGE analysis, I observed a striking defect in DSB repair in the *YRA1* hypomorph (**Fig. 25A**), where the allele leads to an 8-fold reduction in mRNA levels (**Fig. 25D**). Consistent with a central role of Yra1 in DSB repair, the DNA damage checkpoint was persistently maintained in an active state following washing out the zeocin (**Fig. 25B**). These data uncover a profound role for Yra1 in global DSB repair.

A

Post zeocin (hr)   Post zeocin (hr)

M Unt Zeo 2 4 6 8 Unt Zeo 2 4 6 8

Chr

XII
IV

XV, VII

XVI
XIII

II
XIV
X
XI
V
VIII
IX
III
VI
I

WT   *YRA1* DAmP

B

Post zeocin (hr)   Post zeocin (hr)

Unt Zeo 1 2 3 4 5 6 7 8 9   Unt Zeo 1 2 3 4 5 6 7 8 9

Rad53-P
Rad53

G6PDH

WT   *YRA1* DAmP

C

WT *YRA1* DAmP

Rad51

Gapdh

Rad51/Gapdh (%)   100   40

D

Relative *YRA1* mRNA level

1.0

0.5

0.0
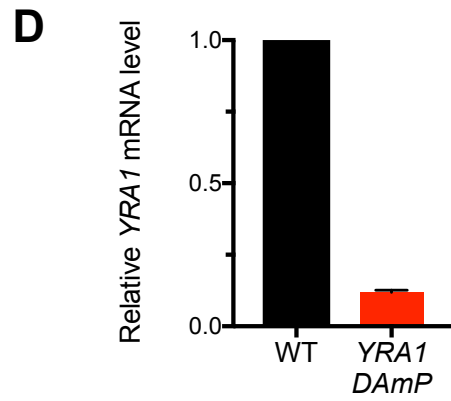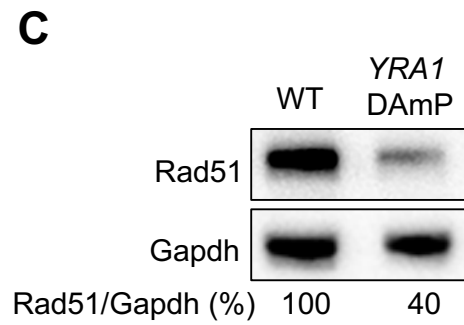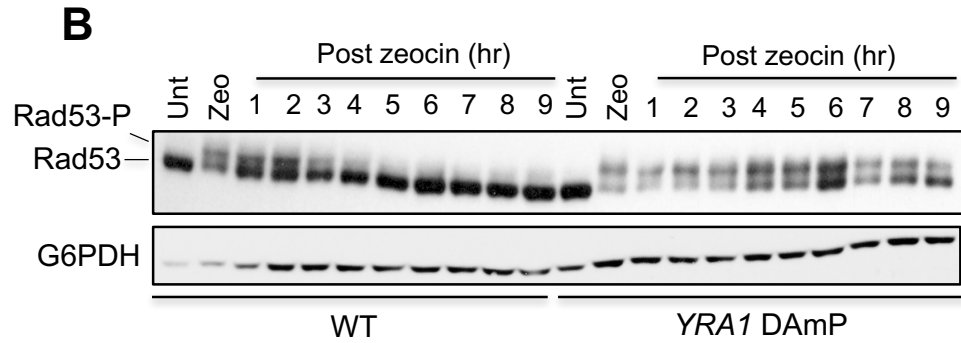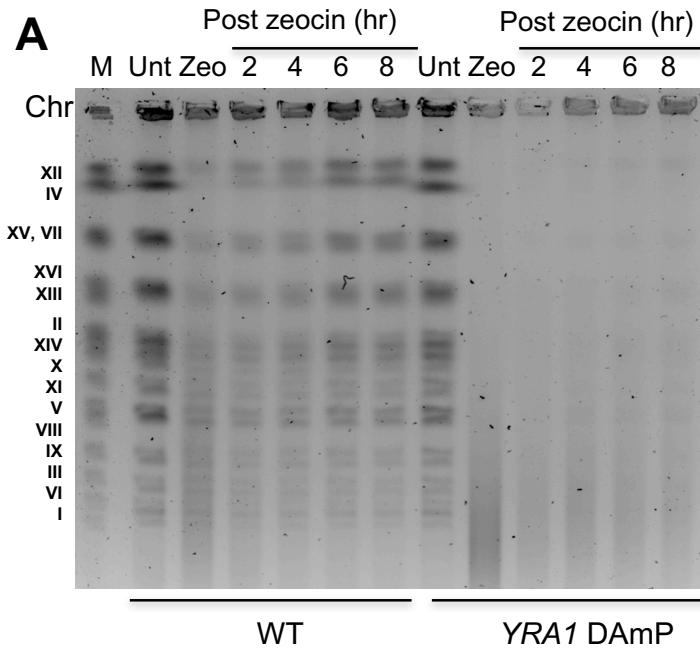
WT   *YRA1* DAmP

Figure 25. *YRA1* **DAmP mutant is defective in global DSB repair. (A)** *YRA1* DAmP mutant is defective in restoration of intact chromosomes after a transient zeocin treatment. The PFGE analysis as described in **Fig. 18**. **(B)** *YRA1* DAmP mutant is defective in dephosphorylating Rad53 after release from a transient zeocin treatment. Procedures as described in **Fig. 15**. **(C)** The Rad51 protein level in the *YRA1* DAmP mutant was about 40% as much as that in the WT strain. Whole cell extract was subjected to western blot analysis for Rad51 normalized to Gapdh as a control. **(D)** *YRA1* mRNA transcript level was reduced about 8 fold in *YRA1* DAmP mutant compared to its isogenic WT. Exponentially growing yeast cells either WT or *YRA1* DAmP were subjected to extraction for RNA, which was reverse transcribed and subject to quantitative PCR analysis for *YRA1* transcript level normalized to *ACT1* as a control.

Interestingly, we found that the Rad51 protein level in the *YRA1* DAmP strain was reduced to about 40% compared to its isogenic wild type strain (**Fig. 25C**), which probably contributed to the DSB repair defect in the *YRA1* DAmP mutant since Rad51 is of critical importance to DSB repair by homologous recombination. This data also suggested that the role of Yra1 in regulating *RAD51* mRNA export and thereby affecting Rad51 protein expression is conserved from yeast to human, given that ALY as the human counterpart of Yra1 is required for *RAD51* mRNA export (Wickramasinghe et al., 2013).

4.2.5. ChIP assays failed to show enrichment of Tom1, Sit4, Def1 or Yra1 at an HO-induced DSB at *MAT*

As mentioned earlier, the candidate proteins Tom1, Sit4, Def1 and Yra1 that I selected for functional characterization were identified as enriched at an HO lesion by our DSB-ChAP-MS analyses. Next, I asked whether I could detect their enrichment at the *MAT* HO site by chromatin immunoprecipitation assays. Under the conditions I used in **Fig. 26A-D**, none of these four candidate proteins show enrichment at the *MAT* HO site undergoing repair. The primers I used for quantitative PCR analyses following chromatin immunoprecipitation were about 500 bp to the right of the HO site (**Table 3**). As ChIP positive controls, Rad51 and Exo1 were both detected to be enriched at the HO site (**Fig. 26E, F**).

Although I did not find enrichment of the candidate proteins close to the *MAT* HO site, it is possible that mass spectrometric analysis is more sensitive in detecting a DSB binding protein than the ChIP assay. Also, an alternative explanation for the discrepancy between proteomic analyses and ChIP assays is that the existence of a protein at a DSB site may be too dynamic to be detected as significantly enriched by ChIP using a few discrete time points over the time course and a specific PCR region that I used. In addition, the ChIP / Input value of a protein at a certain time point was normalized to the value at the time point before DSB induction. Therefore, no enrichment of a protein at the DSB site may just mean there is no increase in the amount of the protein binding to the tested region after DSB generation as detected by ChIP, thereby it is still possible the protein plays an important role at the tested region during the DSB response.
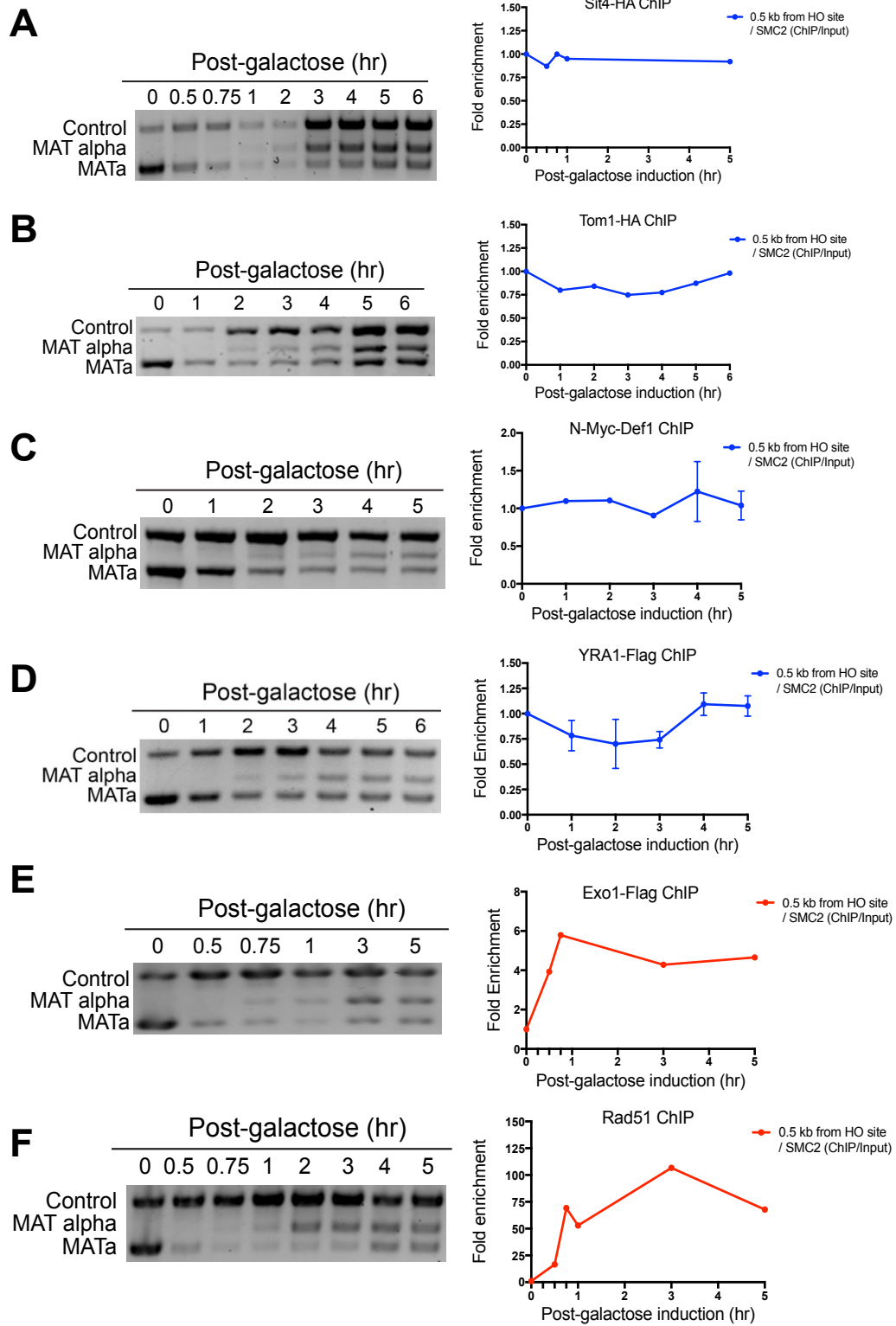
Figure 26. Sit4, Tom1, Yra1 and Def1 were not detected as enriched at the HO-induced DSB site at *MAT* by ChIP assays. The left panels represent the PCR analyses for the HO cutting and repair dynamics of the time course where the corresponding ChIP samples were collected. **(A)** Sit4 was not detected as enriched at the HO site by ChIP using HA antibody. Strain PWY035 was induced for HO cutting and repair in YEPL media. **(B)** Tom1 was not detected as enriched at the HO site by ChIP using HA antibody. Strain PWY042 was induced for HO cutting and repair in YEPR media. **(C)** Def1 was not detected as enriched at the HO site by ChIP using Myc antibody. Strain PWY106 was induced for HO cutting and repair in SC-uracil media supplemented with 2% raffinose. **(D)** Yra1 was not detected as enriched at the HO site by ChIP using Flag antibody. Strain PWY095 was induced for HO cutting and repair in YEPR media. **(E)** A ChIP positive control using Flag antibody to immunoprecipitate Flag-tagged Exo1, which is known to be enriched at a DSB site and difficult to ChIP with. Strain PWY066 was used in **E**. **(F)** A ChIP positive control using an antibody directly targeting Rad51, which is known to be highly enriched at a DSB site. Strain BAT009 was used in **F**. Glucose was added at 0.75 hr post-galactose treatment in **A, E** and **F**, whereas at 2 hr post-galactose induction in **B, C** and **D**, to repress the HO endonuclease expression and allow repair. ChIP primers were about 500 bp distal to the right of the HO site at *MAT*. At each time point, the ChIP / Input value of the 500 bp region was normalized to a control *SMC2* region. Fold enrichment of each time point represents the ratio of the normalized ChIP / Input value of the time point versus that of the 0 hr time point (i.e. prior to galactose induction).

4.3. Discussion

In this chapter, I sought to characterize the potential functions of four candidate proteins that we identified as enriched at a site-specific chromosomal DSB undergoing repair by the DSB-ChAP-MS method that I described in **Chapter 3**. These proteins include Sit4, Tom1, Def1 and Yra1, which I prioritized for mechanistic studies, due to their protein modifying activity, association with other processes such as transcription, cell cycle regulation and RNA metabolism, or having a known human homolog.

I found that Sit4 is not required for DSB repair *per se*, but is required for checkpoint recovery (**Fig. 16, 17 and 18**). Yeast Sit4 is similar to the human phosphatase PP6 (Bastians and Ponstingl, 1996). In agreement with our proposed role for yeast Sit4 in checkpoint recovery, depletion of PP6 in human cells increases sensitivity to ionizing radiation (IR), due to a delay in release from the DSB-induced checkpoint, and caused a defect in dephosphorylation of γH2AX after IR (Douglas et al., 2010). Also, there is no apparent DSB repair defect in PP6-depleted cells, consistent with the lack of a DSB repair defect in yeast *sit4* mutants (**Fig. 16 and 18**). PP6 interacts with the NHEJ protein DNA-PK leading to a model in which DNA-PK helps to recruit PP6 to DSBs to facilitate the dephosphorylation of γH2AX and checkpoint recovery (Douglas et al., 2010). Our findings on Sit4 suggest that the role of this family of phosphatases during checkpoint recovery is conserved from yeast to human. Mechanistically, how are Sit4 and PP6 promoting checkpoint recovery? It is unlikely that Sit4 dephosphorylates γH2A directly given that Pph3 is already known to be the γH2A

phosphatase (Keogh et al., 2006). Moreover, the persistent Rad53 phosphorylation in the *sit4* mutant suggests that Rad53 dephosphorylation is also influenced by Sit4. Noteworthy, Mec1, the yeast counterpart of human ATR, is responsible for phosphorylating both H2A and Rad53 during the DNA damage response, making inactivation of Mec1 a likely indirect target of Sit4, in order to enable dephosphorylation of Rad53 and γH2A. A role for Sit4 in down-regulating Mec1 activity after DSB repair to promote checkpoint recovery could potentially occur through Pkc1. The rationale for this suggestion is because Pkc1 is required for Mec1 and Tel1 (the yeast equivalent of human ATM) activity in response to DSBs (Soriano-Carot et al., 2014). Likewise, the human counterpart of Pkc1, PKCδ, is also required for activation of the DNA integrity checkpoint PKCδ (Soriano-Carot et al., 2014). Meanwhile, Sit4 is required for down-regulating Pkc1 activity, seeing as Pkc1 is overactive in the absence of Sit4 (Angeles de la Torre-Ruiz et al., 2002). As such, Sit4 could potentially dephosphorylate Pkc1, which is known to be phosphorylated by the central checkpoint kinases potentially in a feedback loop (Soriano-Carot et al., 2014), in order to inactivate Mec1 to allow checkpoint recovery.

I found that although the Tom1 HECT3 E3 ligase protein localizes to DSBs, it is not required for checkpoint recovery or DSB repair (**Fig. 13 and 15**). As such, it seems likely that the excess histones that are present in the *tom1* mutant (Singh et al., 2009) themselves are toxic to the cells following DNA damage, leading to the growth defect observed with zeocin and upon induction of a single HO lesion at *MAT*. Intriguingly, I did not observe sensitivity to the HO

lesion induced in the SSA assay system in the *tom1* mutant (**Fig. 14**). However, one key difference between the HO at *MAT* and the HO induced in the SSA system is that the HO at *MAT* is continuously cleaved and repaired over the three days of growth, while the HO in the SSA system is cut and repaired only once. The fact that Tom1 was recruited to the DSB breaks suggests that the role of Tom1 in ubiquitinating histones actually occurs at the site of repair (Singh et al., 2009), perhaps promoting degradation of the histones as they are removed from around the DSB lesion.

As for Def1, I found it promotes the repair of global DSBs. *DEF1* was shown to be required for the degradation of the largest subunit of RNA pol II in response to UV damage (Woudstra et al., 2002). In this way, RNA pol II is removed from genes within the UV-induced DNA lesions to enable their transcription-coupled repair. Another known degradation target of *DEF1* is Pol3, which is the catalytic subunit of DNA polymerase δ (Daraba et al., 2014). This Def1 mediated Pol3 degradation after UV irradiation was suggested to allow the translesion synthesis polymerase to take the place of Pol3 and mediate error-prone DNA synthesis (Daraba et al., 2014). However, I do not consider that Def1 is promoting DSB repair via a role in degradation of RNA pol II after DSB damage, because I did not observe any role for Def1 in repair of a DSB within a highly transcribed gene (**Fig. 19D**). Furthermore, I observed no effect of *DEF1* deletion on RNA pol II levels after inducing DSB damage (**Fig. 20**). Perhaps the role of Def1 in repair of global DSBs is related to the function of *DEF1* in telomere maintenance (Chen et al., 2005), which depends on the NHEJ machinery. As such, a role for Def1

related to NHEJ could explain the lack of any HR defects during HO repair in the *def1* mutant, while there was reduced global DSB repair (**Fig. 22A**). Def1 has also been implicated in meiotic DNA processing (Jordan et al., 2007) which could be related to the role we found for Def1 during DSB repair. We propose that Def1 coordinates the degradation of specific protein(s) (yet to be determined) at the site of DSB repair that promotes efficient DSB repair.

YRA1 mutants were as sensitive to DSBs as yeast lacking the central Rad52 repair protein (**Fig. 9 and 23**). Furthermore, this sensitivity to DSBs was due to a profound defect in DSB repair *per se* (**Fig. 25**). Yra1 is an mRNA export protein, and is essential for yeast viability (Portman et al., 1997; Preker et al., 2002). Strikingly, overexpression of Yra1 leads to the accumulation of DSBs and genomic instability (Gavalda et al., 2016). Mechanistically, the overexpressed Yra1 and associated mRNAs remain on chromatin, leading to the accumulation of R-loops, which are problematic for replication forks resulting in DSB formation (Gavalda et al., 2016). In response to DSBs, local transcription is halted and this is required for DSB repair within transcribed genes (Pankotai and Soutoglou, 2013). It is possible that Yra1 is recruited to the vicinity of DSBs to export the transcripts after RNA pol II has been halted. When Yra1 levels are reduced, the resulting R loops may interfere with homologous recombinational repair of DSBs, in a similar way that the R loops block the replication machinery. If this is the case, overexpression of RNaseH1 should reverse the DNA damage sensitivity observed upon Yra1 depletion. An alternative mechanism by which Yra1 could influence DSB repair would be a consequence of reduced export of mRNAs for

key DSB repair proteins. Interestingly, the Rad51 protein level was reduced in the *YRA1* hypomorphic mutant (**Fig. 25C**). In agreement, the human counterpart of Yra1, ALY, is required for export of Rad51 (Wickramasinghe et al., 2013). Noteworthy, there was no defect in HR repair of a single HO site at *MAT* in the *YRA1* AA mutants (**Fig. 24**). This would suggest that the Rad51 levels would be sufficient for repair of a single DSB, but that the levels are insufficient to repair global DNA breaks (**Fig. 25A**). However, the Rad51 levels in the *YRA1* hypomorphic mutant were approximately 40% of that in wild type, which seems unlikely to be enough of a reduction to lead to such a profound defect in HR.

Chapter 5

Conclusions & future directions

The details of genomic processes have been limited by the lack of knowledge of the identity of all the players acting at a specific genomic region at any given time. To address this issue, several attempts have been made to purify specific endogenous chromatin loci over the past 30 years (Boffa et al., 1995; Jasinskas and Hamkalo, 1999; Workman and Langmore, 1985; Zhang and Horz, 1982). Unfortunately, most of these methods have failed to identify new locus-specific proteins, indicating that this is a complicated biochemical challenge. This is likely due to the low abundance of the putative novel target proteins, which require a high degree of enrichment to be detectable.

One method was successful at purifying novel components on chromatin, but this required affinity purification of proteins using antibodies to the protein, rather than targeting a specific locus (Wang et al., 2013). An alternative method to isolate a specific chromosomal locus is the Proteomics of isolated chromatin fragment approach (PICh), which was used previously by Robert Kingston's lab to purify telomeres (Dejardin and Kingston, 2009). This utilized specific hybridization of nucleic acid probes to the telomeric DNA. The advantage of this approach is that it enables purification of the endogenous locus without addition of exogenous DNA sequences. The drawback of PICh, however, is that the level of sensitivity of detection is so low that it only works on repeated DNA sequences, such as telomeric DNA or the rDNA (Dejardin and Kingston, 2009; Ide and Dejardin, 2015). Roger Kornberg's lab devised an ingenious method that enabled excision of a single copy *PHO5* locus from the yeast genome and its subsequent circularization using the R recombinase, followed by differential

centrifugation to isolate the circular chromatin locus from the intact chromosomes (Griesenbeck et al., 2003). The problem with this approach though is that there is no negative control *per se* that could be used for quantitative mass spectrometric analysis, to identify proteins specifically enriched at the particular locus of interest.

The approach that we were most impressed for the isolation of a single-copy endogenous chromosomal locus was ChAP-MS (Byrum et al., 2012). The advantage here was that the method allowed rapid and specific isolation of the chromatin fragments, via incorporation of the *LEXA* DNA binding sites into the genome. To date, all of these approaches to isolate endogenous chromatin fragments and identify their associated proteins in an unbiased manner have only been applied to learn more about gene expression or repression. Similar approaches had not been applied to the field of DNA repair, which was our area of interest. Accordingly, we adapted the ChAP-MS approach to purify the chromatin fragments adjacent to a DSB lesion, hence the name DSB-ChAP-MS. The work presented in the previous two chapters demonstrates that the DSB-ChAP-MS can successfully identify both known and novel histone PTMs and proteins at a single site-specific chromosomal DSB.

Using the DSB-ChAP-MS approach, we identified numerous histone PTMs enriched around a DSB in yeast that have not been previously implicated in the DSB response in the literature. However, further validation of the roles of those histone PTMs during the DSB response is necessary. The development of specific antibodies to each of these modifications is needed to validate their

enrichment at the break, and the dynamics of their enrichment during DSB repair. The use of histone point mutations that either mimic or prevent these histone modifications, and examination of their effects on DSB repair would also provide insight whether they are required for DSB repair. Identification of the relevant writer and eraser enzymes will enable further manipulation of these histone PTMs to examine their role in DSB repair. Furthermore, identification of the reader domains that bind to these histone PTMs will provide insight into their exact function in the repair process.

Interestingly, one of the histone PTMs enriched at the DSB has never been identified previously before, not even on bulk chromatin. This modification is H3 K125me. The fact that this modification was detected only by DSB-ChAP-MS suggests that its function may be specific to the DNA damage response. It would be valuable to mutate the H3 K125 to a variety of amino acids to prevent it from being modified, such as A or R and examine the consequence on the DSB response, as well as its consequence in general. The interpretation of these experiments would need to consider that this residue is also ubiquitinated during chromatin assembly (Han et al., 2013). It would be useful to test the known histone methyl transferases to examine which of them is responsible for methylating H3 K125, followed by examination of any defects in DSB repair upon deletion of the enzyme. The effect of this methylation on chromatin assembly would also be of interest to examine.

Using the DSB-ChAP-MS approach, we identified many proteins enriched at a DSB that were not previously implicated in DSB repair. We found that over a

dozen of these proteins play novel roles in the response to DSBs. We only further investigated how Tom1, Sit4, Def1 and Yra1 contribute to the DNA damage response and our analyses indicate that additional levels of regulation of the DNA damage response exist and remain to be delineated. Future experiments and proposed molecular models for the further analysis of these four proteins were described in the Discussion Section of the previous chapter. Clearly the analysis of the other novel DSB response proteins remains to be performed, and may also provide new biological insight into the DSB response, and illuminate new links between repair and other cellular processes. In addition, there were dozens of proteins enriched at DSBs that were not required for resistance to radiomimetics. Among the list of proteins (**Appendix 1**) that were identified by our DSB-ChAP-MS analyses as enriched at a DSB undergoing repair, there may well be other novel proteins that play an important role in the DSB response. While they may not be essential for global DSB repair, it would be wise to test in the future whether they are needed for repair of the HO lesion at *MAT*, given that this break has quite unique features. If mutants of these proteins did demonstrate sensitivity to the HO endonuclease, further mechanistic studies as I have performed in **Chapter 3 and 4** would be warranted. It is also possible that some of the proteins are involved in the fidelity of DSB repair, although they do not affect the overall levels of DNA repair. For example, the helicase Mph1 promotes D-loop removal and represses crossover events during homologous recombination, although its absence does not cause defects in the DNA repair kinetics and efficiency (Prakash et al., 2009).

Noteworthy, our analysis was not saturating, as there were many repair proteins that were not enriched at the DSB. Therefore, it would be a good idea to repeat the DSB-ChAP-MS analyses with larger starting cultures and with labeled amino acids in addition to lysine, in order to detect more novel proteins at a DNA break and to detect proteins lacking lysine. This approach is also likely to identify additional histone modifications enriched at a DSB. In addition, performing the DSB-ChAP-MS procedure with yeast strains that are deleted for distinct DSB repair essential genes or at different time points after HO induction will presumably bring valuable insights regarding the temporal involvement of certain proteins or histone PTMs during the DSB response. Furthermore, the mass spectrometric analysis should be extended to identifying protein modifications enriched at a DSB in addition to histones, for example, on DNA repair proteins. While we did observe differences between the proteins identified by DSB-ChAP-MS in the wild type, and *rad52∆* or *rad54∆* strains, repeating the analysis in mutants with larger cultures, and for longer times of HO induction is likely to reveal additional insights.

Given that the DSB response pathways are highly conserved from yeast to larger eukaryotes, our findings in yeast will facilitate our understanding of the complex regulatory events that occur in the mammalian DSB response. Furthermore, the DSB-ChAP-MS method could easily be adapted to site-specific DNA breaks in mammalian cells that can be induced with endonucleases such as ISce-1 and I-PpoI. In this case, in place of introducing the *LEXA* binding sites, one would utilize the Cas9 and guide RNA components of the CRISPR system

for gRNA-directed purification of a discrete section of chromatin (CRISPR-ChAP-MS) adjacent to the induced DSBs. In this case, Protein A is expressed as a fusion protein with Cas9 to enable the purification of the chromosomal locus to which the gRNA is targeted (Waldrip et al., 2014). It would be of particular interest to use this method to examine the DSB response in different types of mammalian cells. For example, pluripotent cells and cancer stem cells have very unusual abilities to accurately repair DSBs, and the basis for this is not clear. DSB-CRISPR-ChAP-MS analysis of repair in these important cell types may provide rare insights into their efficient repair capabilities that could be targeted therapeutically.

Appendix 1: List of candidate proteins identified from the four rounds of DSB-ChAP-MS experiments. The light lysine percentage for each protein in each DSB-ChAP-MS experiment was listed. "N.I" indicates the protein was not identified by our proteomic approach, "N.D" indicates the protein was identified by our proteomic approach but its light lysine percentage was not determined.

	Gene Name	ChAP1	ChAP2	ChAP3	ChAP4
1	SIT4	87.96%	66.58%	N.I	49.71%
2	TOM1	80.60%	N.I	N.I	96.53%
3	DEF1	43.28%	70.55%	65.98%	N.I
4	YRA1	N.I	66.42%	48.89%	N.I
5	NAP1	N.I	64.35%	51.26%	53.31%
6	CDC48	55.33%	56.25%	54.48%	50.36%
7	RAD23	N.I	59.30%	N.I	56.41%
8	TOP2	N.I	N.I	56.43%	N.I
9	NHP6A	N.I	60.40%	38.98%	51.82%
10	RNR4	N.I	60.69%	67.34%	66.00%
11	MMS2	N.I	60.26%	58.81%	57.78%
12	SMT3	54.11%	61.21%	51.44%	48.53%
13	NPL3	N.I	58.21%	42.49%	55.88%
14	SOD1	N.I	52.78%	55.70%	45.39%
15	CPR1	N.I	55.95%	52.44%	53.12%
16	SPT6	N.I	66.03%	42.02%	59.27%
17	WTM1	57.15%	53.47%	58.39%	53.09%
18	PNC1	57.44%	54.74%	56.17%	N.I
19	MBF1	54.45%	56.87%	54.20%	52.56%
20	NPT1	N.I	58.96%	47.81%	N.I
21	YRB1	N.I	63.13%	47.75%	N.I
22	RSP5	N.I	82.33%	44.41%	N.I
23	RNR1	65.10%	59.53%	66.15%	52.96%
24	RTC3	N.I	50.65%	61.30%	N.I
25	GCY1	N.I	54.72%	56.99%	49.03%
26	PPZ1	N.I	N.I	56.71%	N.I

27	SIS1	N.I	N.I	56.56%	53.53%
28	PWP1	N.I	N.I	56.22%	N.I
29	CAR2	N.I	49.73%	54.08%	N.I
30	GRE3	N.I	51.22%	53.71%	57.86%
31	HNT1	56.98%	55.36%	53.01%	47.96%
32	ARO4	N.I	58.23%	52.92%	56.19%
33	ACS2	N.I	60.29%	48.76%	54.36%
34	CDC33	N.I	58.39%	46.88%	68.37%
35	TUB2	N.I	64.14%	50.79%	N.I
36	NOP56	N.I	63.29%	45.94%	55.52%
37	FPR1	54.97%	56.18%	53.78%	52.75%
38	YPL260W	N.I	57.88%	52.75%	N.I
39	GSP2;GSP1	53.16%	54.79%	51.66%	55.56%
40	RBK1	89.78%	N.I	N.I	N.I
41	HOM6	N.I	53.61%	52.76%	52.89%
42	LYS20	N.I	N.I	72.71%	64.27%
43	GPD1	N.I	60.88%	61.52%	58.68%
44	PDC1	N.I	57.52%	60.04%	57.26%
45	RHR2;HOR2	N.I	63.48%	56.30%	53.82%
46	YHB1	60.71%	57.87%	55.60%	54.51%
47	HOM2	N.I	58.40%	52.54%	50.50%
48	RGI1	N.I	55.89%	60.63%	50.46%
49	TUB1	N.I	59.06%	56.53%	N.I
50	OYE2	N.I	51.59%	55.59%	N.I
51	YBR085C-A	N.I	N.I	55.28%	54.14%
52	YOR131C	N.I	N.I	54.89%	N.I
53	YER134C	N.I	64.15%	54.41%	N.I
54	SRP68	N.I	57.57%	53.98%	N.I
55	YMR226C	59.95%	54.51%	53.96%	60.48%
56	PBI2	N.I	50.81%	53.44%	48.94%
57	CRM1	N.I	57.30%	53.25%	53.70%
58	GLR1	N.I	62.43%	51.48%	55.59%
59	KAP123	N.I	60.38%	49.96%	51.92%
60	SUB2	N.I	62.96%	49.60%	53.82%
61	APA1	N.I	62.04%	48.66%	N.I
62	GUK1	56.33%	56.81%	47.93%	53.62%
63	PUS1	N.I	63.75%	47.52%	N.I

64	HMG1	N.I	60.55%	47.38%	49.13%
65	RIB4	N.I	58.88%	45.28%	54.15%
66	NSR1	N.I	63.92%	43.25%	48.80%
67	PUS7	N.I	64.21%	40.32%	N.I
68	DBP2	N.I	69.98%	38.90%	N.I
69	TMA16	N.I	68.50%	38.87%	N.I
70	HPT1	70.61%	70.26%	57.73%	N.I
71	GLN1	N.I	70.53%	54.98%	56.38%
72	GFA1	N.I	60.24%	53.95%	57.65%
73	ESS1	52.89%	63.46%	51.08%	55.29%
74	QNS1	N.I	59.56%	50.22%	62.61%
75	STO1	N.I	63.06%	49.79%	N.I
76	GNA1	N.I	70.53%	49.04%	N.I
77	PCM1	N.I	60.11%	48.54%	N.I
78	YNL010W	N.I	63.73%	46.71%	N.I
79	ERG13	N.I	N.I	50.81%	54.82%
80	LHP1	N.I	61.88%	42.70%	58.84%
81	GAS1	60.03%	52.06%	41.06%	48.36%
82	EGD1	62.05%	55.83%	50.93%	65.08%
83	HIS1	N.I	62.38%	50.36%	55.91%
84	GUA1	N.I	N.I	55.65%	61.99%
85	FCY1	N.I	63.16%	50.37%	60.93%
86	STM1	N.I	N.I	N.I	55.56%
87	YPR010C-A	N.I	N.I	N.I	57.23%
88	SBP1	N.I	N.I	N.I	57.50%
89	CBF1	N.I	N.I	N.I	57.66%
90	GRX1	N.I	N.I	N.I	58.24%
91	ZPR1	N.I	N.I	N.I	62.39%
92	TRA1	N.I	N.I	N.I	54.77%
93	PAT1	56.62%	59.23%	N.D	N.D
94	HEM2	N.I	N.I	49.60%	55.85%
95	SNF4	N.I	N.I	48.81%	N.I
96	MSN5	N.I	N.I	52.14%	N.I
97	HXK2	N.I	N.I	51.78%	51.46%
98	NCL1	N.I	N.I	51.63%	53.77%
99	SXM1	N.I	49.49%	51.59%	40.86%
100	GBP2	N.I	N.I	51.43%	N.I

101	*CYS3*	N.I	52.71%	51.26%	N.I
102	*YPR1*	N.I	N.I	48.88%	N.I
103	*SEH1*	N.I	N.I	48.84%	N.I
104	*TAL1*	N.I	49.77%	48.98%	51.02%
105	*SPE3*	N.I	52.36%	48.00%	48.46%
106	*YGR169C-A*	N.I	N.I	49.85%	N.I
107	*PBP4*	N.I	N.I	N.I	53.69%
108	*TRM112*	N.I	N.I	N.I	53.03%

Appendix 2: A commercial antibody to human histone H3 lysine 122 acetylation is non-specific *in vivo*

The content of this appendix is based on our published paper: Graves, H.K., **Wang, P.**, Lagarde, M., Chen, Z., and Tyler, J.K. (2016). "Mutations that prevent or mimic persistent post-translational modifications of the histone H3 globular domain cause lethality and growth defects in Drosophila". Epigenetics & Chromatin 9, 9. Copyright permission is not required since the copyright policy of the journal of Epigenetics & Chromatin states that "As an author of an article published in Epigenetics & Chromatin you retain the copyright of your article and you are free to reproduce and disseminate your work".

Introduction

Understanding the functions of histone post-translational modifications (PTMs) is of great importance to deciphering the mechanisms underlying various genomic activities. Among the least well-understood histone PTMs *in vivo* are those that occur on the histone globular domains. Biochemical studies have showed that histone globular domain PTMs can directly alter the nucleosome structure if the residue normally mediates the interaction between histone and DNA within a nucleosome (Bowman and Poirier, 2015). However, their *in vivo* functions are poorly appreciated.

Among the histone globular domain PTMs is histone H3 lysine (K) 122 acetylation (H3 K122ac) that occurs at the nucleosome dyad region, where DNA

is wrapped only once around the nucleosome and is therefore more sensitive to perturbation of the histone-DNA contacts (Lawrence et al., 2016). H3 K122ac was identified by mass spectrometry analysis in bovine (Zhang et al., 2004), human (Das et al., 2009; Olsen et al., 2010) and fission yeast (Tropberger et al., 2013). *In vitro* studies suggested that acetylation of H3 K122 loosens the binding between histone and DNA (Iwasaki et al., 2011), and promotes transcription on reconstituted chromatin templates (Tropberger et al., 2013). Using a commercial antibody to H3 K122ac for chromatin immunoprecipitation analysis in mammalian cells, Tropberger et al. found H3 K122ac is enriched in active enhancers, which is consistent with a role for this modification in transcriptional activation (Tropberger et al., 2013). In addition, mutations of H3 K122 in yeast lead to DNA damage sensitivity and defects in transcriptional induction and silencing (English et al., 2006; Xu et al., 2005). Therefore, it is possible that H3 K122ac regulates transcription and DNA repair by altering the chromatin structure in metazoan cells. In order to functionally characterize the function of H3 K122ac *in vivo*, it is necessary to have an antibody that specifically recognizes this modification *in vivo*. Unfortunately, however, I found the only so far available commercial antibody to H3 K122ac, which was previously used to imply a role for H3 K122ac in transcription in metazoans, is actually non-specific *in vivo*.

Methods

Western blots

Plasmids expressing YFP tagged mutant H3.1 (K115R, K122R, T118E or K115RK122R) were generated by site-directed mutagenesis on the pcDNA5-wild type H3.1-YFP using the QuickChange Site-Directed Mutagenesis Kit (Agilent Technologies). HEK293T cells were transiently transfected with YFP-tagged WT or mutant histone H3.1 expression plasmid (or pcDNA5 empty plasmid as a control). Cells were harvested 24 hr post-transfection and processed for histone acid extraction. Acid extracted histones were separated by SDS-PAGE, probed with the anti-H3 K122Ac antibody (Rabbit pAb: Abcam 33309) and anti-GFP antibody (Mouse). The secondary antibody IRDye® 680RD Goat anti-Rabbit IgG (H + L) multiplexed with the IRDye® 800CW Goat anti-Mouse IgG (H + L) was used for the 2-color detection method by the Odyssey LI-COR imaging system.

Immunoprecipitation

Plasmids expressing Flag tagged mutant H3.1 (K115R, K122R or K115RK122R), were generated by site-directed mutagenesis on the pcDNA5/FRT-wild type H3.1-FLAG using QuickChange Site-Directed Mutagenesis Kit (Agilent Technologies). Flp-In™-293 host cells were co-transfected with plasmid pcDNA5/FRT-H3.1-FLAG (either WT or mutant H3.1, i.e. H3.1 K115R, K122R or K115RK122R) and Flp recombinase expression plasmid pOG44, to generate cell lines that stably express Flag tagged WT or mutant histone H3.1. The stable cells lines were selected based on their resistance to hygromycin, sensitivity to zeocin and expression of Flag tagged

histone H3. Stable Flp-In™-293 cells were harvested and processed for nuclear extract, as previously described (Hammond et al., 2014). 20 µl Dynabeads Protein A, and 1 µg of the Abcam anti-H3 K122Ac antibody (Rabbit pAb: Abcam 33309) were used for each IP sample which contained 300 µg of total proteins. The eluted supernatants were separated by SDS-PAGE, probed with the anti-H3 antibody (Rabbit pAb: Abcam 1791) and anti-Flag antibody (Mouse mAb: Sigma 3165). The secondary antibody IRDye® 680RD Goat anti-Rabbit IgG (H + L) multiplexed with the IRDye® 800CW Goat anti-Mouse IgG (H + L) was used for the 2-color detection method by the Odyssey LI-COR imaging system.

Results

I examined the specificity of the antibody directly in human cells. Using cells expressing H3-YFP, I found that the ability of the H3 K122ac antibody to recognize H3-YFP in western blots was identical for wild type and H3 K122R mutant protein (**Fig. 27A**) indicating that it is non-specific in western blots. Given that ChIP and immunofluorescence are based on recognition of the native epitope, I examined whether the H3 K122ac antibody was specific for the native H3 K122ac epitope. I immunoprecipitated histones with the H3 K122ac antibody, and found that it was equally as effective at immunoprecipitating Flag-tagged H3 as Flag-tagged H3 K122R histones (**Fig. 27B**). As such, the antibody that is commonly used to study H3 K122ac is highly non-specific within metazoan cells.
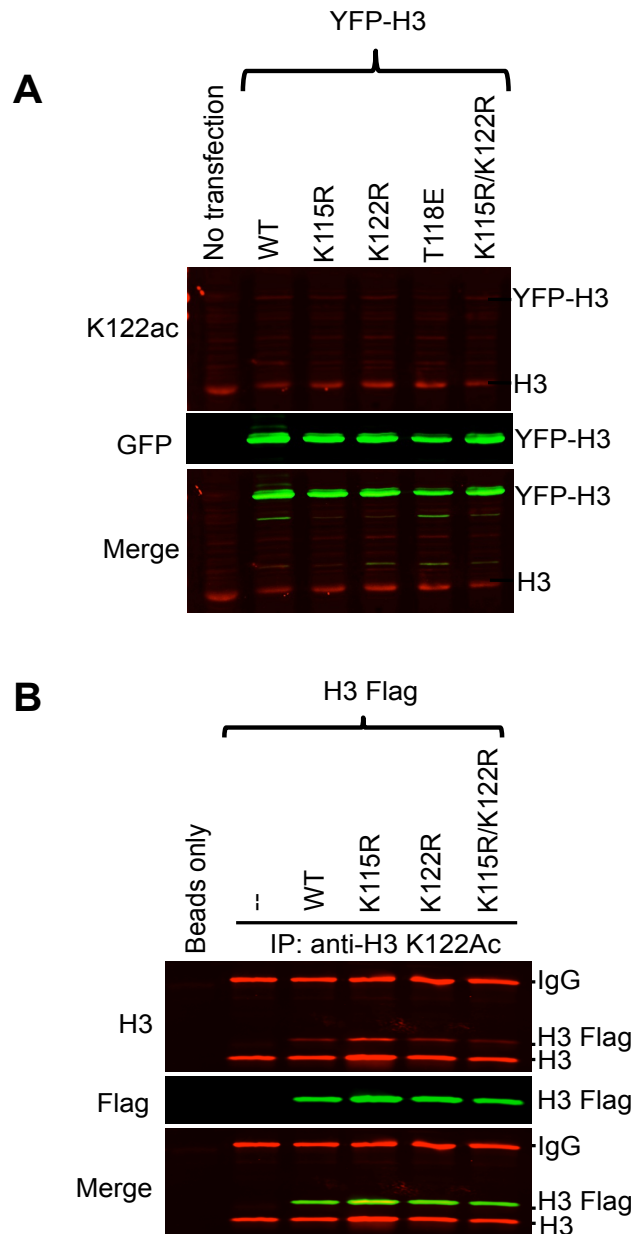
Figure 27. The commercial H3 K122ac antibody is not specific. (A) Western

blot analysis with the anti-H3 K122ac antibody (Abcam 33309) using acid

extracted histones collected from HEK293T cells transiently transfected with

YFP-tagged WT or mutant histone H3 expression plasmid (H3.1 K115R, K122R,

T118E or K115R / K122R) shows that the anti-H3 K122Ac antibody non

specifically recognizes unmodified H3 and / or other modification(s) besides H3 K122ac. **(B)** Immunoprecipitation (IP) analysis with the Abcam anti-H3 K122Ac antibody using nuclear extract from stable cell lines expressing Flag-tagged WT or mutant histone H3 (H3.1 K115R, K122R or K115R / K122R) shows that the anti-H3 K122Ac antibody non specifically recognizes unmodified histone H3 and / or other modification(s) besides H3 K122ac.

Discussion

Since the inferred role of H3 K122ac in transcription in mammalian cells was largely based on its immunolocalization to enhancers (Tropberger et al., 2013) using the commercial antibody that I have found to be non specific, my finding suggests the reported role of H3 K122ac in transcription in metazoans *in vivo* needs to be revisited. Although this antibody is specific in dot blots when all acetylated peptides are present in equal amounts, the H3 K122ac modification is relatively rare compared to N-terminal histone modifications within mammalian cells (Alan Tackett, personal communication). As such, antibody specificity has to be determined in the context of the cell due to the diverse differences in the relative abundance of different histone modifications *in vivo*. Accordingly, I find that the H3 K122ac signal by western analysis or immunoprecipitation is unchanged upon mutation of H3 K122 to a non-acetylatable residue (**Fig. 27**), suggesting that the H3 K122ac antibody favors other histone H3 acetylation sites *in vivo.* Therefore, caution should be taken when interpreting experiments using the Abcam H3 K122ac antibody, which *in vivo* is clearly non-specific. In addition,

developing a specific antibody to H3 K122ac will be highly desirable for future studies on this modification.

Bibliography

Adkins, M.W., Howar, S.R., and Tyler, J.K. (2004). Chromatin disassembly mediated by the histone chaperone Asf1 is essential for transcriptional activation of the yeast PHO5 and PHO8 genes. Molecular cell *14*, 657-666.

Alani, E., Thresher, R., Griffith, J.D., and Kolodner, R.D. (1992). Characterization of DNA-binding and strand-exchange stimulation properties of y-RPA, a yeast single-strand-DNA-binding protein. Journal of molecular biology *227*, 54-71.

Allen, J.B., Zhou, Z., Siede, W., Friedberg, E.C., and Elledge, S.J. (1994). The SAD1/RAD53 protein kinase controls multiple checkpoints and DNA damage-induced transcription in yeast. Genes & development *8*, 2401-2415.

Angeles de la Torre-Ruiz, M., Torres, J., Arino, J., and Herrero, E. (2002). Sit4 is required for proper modulation of the biological functions mediated by Pkc1 and the cell integrity pathway in Saccharomyces cerevisiae. The Journal of biological chemistry *277*, 33468-33476.

Awad, S., Ryan, D., Prochasson, P., Owen-Hughes, T., and Hassan, A.H. (2010). The Snf2 homolog Fun30 acts as a homodimeric ATP-dependent chromatin-remodeling enzyme. The Journal of biological chemistry *285*, 9477-9484.

Aylon, Y., Liefshitz, B., and Kupiec, M. (2004). The CDK regulates repair of double-strand breaks by homologous recombination during the cell cycle. The EMBO journal *23*, 4868-4875.

Ayrapetov, M.K., Gursoy-Yuzugullu, O., Xu, C., Xu, Y., and Price, B.D. (2014). DNA double-strand breaks promote methylation of histone H3 on lysine 9 and transient formation of repressive chromatin. Proceedings of the National Academy of Sciences of the United States of America *111*, 9169-9174.

Ball, H.L., Myers, J.S., and Cortez, D. (2005). ATRIP binding to replication protein A-single-stranded DNA promotes ATR-ATRIP localization but is dispensable for Chk1 phosphorylation. Molecular biology of the cell *16*, 2372-2381.

Bao, Y., and Shen, X. (2007). Chromatin remodeling in DNA double-strand break repair. Current opinion in genetics & development *17*, 126-131.

Bao, Y., and Shen, X. (2011). SnapShot: Chromatin remodeling: INO80 and SWR1. Cell *144*, 158-158 e152.

Bastians, H., and Ponstingl, H. (1996). The novel human protein serine/threonine phosphatase 6 is a functional homologue of budding yeast Sit4p and fission yeast ppe1, which are involved in cell cycle regulation. Journal of cell science *109 (Pt 12)*, 2865-2874.

Bazzi, M., Mantiero, D., Trovesi, C., Lucchini, G., and Longhese, M.P. (2010). Dephosphorylation of gamma H2A by Glc7/protein phosphatase 1 promotes recovery from inhibition of DNA replication. Molecular and cellular biology *30*, 131-145.

Belotserkovskaya, R., Oh, S., Bondarenko, V.A., Orphanides, G., Studitsky, V.M., and Reinberg, D. (2003). FACT facilitates transcription-dependent nucleosome alteration. Science *301*, 1090-1093.

Bergs, J.W., Franken, N.A., Haveman, J., Geijsen, E.D., Crezee, J., and van Bree, C. (2007). Hyperthermia, cisplatin and radiation trimodality treatment: a promising cancer treatment? A review from preclinical studies to clinical application. Int J Hyperthermia *23*, 329-341.

Bird, A.W., Yu, D.Y., Pray-Grant, M.G., Qiu, Q., Harmon, K.E., Megee, P.C., Grant, P.A., Smith, M.M., and Christman, M.F. (2002). Acetylation of histone H4 by Esa1 is required for DNA double-strand break repair. Nature *419*, 411-415.

Boffa, L.C., Carpaneto, E.M., and Allfrey, V.G. (1995). Isolation of active genes containing CAG repeats by DNA strand invasion by a peptide nucleic acid. Proceedings of the National Academy of Sciences of the United States of America *92*, 1901-1905.

Bonilla, C.Y., Melo, J.A., and Toczyski, D.P. (2008). Colocalization of sensors is sufficient to activate the DNA damage checkpoint in the absence of damage. Molecular cell *30*, 267-276.

Bonnerot, C., Boeck, R., and Lapeyre, B. (2000). The two proteins Pat1p (Mrt1p) and Spb8p interact in vivo, are required for mRNA decay, and are functionally linked to Pab1p. Molecular and cellular biology *20*, 5939-5946.

Botuyan, M.V., Lee, J., Ward, I.M., Kim, J.E., Thompson, J.R., Chen, J., and Mer, G. (2006). Structural basis for the methylation state-specific recognition of histone H4-K20 by 53BP1 and Crb2 in DNA repair. Cell *127*, 1361-1373.

Bowman, G.D., and Poirier, M.G. (2015). Post-translational modifications of histones that influence nucleosome dynamics. Chemical reviews *115*, 2274-2295.

Brachmann, C.B., Davies, A., Cost, G.J., Caputo, E., Li, J., Hieter, P., and Boeke, J.D. (1998). Designer deletion strains derived from Saccharomyces cerevisiae S288C: a useful set of strains and plasmids for PCR-mediated gene disruption and other applications. Yeast *14*, 115-132.

Branzei, D., and Foiani, M. (2010). Maintaining genome stability at the replication fork. Nature reviews Molecular cell biology *11*, 208-219.

Bucheli, M.E., and Buratowski, S. (2005). Npl3 is an antagonist of mRNA 3' end formation by RNA polymerase II. The EMBO journal *24*, 2150-2160.

Byrum, S.D., Raman, A., Taverna, S.D., and Tackett, A.J. (2012). ChAP-MS: a method for identification of proteins and histone posttranslational modifications at a single genomic locus. Cell reports *2*, 198-205.

Byrum, S.D., Taverna, S.D., and Tackett, A.J. (2015). Purification of specific chromatin loci for proteomic analysis. Methods in molecular biology *1228*, 83-92.

Cai, M., and Davis, R.W. (1990). Yeast centromere binding protein CBF1, of the helix-loop-helix protein family, is required for chromosome stability and methionine prototrophy. Cell *61*, 437-446.

Cejka, P., Cannavo, E., Polaczek, P., Masuda-Sasa, T., Pokharel, S., Campbell, J.L., and Kowalczykowski, S.C. (2010). DNA end resection by Dna2-Sgs1-RPA and its stimulation by Top3-Rmi1 and Mre11-Rad50-Xrs2. Nature *467*, 112-116.

Chai, B., Huang, J., Cairns, B.R., and Laurent, B.C. (2005). Distinct roles for the RSC and Swi/Snf ATP-dependent chromatin remodelers in DNA double-strand break repair. Genes & development *19*, 1656-1661.

Chapman, J.R., Taylor, M.R., and Boulton, S.J. (2012). Playing the end game: DNA double-strand break repair pathway choice. Molecular cell *47*, 497-510.

Chaurasia, P., Sen, R., Pandita, T.K., and Bhaumik, S.R. (2012). Preferential repair of DNA double-strand break at the active gene in vivo. The Journal of biological chemistry *287*, 36414-36422.

Chen, C.C., Carson, J.J., Feser, J., Tamburini, B., Zabaronick, S., Linger, J., and Tyler, J.K. (2008). Acetylated lysine 56 on histone H3 drives chromatin assembly after repair and signals for the completion of repair. Cell *134*, 231-243.

Chen, L., Trujillo, K., Ramos, W., Sung, P., and Tomkinson, A.E. (2001). Promotion of Dnl4-catalyzed DNA end-joining by the Rad50/Mre11/Xrs2 and Hdf1/Hdf2 complexes. Molecular cell *8*, 1105-1115.

Chen, S.H., Smolka, M.B., and Zhou, H. (2007). Mechanism of Dun1 activation by Rad53 phosphorylation in Saccharomyces cerevisiae. The Journal of biological chemistry *282*, 986-995.

Chen, X., Cui, D., Papusha, A., Zhang, X., Chu, C.D., Tang, J., Chen, K., Pan, X., and Ira, G. (2012). The Fun30 nucleosome remodeller promotes resection of DNA double-strand break ends. Nature *489*, 576-580.

Chen, X., Niu, H., Chung, W.H., Zhu, Z., Papusha, A., Shim, E.Y., Lee, S.E., Sung, P., and Ira, G. (2011). Cell cycle regulation of DNA double-strand break end resection by Cdk1-dependent Dna2 phosphorylation. Nature structural & molecular biology *18*, 1015-1019.

Chen, Y.B., Yang, C.P., Li, R.X., Zeng, R., and Zhou, J.Q. (2005). Def1p is involved in telomere maintenance in budding yeast. The Journal of biological chemistry *280*, 24784-24791.

Cheung, W.L., Turner, F.B., Krishnamoorthy, T., Wolner, B., Ahn, S.H., Foley, M., Dorsey, J.A., Peterson, C.L., Berger, S.L., and Allis, C.D. (2005). Phosphorylation of histone H4 serine 1 during DNA damage requires casein kinase II in S. cerevisiae. Current biology : CB *15*, 656-660.

Chowdhury, D., Keogh, M.C., Ishii, H., Peterson, C.L., Buratowski, S., and Lieberman, J. (2005). gamma-H2AX dephosphorylation by protein phosphatase 2A facilitates DNA double-strand break repair. Molecular cell *20*, 801-809.

Ciccia, A., and Elledge, S.J. (2010). The DNA damage response: making it safe to play with knives. Molecular cell *40*, 179-204.

Ciosk, R., Zachariae, W., Michaelis, C., Shevchenko, A., Mann, M., and Nasmyth, K. (1998). An ESP1/PDS1 complex regulates loss of sister chromatid cohesion at the metaphase to anaphase transition in yeast. Cell *93*, 1067-1076.

Clerici, M., Mantiero, D., Guerini, I., Lucchini, G., and Longhese, M.P. (2008). The Yku70-Yku80 complex contributes to regulate double-strand break processing and checkpoint activation during the cell cycle. EMBO reports *9*, 810-818.

Clerici, M., Mantiero, D., Lucchini, G., and Longhese, M.P. (2006). The Saccharomyces cerevisiae Sae2 protein negatively regulates DNA damage checkpoint signalling. EMBO reports *7*, 212-218.

Costelloe, T., Louge, R., Tomimatsu, N., Mukherjee, B., Martini, E., Khadaroo, B., Dubois, K., Wiegant, W.W., Thierry, A., Burma, S., *et al.* (2012). The yeast Fun30 and human SMARCAD1 chromatin remodellers promote DNA end resection. Nature *489*, 581-584.

Daraba, A., Gali, V.K., Halmai, M., Haracska, L., and Unk, I. (2014). Def1 promotes the degradation of Pol3 for polymerase exchange to occur during DNA-damage--induced mutagenesis in Saccharomyces cerevisiae. PLoS biology *12*, e1001771.

Das, C., Lucia, M.S., Hansen, K.C., and Tyler, J.K. (2009). CBP/p300-mediated acetylation of histone H3 on lysine 56. Nature *459*, 113-117.

Dejardin, J., and Kingston, R.E. (2009). Purification of proteins associated with specific genomic Loci. Cell *136*, 175-186.

Dermody, J.L., Dreyfuss, J.M., Villen, J., Ogundipe, B., Gygi, S.P., Park, P.J., Ponticelli, A.S., Moore, C.L., Buratowski, S., and Bucheli, M.E. (2008). Unphosphorylated SR-like protein Npl3 stimulates RNA polymerase II elongation. PloS one *3*, e3273.

Doil, C., Mailand, N., Bekker-Jensen, S., Menard, P., Larsen, D.H., Pepperkok, R., Ellenberg, J., Panier, S., Durocher, D., Bartek, J., *et al.* (2009). RNF168 binds and amplifies ubiquitin conjugates on damaged chromosomes to allow accumulation of repair proteins. Cell *136*, 435-446.

Dong, A., Zhu, Y., Yu, Y., Cao, K., Sun, C., and Shen, W.H. (2003). Regulation of biosynthesis and intracellular localization of rice and tobacco homologues of nucleosome assembly protein 1. Planta *216*, 561-570.

Donham, D.C., 2nd, Scorgie, J.K., and Churchill, M.E. (2011). The activity of the histone chaperone yeast Asf1 in the assembly and disassembly of histone H3/H4-DNA complexes. Nucleic acids research *39*, 5449-5458.

Douglas, P., Zhong, J., Ye, R., Moorhead, G.B., Xu, X., and Lees-Miller, S.P. (2010). Protein phosphatase 6 interacts with the DNA-dependent protein kinase catalytic subunit and dephosphorylates gamma-H2AX. Molecular and cellular biology *30*, 1368-1381.

Durocher, D., and Jackson, S.P. (2002). The FHA domain. FEBS letters *513*, 58-66.

Eapen, V.V., Sugawara, N., Tsabar, M., Wu, W.H., and Haber, J.E. (2012). The Saccharomyces cerevisiae chromatin remodeler Fun30 regulates DNA end resection and checkpoint deactivation. Molecular and cellular biology *32*, 4727-4740.

English, C.M., Adkins, M.W., Carson, J.J., Churchill, M.E., and Tyler, J.K. (2006). Structural basis for the histone chaperone activity of Asf1. Cell *127*, 495-508.

Ferguson, D.O., and Holloman, W.K. (1996). Recombinational repair of gaps in DNA is asymmetric in Ustilago maydis and can be explained by a migrating D-loop model. Proceedings of the National Academy of Sciences of the United States of America *93*, 5419-5424.

Finn, K., Lowndes, N.F., and Grenon, M. (2012). Eukaryotic DNA damage checkpoint activation in response to double-strand breaks. Cellular and molecular life sciences : CMLS *69*, 1447-1473.

Fiorani, S., Mimun, G., Caleca, L., Piccini, D., and Pellicioli, A. (2008). Characterization of the activation domain of the Rad53 checkpoint kinase. Cell cycle *7*, 493-499.

Fnu, S., Williamson, E.A., De Haro, L.P., Brenneman, M., Wray, J., Shaheen, M., Radhakrishnan, K., Lee, S.H., Nickoloff, J.A., and Hromas, R. (2011). Methylation of histone H3 lysine 36 enhances DNA repair by nonhomologous end-joining. Proceedings of the National Academy of Sciences of the United States of America *108*, 540-545.

Fradet-Turcotte, A., Canny, M.D., Escribano-Diaz, C., Orthwein, A., Leung, C.C., Huang, H., Landry, M.C., Kitevski-LeBlanc, J., Noordermeer, S.M., Sicheri, F*., et al.* (2013). 53BP1 is a reader of the DNA-damage-induced H2A Lys 15 ubiquitin mark. Nature *499*, 50-54.

Franken, N.A., and Barendsen, G.W. (2014). Enhancement of radiation effectiveness by hyperthermia and incorporation of halogenated pyrimidines at low radiation doses as compared with high doses: implications for mechanisms. Int J Radiat Biol *90*, 313-317.

Funakoshi, M., and Hochstrasser, M. (2009). Small epitope-linker modules for PCR-based C-terminal tagging in Saccharomyces cerevisiae. Yeast *26*, 185-192.

Gao, J., Zhu, Y., Zhou, W., Molinier, J., Dong, A., and Shen, W.H. (2012). NAP1 family histone chaperones are required for somatic homologous recombination in Arabidopsis. The Plant cell *24*, 1437-1447.

Gardner, R., Putnam, C.W., and Weinert, T. (1999). RAD53, DUN1 and PDS1 define two parallel G2/M checkpoint pathways in budding yeast. The EMBO journal *18*, 3173-3185.

Gavalda, S., Santos-Pereira, J.M., Garcia-Rubio, M.L., Luna, R., and Aguilera, A. (2016). Excess of Yra1 RNA-Binding Factor Causes Transcription-Dependent Genome Instability, Replication Impairment and Telomere Shortening. PLoS genetics *12*, e1005966.

Giaever, G., Chu, A.M., Ni, L., Connelly, C., Riles, L., Veronneau, S., Dow, S., Lucau-Danila, A., Anderson, K., Andre, B.*, et al.* (2002). Functional profiling of the Saccharomyces cerevisiae genome. Nature *418*, 387-391.

Giannattasio, M., Lazzaro, F., Plevani, P., and Muzi-Falconi, M. (2005). The DNA damage checkpoint response requires histone H2B ubiquitination by Rad6-Bre1 and H3 methylation by Dot1. The Journal of biological chemistry *280*, 9879-9886.

Gietz, D., St Jean, A., Woods, R.A., and Schiestl, R.H. (1992). Improved method for high efficiency transformation of intact yeast cells. Nucleic acids research *20*, 1425.

Gilbert, C.S., Green, C.M., and Lowndes, N.F. (2001). Budding yeast Rad9 is an ATP-dependent Rad53 activating machine. Molecular cell *8*, 129-136.

Gobbini, E., Cesena, D., Galbiati, A., Lockhart, A., and Longhese, M.P. (2013). Interplays between ATM/Tel1 and ATR/Mec1 in sensing and signaling DNA double-strand breaks. DNA repair *12*, 791-799.

Grenon, M., Costelloe, T., Jimeno, S., O'Shaughnessy, A., Fitzgerald, J., Zgheib, O., Degerth, L., and Lowndes, N.F. (2007). Docking onto chromatin via the Saccharomyces cerevisiae Rad9 Tudor domain. Yeast *24*, 105-119.

Griesenbeck, J., Boeger, H., Strattan, J.S., and Kornberg, R.D. (2003). Affinity purification of specific chromatin segments from chromosomal loci in yeast. Molecular and cellular biology *23*, 9275-9282.

Gursoy-Yuzugullu, O., Ayrapetov, M.K., and Price, B.D. (2015). Histone chaperone Anp32e removes H2A.Z from DNA double-strand breaks and promotes nucleosome reorganization and DNA repair. Proceedings of the National Academy of Sciences of the United States of America *112*, 7507-7512.

Haber, J.E. (2012). Mating-type genes and MAT switching in Saccharomyces cerevisiae. Genetics *191*, 33-64.

Hagen, U. (1994). Mechanisms of induction and repair of DNA double-strand breaks by ionizing radiation: some contradictions. Radiation and environmental biophysics *33*, 45-61.

Hammond, S.L., Byrum, S.D., Namjoshi, S., Graves, H.K., Dennehey, B.K., Tackett, A.J., and Tyler, J.K. (2014). Mitotic phosphorylation of histone H3 threonine 80. Cell cycle *13*, 440-452.

Han, J., Zhang, H., Zhang, H., Wang, Z., Zhou, H., and Zhang, Z. (2013). A Cul4 E3 ubiquitin ligase regulates histone hand-off during nucleosome assembly. Cell *155*, 817-829.

Harrison, J.C., and Haber, J.E. (2006). Surviving the breakup: the DNA damage checkpoint. Annual review of genetics *40*, 209-235.

Haruki, H., Nishikawa, J., and Laemmli, U.K. (2008). The anchor-away technique: rapid, conditional establishment of yeast mutant phenotypes. Molecular cell *31*, 925-932.

Heideker, J., Lis, E.T., and Romesberg, F.E. (2007). Phosphatases, DNA damage checkpoints and checkpoint deactivation. Cell cycle *6*, 3058-3064.

Helleday, T., Eshtad, S., and Nik-Zainal, S. (2014). Mechanisms underlying mutational signatures in human cancers. Nature reviews Genetics *15*, 585-598.

Heo, K., Kim, H., Choi, S.H., Choi, J., Kim, K., Gu, J., Lieber, M.R., Yang, A.S., and An, W. (2008). FACT-mediated exchange of histone variant H2AX regulated by phosphorylation of H2AX and ADP-ribosylation of Spt16. Molecular cell *30*, 86-97.

Herskowitz, I., and Jensen, R.E. (1991). Putting the HO gene to work: practical uses for mating-type switching. Methods in enzymology *194*, 132-146.

Hill, R., and Lee, P.W. (2010). The DNA-dependent protein kinase (DNA-PK): More than just a case of making ends meet? Cell cycle *9*, 3460-3469.

Hsiao, K.Y., and Mizzen, C.A. (2013). Histone H4 deacetylation facilitates 53BP1 DNA damage signaling and double-strand break repair. Journal of molecular cell biology *5*, 157-165.

Huen, M.S., Grant, R., Manke, I., Minn, K., Yu, X., Yaffe, M.B., and Chen, J. (2007). RNF8 transduces the DNA-damage signal via histone ubiquitylation and checkpoint protein assembly. Cell *131*, 901-914.

Huertas, P., Cortes-Ledesma, F., Sartori, A.A., Aguilera, A., and Jackson, S.P. (2008). CDK targets Sae2 to control DNA-end resection and homologous recombination. Nature *455*, 689-692.

Hunt, C.R., Dix, D.J., Sharma, G.G., Pandita, R.K., Gupta, A., Funk, M., and Pandita, T.K. (2004). Genomic instability and enhanced radiosensitivity in Hsp70.1- and Hsp70.3-deficient mice. Molecular and cellular biology *24*, 899-911.

Hunt, C.R., Pandita, R.K., Laszlo, A., Higashikubo, R., Agarwal, M., Kitamura, T., Gupta, A., Rief, N., Horikoshi, N., Baskaran, R.*, et al.* (2007). Hyperthermia activates a subset of ataxia-telangiectasia mutated effectors independent of DNA strand breaks and heat shock protein 70 status. Cancer Res *67*, 3010-3017.

Hustedt, N., Gasser, S.M., and Shimada, K. (2013). Replication checkpoint: tuning and coordination of replication forks in s phase. Genes *4*, 388-434.

Huyen, Y., Zgheib, O., Ditullio, R.A., Jr., Gorgoulis, V.G., Zacharatos, P., Petty, T.J., Sheston, E.A., Mellert, H.S., Stavridi, E.S., and Halazonetis, T.D. (2004). Methylated lysine 79 of histone H3 targets 53BP1 to DNA double-strand breaks. Nature *432*, 406-411.

Ide, S., and Dejardin, J. (2015). End-targeting proteomics of isolated chromatin segments of a mammalian ribosomal RNA gene promoter. Nature communications *6*, 6674.

Ikura, T., Tashiro, S., Kakino, A., Shima, H., Jacob, N., Amunugama, R., Yoder, K., Izumi, S., Kuraoka, I., Tanaka, K.*, et al.* (2007). DNA damage-

dependent acetylation and ubiquitination of H2AX enhances chromatin dynamics. Molecular and cellular biology *27*, 7028-7040.

Ira, G., Pellicioli, A., Balijja, A., Wang, X., Fiorani, S., Carotenuto, W., Liberi, G., Bressan, D., Wan, L., Hollingsworth, N.M.*, et al.* (2004). DNA end resection, homologous recombination and DNA damage checkpoint activation require CDK1. Nature *431*, 1011-1017.

Ivanov, E.L., Sugawara, N., Fishman-Lobell, J., and Haber, J.E. (1996). Genetic requirements for the single-strand annealing pathway of double-strand break repair in Saccharomyces cerevisiae. Genetics *142*, 693-704.

Iwasaki, W., Tachiwana, H., Kawaguchi, K., Shibata, T., Kagawa, W., and Kurumizaka, H. (2011). Comprehensive structural analysis of mutant nucleosomes containing lysine to glutamine (KQ) substitutions in the H3 and H4 histone-fold domains. Biochemistry *50*, 7822-7832.

Jackson, S.P. (2002). Sensing and repairing DNA double-strand breaks. Carcinogenesis *23*, 687-696.

Jackson, S.P., and Bartek, J. (2009). The DNA-damage response in human biology and disease. Nature *461*, 1071-1078.

Jasinskas, A., and Hamkalo, B.A. (1999). Purification and initial characterization of primate satellite chromatin. Chromosome research : an international journal on the molecular, supramolecular and evolutionary aspects of chromosome biology *7*, 341-354.

Jha, D.K., and Strahl, B.D. (2014). An RNA polymerase II-coupled function for histone H3K36 methylation in checkpoint activation and DSB repair. Nature communications *5*, 3965.

Jiang, X., Xu, Y., and Price, B.D. (2010). Acetylation of H2AX on lysine 36 plays a key role in the DNA double-strand break repair pathway. FEBS letters *584*, 2926-2930.

Jordan, P.W., Klein, F., and Leach, D.R. (2007). Novel roles for selected genes in meiotic DNA processing. PLoS genetics *3*, e222.

Kalocsay, M., Hiller, N.J., and Jentsch, S. (2009). Chromosome-wide Rad51 spreading and SUMO-H2A.Z-dependent chromosome fixation in response to a persistent DNA double-strand break. Molecular cell *33*, 335-343.

Kampinga, H.H., and Konings, A.W. (1987). Inhibition of repair of X-ray-induced DNA damage by heat: the role of hyperthermic inhibition of DNA polymerase alpha activity. Radiat Res *112*, 86-98.

Kent, N.A., Chambers, A.L., and Downs, J.A. (2007). Dual chromatin remodeling roles for RSC during DNA double strand break induction and repair at the yeast MAT locus. The Journal of biological chemistry *282*, 27693-27701.

Keogh, M.C., Kim, J.A., Downey, M., Fillingham, J., Chowdhury, D., Harrison, J.C., Onishi, M., Datta, N., Galicia, S., Emili, A.*, et al.* (2006). A phosphatase complex that dephosphorylates gammaH2AX regulates DNA damage checkpoint recovery. Nature *439*, 497-501.

Kim, H.S., Vijayakumar, S., Reger, M., Harrison, J.C., Haber, J.E., Weil, C., and Petrini, J.H. (2008). Functional interactions between Sae2 and the Mre11 complex. Genetics *178*, 711-723.

Klar, A.J., Hicks, J.B., and Strathern, J.N. (1982). Directionality of yeast mating-type interconversion. Cell *28*, 551-561.

Koch, M.R., and Pillus, L. (2009). The glucanosyltransferase Gas1 functions in transcriptional silencing. Proceedings of the National Academy of Sciences of the United States of America *106*, 11224-11229.

Kolas, N.K., Chapman, J.R., Nakada, S., Ylanko, J., Chahwan, R., Sweeney, F.D., Panier, S., Mendez, M., Wildenhain, J., Thomson, T.M.*, et al.* (2007). Orchestration of the DNA-damage response by the RNF8 ubiquitin ligase. Science *318*, 1637-1640.

Kondo, T., Wakayama, T., Naiki, T., Matsumoto, K., and Sugimoto, K. (2001). Recruitment of Mec1 and Ddc1 checkpoint proteins to double-strand breaks through distinct mechanisms. Science *294*, 867-870.

Kress, T.L., Krogan, N.J., and Guthrie, C. (2008). A single SR-like protein, Npl3, promotes pre-mRNA splicing in budding yeast. Molecular cell *32*, 727-734.

Krogh, B.O., and Symington, L.S. (2004). Recombination proteins in yeast. Annual review of genetics *38*, 233-271.

Kuras, L., Cherest, H., Surdin-Kerjan, Y., and Thomas, D. (1996). A heteromeric complex containing the centromere binding factor 1 and two basic leucine zipper factors, Met4 and Met28, mediates the transcription activation of yeast sulfur metabolism. The EMBO journal *15*, 2519-2529.

Kushnirov, V.V. (2000). Rapid and reliable protein extraction from yeast. Yeast *16*, 857-860.

Labib, K., and Hodgson, B. (2007). Replication fork barriers: pausing for a break or stalling for time? EMBO reports *8*, 346-353.

Lam, I., and Keeney, S. (2014). Mechanism and regulation of meiotic recombination initiation. Cold Spring Harbor perspectives in biology *7*, a016634.

Lawrence, M., Daujat, S., and Schneider, R. (2016). Lateral Thinking: How Histone Modifications Regulate Gene Expression. Trends in genetics : TIG *32*, 42-56.

Lazzaro, F., Giannattasio, M., Puddu, F., Granata, M., Pellicioli, A., Plevani, P., and Muzi-Falconi, M. (2009). Checkpoint mechanisms at the intersection between DNA damage and repair. DNA repair *8*, 1055-1067.

Lazzaro, F., Sapountzi, V., Granata, M., Pellicioli, A., Vaze, M., Haber, J.E., Plevani, P., Lydall, D., and Muzi-Falconi, M. (2008). Histone methyltransferase Dot1 and Rad9 inhibit single-stranded DNA accumulation at DSBs and uncapped telomeres. The EMBO journal *27*, 1502-1512.

Lecoq, K., Konrad, M., and Daignan-Fornier, B. (2000). Yeast GMP kinase mutants constitutively express AMP biosynthesis genes by phenocopying a hypoxanthine-guanine phosphoribosyltransferase defect. Genetics *156*, 953-961.

Lee, H.S., Park, J.H., Kim, S.J., Kwon, S.J., and Kwon, J. (2010). A cooperative activation loop among SWI/SNF, gamma-H2AX and H3 acetylation for DNA double-strand break repair. The EMBO journal *29*, 1434-1445.

Lee, S.E., Moore, J.K., Holmes, A., Umezu, K., Kolodner, R.D., and Haber, J.E. (1998). Saccharomyces Ku70, mre11/rad50 and RPA proteins regulate adaptation to G2/M arrest after DNA damage. Cell *94*, 399-409.

Leroy, C., Lee, S.E., Vaze, M.B., Ochsenbein, F., Guerois, R., Haber, J.E., and Marsolier-Kergoat, M.C. (2003). PP2C phosphatases Ptc2 and Ptc3 are required for DNA checkpoint inactivation after a double-strand break. Molecular cell *11*, 827-835.

Li, X., Corsa, C.A., Pan, P.W., Wu, L., Ferguson, D., Yu, X., Min, J., and Dou, Y. (2010). MOF and H4 K16 acetylation play important roles in DNA damage repair by modulating recruitment of DNA damage repair protein Mdc1. Molecular and cellular biology *30*, 5335-5347.

Liang, B., Qiu, J., Ratnakumar, K., and Laurent, B.C. (2007). RSC functions as an early double-strand-break sensor in the cell's response to DNA damage. Current biology : CB *17*, 1432-1437.

Lieber, M.R. (2010). The mechanism of double-strand DNA break repair by the nonhomologous DNA end-joining pathway. Annu Rev Biochem *79*, 181-211.

Linger, J.G., and Tyler, J.K. (2007). Chromatin disassembly and reassembly during DNA repair. Mutation research *618*, 52-64.

Lisby, M., Barlow, J.H., Burgess, R.C., and Rothstein, R. (2004). Choreography of the DNA damage response: spatiotemporal relationships among checkpoint and repair proteins. Cell *118*, 699-713.

Llorente, B., Smith, C.E., and Symington, L.S. (2008). Break-induced replication: what is it and what is it for? Cell cycle *7*, 859-864.

Lok, B.H., and Powell, S.N. (2012). Molecular pathways: understanding the role of Rad52 in homologous recombination for therapeutic advancement. Clinical cancer research : an official journal of the American Association for Cancer Research *18*, 6400-6406.

Longtine, M.S., McKenzie, A., 3rd, Demarini, D.J., Shah, N.G., Wach, A., Brachat, A., Philippsen, P., and Pringle, J.R. (1998). Additional modules for versatile and economical PCR-based gene deletion and modification in Saccharomyces cerevisiae. Yeast *14*, 953-961.

Lu, Z., and Cyr, D.M. (1998). Protein folding activity of Hsp70 is modified differentially by the hsp40 co-chaperones Sis1 and Ydj1. The Journal of biological chemistry *273*, 27824-27830.

Luger, K., Mader, A.W., Richmond, R.K., Sargent, D.F., and Richmond, T.J. (1997). Crystal structure of the nucleosome core particle at 2.8 A resolution. Nature *389*, 251-260.

Luk, E., Vu, N.D., Patteson, K., Mizuguchi, G., Wu, W.H., Ranjan, A., Backus, J., Sen, S., Lewis, M., Bai, Y*., et al.* (2007). Chz1, a nuclear chaperone for histone H2AZ. Molecular cell *25*, 357-368.

Maas, N.L., Miller, K.M., DeFazio, L.G., and Toczyski, D.P. (2006). Cell cycle and checkpoint regulation of histone H3 K56 acetylation by Hst3 and Hst4. Molecular cell *23*, 109-119.

Maeshima, K., Imai, R., Tamura, S., and Nozaki, T. (2014). Chromatin as dynamic 10-nm fibers. Chromosoma *123*, 225-237.

Mailand, N., Bekker-Jensen, S., Faustrup, H., Melander, F., Bartek, J., Lukas, C., and Lukas, J. (2007). RNF8 ubiquitylates histones at DNA double-strand breaks and promotes assembly of repair proteins. Cell *131*, 887-900.

Majka, J., Niedziela-Majka, A., and Burgers, P.M. (2006). The checkpoint clamp activates Mec1 kinase during initiation of the DNA damage checkpoint. Molecular cell *24*, 891-901.

Malkova, A., Ivanov, E.L., and Haber, J.E. (1996). Double-strand break repair in the absence of RAD51 in yeast: a possible role for break-induced DNA replication. Proceedings of the National Academy of Sciences of the United States of America *93*, 7131-7136.

Masumoto, H., Hawke, D., Kobayashi, R., and Verreault, A. (2005). A role for cell-cycle-regulated histone H3 lysine 56 acetylation in the DNA damage response. Nature *436*, 294-298.

Matos, J., Blanco, M.G., Maslen, S., Skehel, J.M., and West, S.C. (2011). Regulatory control of the resolution of DNA recombination intermediates during meiosis and mitosis. Cell *147*, 158-172.

Mattiroli, F., Vissers, J.H., van Dijk, W.J., Ikpa, P., Citterio, E., Vermeulen, W., Marteijn, J.A., and Sixma, T.K. (2012). RNF168 ubiquitinates K13-15 on H2A/H2AX to drive DNA damage signaling. Cell *150*, 1182-1195.

McEachern, M.J., and Haber, J.E. (2006). Break-induced replication and recombinational telomere elongation in yeast. Annu Rev Biochem *75*, 111-135.

Mehta, A., and Haber, J.E. (2014). Sources of DNA double-strand breaks and models of recombinational DNA repair. Cold Spring Harbor perspectives in biology *6*, a016428.

Mello, J.A., Sillje, H.H., Roche, D.M., Kirschner, D.B., Nigg, E.A., and Almouzni, G. (2002). Human Asf1 and CAF-1 interact and synergize in a repair-coupled nucleosome assembly pathway. EMBO reports *3*, 329-334.

Mellor, J., Jiang, W., Funk, M., Rathjen, J., Barnes, C.A., Hinz, T., Hegemann, J.H., and Philippsen, P. (1990). CPF1, a yeast protein which functions in centromeres and promoters. The EMBO journal *9*, 4017-4026.

Melo, J.A., Cohen, J., and Toczyski, D.P. (2001). Two checkpoint complexes are independently recruited to sites of DNA damage in vivo. Genes & development *15*, 2809-2821.

Merrikh, H., Zhang, Y., Grossman, A.D., and Wang, J.D. (2012). Replication-transcription conflicts in bacteria. Nature reviews Microbiology *10*, 449-458.

Miller, K.M., Tjeertes, J.V., Coates, J., Legube, G., Polo, S.E., Britton, S., and Jackson, S.P. (2010). Human HDAC1 and HDAC2 function in the DNA-damage response to promote DNA nonhomologous end-joining. Nature structural & molecular biology *17*, 1144-1151.

Mimitou, E.P., and Symington, L.S. (2008). Sae2, Exo1 and Sgs1 collaborate in DNA double-strand break processing. Nature *455*, 770-774.

Mizuguchi, G., Shen, X., Landry, J., Wu, W.H., Sen, S., and Wu, C. (2004). ATP-driven exchange of histone H2AZ variant catalyzed by SWR1 chromatin remodeling complex. Science *303*, 343-348.

Moreau, S., Morgan, E.A., and Symington, L.S. (2001). Overlapping functions of the Saccharomyces cerevisiae Mre11, Exo1 and Rad27 nucleases in DNA metabolism. Genetics *159*, 1423-1433.

Morrison, A.J., Highland, J., Krogan, N.J., Arbel-Eden, A., Greenblatt, J.F., Haber, J.E., and Shen, X. (2004). INO80 and gamma-H2AX interaction links ATP-dependent chromatin remodeling to DNA damage repair. Cell *119*, 767-775.

Morrison, A.J., Kim, J.A., Person, M.D., Highland, J., Xiao, J., Wehr, T.S., Hensley, S., Bao, Y., Shen, J., Collins, S.R.*, et al.* (2007). Mec1/Tel1 phosphorylation of the INO80 chromatin remodeling complex influences DNA damage checkpoint responses. Cell *130*, 499-511.

Moyal, L., Lerenthal, Y., Gana-Weisz, M., Mass, G., So, S., Wang, S.Y., Eppink, B., Chung, Y.M., Shalev, G., Shema, E.*, et al.* (2011). Requirement of ATM-dependent monoubiquitylation of histone H2B for timely repair of DNA double-strand breaks. Molecular cell *41*, 529-542.

Murr, R., Loizou, J.I., Yang, Y.G., Cuenin, C., Li, H., Wang, Z.Q., and Herceg, Z. (2006). Histone acetylation by Trrap-Tip60 modulates loading of repair proteins and repair of DNA double-strand breaks. Nature cell biology *8*, 91-99.

Nagai, S., Dubrana, K., Tsai-Pflugfelder, M., Davidson, M.B., Roberts, T.M., Brown, G.W., Varela, E., Hediger, F., Gasser, S.M., and Krogan, N.J. (2008). Functional targeting of DNA damage to a nuclear pore-associated SUMO-dependent ubiquitin ligase. Science *322,* 597-602.

Nakada, D., Matsumoto, K., and Sugimoto, K. (2003). ATM-related Tel1 associates with double-strand breaks through an Xrs2-dependent mechanism. Genes & development *17*, 1957-1962.

Navadgi-Patil, V.M., and Burgers, P.M. (2009a). A tale of two tails: activation of DNA damage checkpoint kinase Mec1/ATR by the 9-1-1 clamp and by Dpb11/TopBP1. DNA repair *8*, 996-1003.

Navadgi-Patil, V.M., and Burgers, P.M. (2009b). The unstructured C-terminal tail of the 9-1-1 clamp subunit Ddc1 activates Mec1/ATR via two distinct mechanisms. Molecular cell *36*, 743-753.

Nicolette, M.L., Lee, K., Guo, Z., Rani, M., Chow, J.M., Lee, S.E., and Paull, T.T. (2010). Mre11-Rad50-Xrs2 and Sae2 promote 5' strand resection of DNA double-strand breaks. Nature structural & molecular biology *17*, 1478-1485.

Oberle, C., and Blattner, C. (2010). Regulation of the DNA Damage Response to DSBs by Post-Translational Modifications. Current genomics *11*, 184-198.

Ogiwara, H., Ui, A., Otsuka, A., Satoh, H., Yokomi, I., Nakajima, S., Yasui, A., Yokota, J., and Kohno, T. (2011). Histone acetylation by CBP and p300 at double-strand break sites facilitates SWI/SNF chromatin remodeling and the recruitment of non-homologous end joining factors. Oncogene *30*, 2135-2146.

Olsen, J.V., Vermeulen, M., Santamaria, A., Kumar, C., Miller, M.L., Jensen, L.J., Gnad, F., Cox, J., Jensen, T.S., Nigg, E.A*., et al.* (2010). Quantitative phosphoproteomics reveals widespread full phosphorylation site occupancy during mitosis. Science signaling *3*, ra3.

Oum, J.H., Seong, C., Kwon, Y., Ji, J.H., Sid, A., Ramakrishnan, S., Ira, G., Malkova, A., Sung, P., Lee, S.E., *et al.* (2011). RSC facilitates Rad59-dependent homologous recombination between sister chromatids by promoting cohesin loading at DNA double-strand breaks. Molecular and cellular biology *31*, 3924-3937.

Paciotti, V., Clerici, M., Lucchini, G., and Longhese, M.P. (2000). The checkpoint protein Ddc2, functionally related to S. pombe Rad26, interacts with Mec1 and is regulated by Mec1-dependent phosphorylation in budding yeast. Genes & development *14*, 2046-2059.

Pandita, T.K., Pandita, S., and Bhaumik, S.R. (2009). Molecular parameters of hyperthermia for radiosensitization. Crit Rev Eukaryot Gene Expr *19*, 235-251.

Pankotai, T., and Soutoglou, E. (2013). Double strand breaks: hurdles for RNA polymerase II transcription? Transcription *4*, 34-38.

Park, Y.J., and Luger, K. (2006). Structure and function of nucleosome assembly proteins. Biochemistry and cell biology = Biochimie et biologie cellulaire *84*, 549-558.

Parks, L.W., Smith, S.J., and Crowley, J.H. (1995). Biochemical and physiological effects of sterol alterations in yeast--a review. Lipids *30*, 227-230.

Pei, H., Zhang, L., Luo, K., Qin, Y., Chesi, M., Fei, F., Bergsagel, P.L., Wang, L., You, Z., and Lou, Z. (2011). MMSET regulates histone H4K20 methylation and 53BP1 accumulation at DNA damage sites. Nature *470*, 124-128.

Pellicioli, A., Lee, S.E., Lucca, C., Foiani, M., and Haber, J.E. (2001). Regulation of Saccharomyces Rad53 checkpoint kinase during adaptation from DNA damage-induced G2/M arrest. Molecular cell *7*, 293-300.

Pellicioli, A., Lucca, C., Liberi, G., Marini, F., Lopes, M., Plevani, P., Romano, A., Di Fiore, P.P., and Foiani, M. (1999). Activation of Rad53 kinase in response to DNA damage and its effect in modulating phosphorylation of the lagging strand DNA polymerase. The EMBO journal *18*, 6561-6572.

Pfister, S.X., Ahrabi, S., Zalmas, L.P., Sarkar, S., Aymard, F., Bachrati, C.Z., Helleday, T., Legube, G., La Thangue, N.B., Porter, A.C.*, et al.* (2014). SETD2-dependent histone H3K36 trimethylation is required for homologous recombination repair and genome stability. Cell reports *7*, 2006-2018.

Pike, B.L., Yongkiettrakul, S., Tsai, M.D., and Heierhorst, J. (2003). Diverse but overlapping functions of the two forkhead-associated (FHA) domains in Rad53 checkpoint kinase activation. The Journal of biological chemistry *278*, 30421-30424.

Polo, S.E., and Jackson, S.P. (2011). Dynamics of DNA damage response proteins at DNA breaks: a focus on protein modifications. Genes & development *25*, 409-433.

Portman, D.S., O'Connor, J.P., and Dreyfuss, G. (1997). YRA1, an essential Saccharomyces cerevisiae gene, encodes a novel nuclear protein with RNA annealing activity. Rna *3*, 527-537.

Povirk, L.F. (1996). DNA damage and mutagenesis by radiomimetic DNA-cleaving agents: bleomycin, neocarzinostatin and other enediynes. Mutation research *355*, 71-89.

Prakash, R., Satory, D., Dray, E., Papusha, A., Scheller, J., Kramer, W., Krejci, L., Klein, H., Haber, J.E., Sung, P*., et al.* (2009). Yeast Mph1 helicase dissociates Rad51-made D-loops: implications for crossover control in mitotic recombination. Genes & development *23*, 67-79.

Preker, P.J., Kim, K.S., and Guthrie, C. (2002). Expression of the essential mRNA export factor Yra1p is autoregulated by a splicing-dependent mechanism. Rna *8*, 969-980.

Price, B.D., and D'Andrea, A.D. (2013). Chromatin remodeling at DNA double-strand breaks. Cell *152*, 1344-1354.

Ray, B.L., White, C.I., and Haber, J.E. (1991). Heteroduplex formation and mismatch repair of the "stuck" mutation during mating-type switching in Saccharomyces cerevisiae. Molecular and cellular biology *11*, 5372-5380.

Robzyk, K., Recht, J., and Osley, M.A. (2000). Rad6-dependent ubiquitination of histone H2B in yeast. Science *287*, 501-504.

Rossetto, D., Truman, A.W., Kron, S.J., and Cote, J. (2010). Epigenetic modifications in double-strand break DNA damage signaling and repair. Clinical cancer research : an official journal of the American Association for Cancer Research *16*, 4543-4552.

Saleh, A., Collart, M., Martens, J.A., Genereaux, J., Allard, S., Cote, J., and Brandl, C.J. (1998). TOM1p, a yeast hect-domain protein which mediates

transcriptional regulation through the ADA/SAGA coactivator complexes. Journal of molecular biology *282*, 933-946.

Sanchez, Y., Bachant, J., Wang, H., Hu, F., Liu, D., Tetzlaff, M., and Elledge, S.J. (1999). Control of the DNA damage checkpoint by chk1 and rad53 protein kinases through distinct mechanisms. Science *286*, 1166-1171.

Sanchez, Y., Desany, B.A., Jones, W.J., Liu, Q., Wang, B., and Elledge, S.J. (1996). Regulation of RAD53 by the ATM-like kinases MEC1 and TEL1 in yeast cell cycle checkpoint pathways. Science *271*, 357-360.

Sandell, L.L., and Zakian, V.A. (1993). Loss of a yeast telomere: arrest, recovery, and chromosome loss. Cell *75*, 729-739.

Sanematsu, F., Takami, Y., Barman, H.K., Fukagawa, T., Ono, T., Shibahara, K., and Nakayama, T. (2006). Asf1 is required for viability and chromatin assembly during DNA replication in vertebrate cells. The Journal of biological chemistry *281*, 13817-13827.

Scheller, N., Resa-Infante, P., de la Luna, S., Galao, R.P., Albrecht, M., Kaestner, L., Lipp, P., Lengauer, T., Meyerhans, A., and Diez, J. (2007). Identification of PatL1, a human homolog to yeast P body component Pat1. Biochimica et biophysica acta *1773*, 1786-1792.

Schipler, A., and Iliakis, G. (2013). DNA double-strand-break complexity levels and their possible contributions to the probability for error-prone processing and repair pathway choice. Nucleic acids research *41*, 7589-7605.

Schuldiner, M., Collins, S.R., Thompson, N.J., Denic, V., Bhamidipati, A., Punna, T., Ihmels, J., Andrews, B., Boone, C., Greenblatt, J.F.*, et al.* (2005).

Exploration of the function and organization of the yeast early secretory pathway through an epistatic miniarray profile. Cell *123*, 507-519.

Schwartz, M.F., Duong, J.K., Sun, Z., Morrow, J.S., Pradhan, D., and Stern, D.F. (2002). Rad9 phosphorylation sites couple Rad53 to the Saccharomyces cerevisiae DNA damage checkpoint. Molecular cell *9*, 1055-1065.

Schwertman, P., Bekker-Jensen, S., and Mailand, N. (2016). Regulation of DNA double-strand break repair by ubiquitin and ubiquitin-like modifiers. Nature reviews Molecular cell biology *17*, 379-394.

Seeber, A., Hauer, M., and Gasser, S.M. (2013). Nucleosome remodelers in double-strand break repair. Current opinion in genetics & development *23*, 174-184.

Sharma, G.G., So, S., Gupta, A., Kumar, R., Cayrou, C., Avvakumov, N., Bhadra, U., Pandita, R.K., Porteus, M.H., Chen, D.J.*, et al.* (2010). MOF and histone H4 acetylation at lysine 16 are critical for DNA damage response and double-strand break repair. Molecular and cellular biology *30*, 3582-3595.

Sharp, J.A., Fouts, E.T., Krawitz, D.C., and Kaufman, P.D. (2001). Yeast histone deposition protein Asf1p requires Hir proteins and PCNA for heterochromatic silencing. Current biology : CB *11*, 463-473.

Shim, E.Y., Chung, W.H., Nicolette, M.L., Zhang, Y., Davis, M., Zhu, Z., Paull, T.T., Ira, G., and Lee, S.E. (2010). Saccharomyces cerevisiae Mre11/Rad50/Xrs2 and Ku proteins regulate association of Exo1 and Dna2 with DNA breaks. The EMBO journal *29*, 3370-3380.

Shroff, R., Arbel-Eden, A., Pilch, D., Ira, G., Bonner, W.M., Petrini, J.H., Haber, J.E., and Lichten, M. (2004). Distribution and dynamics of chromatin modification induced by a defined DNA double-strand break. Current biology : CB *14*, 1703-1711.

Singh, R.K., Kabbaj, M.H., Paik, J., and Gunjan, A. (2009). Histone levels are regulated by phosphorylation and ubiquitylation-dependent proteolysis. Nature cell biology *11*, 925-933.

Smith, D.J., Proudfoot, A., Friedli, L., Klig, L.S., Paravicini, G., and Payton, M.A. (1992). PMI40, an intron-containing gene required for early steps in yeast mannosylation. Molecular and cellular biology *12*, 2924-2930.

Smith, J.S., Brachmann, C.B., Celic, I., Kenna, M.A., Muhammad, S., Starai, V.J., Avalos, J.L., Escalante-Semerena, J.C., Grubmeyer, C., Wolberger, C.*, et al.* (2000). A phylogenetically conserved NAD+-dependent protein deacetylase activity in the Sir2 protein family. Proceedings of the National Academy of Sciences of the United States of America *97*, 6658-6663.

Soriano-Carot, M., Quilis, I., Bano, M.C., and Igual, J.C. (2014). Protein kinase C controls activation of the DNA integrity checkpoint. Nucleic acids research *42*, 7084-7095.

Soulas-Sprauel, P., Rivera-Munoz, P., Malivert, L., Le Guyader, G., Abramowski, V., Revy, P., and de Villartay, J.P. (2007). V(D)J and immunoglobulin class switch recombinations: a paradigm to study the regulation of DNA end-joining. Oncogene *26*, 7780-7791.

157

Stanlie, A., Aida, M., Muramatsu, M., Honjo, T., and Begum, N.A. (2010). Histone3 lysine4 trimethylation regulated by the facilitates chromatin transcription complex is critical for DNA cleavage in class switch recombination. Proceedings of the National Academy of Sciences of the United States of America *107*, 22190-22195.

Stefansson, B., and Brautigan, D.L. (2006). Protein phosphatase 6 subunit with conserved Sit4-associated protein domain targets IkappaBepsilon. The Journal of biological chemistry *281*, 22624-22634.

Stewart, G.S., Wang, B., Bignell, C.R., Taylor, A.M., and Elledge, S.J. (2003). MDC1 is a mediator of the mammalian DNA damage checkpoint. Nature *421*, 961-966.

Strasser, K., and Hurt, E. (2000). Yra1p, a conserved nuclear RNA-binding protein, interacts directly with Mex67p and is required for mRNA export. The EMBO journal *19*, 410-420.

Su, T.T. (2006). Cellular responses to DNA damage: one signal, multiple choices. Annual review of genetics *40*, 187-208.

Sugawara, N., Ira, G., and Haber, J.E. (2000). DNA length dependence of the single-strand annealing pathway and the role of Saccharomyces cerevisiae RAD59 in double-strand break repair. Molecular and cellular biology *20*, 5300-5309.

Summers, D.W., Wolfe, K.J., Ren, H.Y., and Cyr, D.M. (2013). The Type II Hsp40 Sis1 cooperates with Hsp70 and the E3 ligase Ubr1 to promote degradation of terminally misfolded cytosolic protein. PloS one *8*, e52099.

Sun, Y., Jiang, X., Xu, Y., Ayrapetov, M.K., Moreau, L.A., Whetstine, J.R., and Price, B.D. (2009). Histone H3 methylation links DNA damage detection to activation of the tumour suppressor Tip60. Nature cell biology *11*, 1376-1382.

Sun, Z., Hsiao, J., Fay, D.S., and Stern, D.F. (1998). Rad53 FHA domain associated with phosphorylated Rad9 in the DNA damage checkpoint. Science *281*, 272-274.

Sutton, A., Immanuel, D., and Arndt, K.T. (1991). The SIT4 protein phosphatase functions in late G1 for progression into S phase. Molecular and cellular biology *11*, 2133-2148.

Takahashi, H., McCaffery, J.M., Irizarry, R.A., and Boeke, J.D. (2006). Nucleocytosolic acetyl-coenzyme a synthetase is required for histone acetylation and global transcription. Molecular cell *23*, 207-217.

Tamburini, B.A., and Tyler, J.K. (2005). Localized histone acetylation and deacetylation triggered by the homologous recombination pathway of double-strand DNA repair. Molecular and cellular biology *25*, 4903-4913.

Thomas, B.J., and Rothstein, R. (1989). The genetic control of direct-repeat recombination in Saccharomyces: the effect of rad52 and rad1 on mitotic recombination at GAL10, a transcriptionally regulated gene. Genetics *123*, 725-738.

Thompson, L.H. (2012). Recognition, signaling, and repair of DNA double-strand breaks produced by ionizing radiation in mammalian cells: the molecular choreography. Mutation research *751*, 158-246.

Toh, G.W., and Lowndes, N.F. (2003). Role of the Saccharomyces cerevisiae Rad9 protein in sensing and responding to DNA damage. Biochemical Society transactions *31*, 242-246.

Tropberger, P., Pott, S., Keller, C., Kamieniarz-Gdula, K., Caron, M., Richter, F., Li, G., Mittler, G., Liu, E.T., Buhler, M.*, et al.* (2013). Regulation of transcription through acetylation of H3K122 on the lateral surface of the histone octamer. Cell *152*, 859-872.

Tsabar, M., Waterman, D.P., Aguilar, F., Katsnelson, L., Eapen, V.V., Memisoglu, G., and Haber, J.E. (2016). Asf1 facilitates dephosphorylation of Rad53 after DNA double-strand break repair. Genes & development *30*, 1211-1224.

Tsukuda, T., Fleming, A.B., Nickoloff, J.A., and Osley, M.A. (2005). Chromatin remodelling at a DNA double-strand break site in Saccharomyces cerevisiae. Nature *438*, 379-383.

Usui, T., Foster, S.S., and Petrini, J.H. (2009). Maintenance of the DNA-damage checkpoint requires DNA-damage-induced mediator protein oligomerization. Molecular cell *33*, 147-159.

Valko, M., Leibfritz, D., Moncol, J., Cronin, M.T., Mazur, M., and Telser, J. (2007). Free radicals and antioxidants in normal physiological functions and human disease. The international journal of biochemistry & cell biology *39*, 44-84.

van Attikum, H., Fritsch, O., and Gasser, S.M. (2007). Distinct roles for SWR1 and INO80 chromatin remodeling complexes at chromosomal double-strand breaks. The EMBO journal *26*, 4113-4125.

van Attikum, H., Fritsch, O., Hohn, B., and Gasser, S.M. (2004). Recruitment of the INO80 complex by H2A phosphorylation links ATP-dependent chromatin remodeling with DNA double-strand break repair. Cell *119*, 777-788.

Vaze, M.B., Pellicioli, A., Lee, S.E., Ira, G., Liberi, G., Arbel-Eden, A., Foiani, M., and Haber, J.E. (2002). Recovery from checkpoint-mediated arrest after repair of a double-strand break requires Srs2 helicase. Molecular cell *10*, 373-385.

Venkitaraman, A.R. (2001). Functions of BRCA1 and BRCA2 in the biological response to DNA damage. Journal of cell science *114*, 3591-3598.

Waldrip, Z.J., Byrum, S.D., Storey, A.J., Gao, J., Byrd, A.K., Mackintosh, S.G., Wahls, W.P., Taverna, S.D., Raney, K.D., and Tackett, A.J. (2014). A CRISPR-based approach for proteomic analysis of a single genomic locus. Epigenetics *9*, 1207-1211.

Walker, J.R., Corpina, R.A., and Goldberg, J. (2001). Structure of the Ku heterodimer bound to DNA and its implications for double-strand break repair. Nature *412*, 607-614.

Wang, B., Matsuoka, S., Carpenter, P.B., and Elledge, S.J. (2002). 53BP1, a mediator of the DNA damage checkpoint. Science *298*, 1435-1438.

Wang, C.I., Alekseyenko, A.A., LeRoy, G., Elia, A.E., Gorchakov, A.A., Britton, L.M., Elledge, S.J., Kharchenko, P.V., Garcia, B.A., and Kuroda, M.I. (2013).

Chromatin proteins captured by ChIP-mass spectrometry are linked to dosage compensation in Drosophila. Nature structural & molecular biology *20*, 202-209.

Wang, H., Li, Y., Truong, L.N., Shi, L.Z., Hwang, P.Y.-H., He, J., Do, J., Cho, M.J., Li, H., Negrete, A*., et al.* (2014). CtIP maintains stability at common fragile sites and inverted repeats by end resection-independent endonuclease activity. Molecular cell *54*, 1012-1021.

Wang, X., Watt, P.M., Borts, R.H., Louis, E.J., and Hickson, I.D. (1999). The topoisomerase II-associated protein, Pat1p, is required for maintenance of rDNA locus stability in Saccharomyces cerevisiae. Molecular & general genetics : MGG *261*, 831-840.

Wickramasinghe, V.O., Savill, J.M., Chavali, S., Jonsdottir, A.B., Rajendra, E., Gruner, T., Laskey, R.A., Babu, M.M., and Venkitaraman, A.R. (2013). Human inositol polyphosphate multikinase regulates transcript-selective nuclear mRNA export to preserve genome integrity. Molecular cell *51*, 737-750.

Wilson, M.D., Harreman, M., Taschner, M., Reid, J., Walker, J., Erdjument-Bromage, H., Tempst, P., and Svejstrup, J.Q. (2013). Proteasome-mediated processing of Def1, a critical step in the cellular response to transcription stress. Cell *154*, 983-995.

Winkler, D.D., Muthurajan, U.M., Hieb, A.R., and Luger, K. (2011). Histone chaperone FACT coordinates nucleosome interaction through multiple synergistic binding events. The Journal of biological chemistry *286*, 41883-41892.

Workman, J.L., and Langmore, J.P. (1985). Nucleoprotein hybridization: a method for isolating specific genes as high molecular weight chromatin. Biochemistry *24*, 7486-7497.

Woudstra, E.C., Gilbert, C., Fellows, J., Jansen, L., Brouwer, J., Erdjument-Bromage, H., Tempst, P., and Svejstrup, J.Q. (2002). A Rad26-Def1 complex coordinates repair and RNA pol II proteolysis in response to DNA damage. Nature *415*, 929-933.

Wu, D., Topper, L.M., and Wilson, T.E. (2008). Recruitment and dissociation of nonhomologous end joining proteins at a DNA double-strand break in Saccharomyces cerevisiae. Genetics *178*, 1237-1249.

Wu, L., and Hickson, I.D. (2003). The Bloom's syndrome helicase suppresses crossing over during homologous recombination. Nature *426*, 870-874.

Xiao, A., Li, H., Shechter, D., Ahn, S.H., Fabrizio, L.A., Erdjument-Bromage, H., Ishibe-Murakami, S., Wang, B., Tempst, P., Hofmann, K.*, et al.* (2009). WSTF regulates the H2A.X DNA damage response via a novel tyrosine kinase activity. Nature *457*, 57-62.

Xie, A., Odate, S., Chandramouly, G., and Scully, R. (2010). H2AX post-translational modifications in the ionizing radiation response and homologous recombination. Cell cycle *9*, 3602-3610.

Xu, E.Y., Bi, X., Holland, M.J., Gottschling, D.E., and Broach, J.R. (2005). Mutations in the nucleosome core enhance transcriptional silencing. Molecular and cellular biology *25*, 1846-1859.

Xu, Y., Ayrapetov, M.K., Xu, C., Gursoy-Yuzugullu, O., Hu, Y., and Price, B.D. (2012). Histone H2A.Z controls a critical chromatin remodeling step required for DNA double-strand break repair. Molecular cell *48*, 723-733.

Yan, Q., Dutt, S., Xu, R., Graves, K., Juszczynski, P., Manis, J.P., and Shipp, M.A. (2009). BBAP monoubiquitylates histone H4 at lysine 91 and selectively modulates the DNA damage response. Molecular cell *36*, 110-120.

Yenush, L., Mulet, J.M., Arino, J., and Serrano, R. (2002). The Ppz protein phosphatases are key regulators of K+ and pH homeostasis: implications for salt tolerance, cell wall integrity and cell cycle progression. The EMBO journal *21*, 920-929.

Yeung, M., and Durocher, D. (2011). Srs2 enables checkpoint recovery by promoting disassembly of DNA damage foci from chromatin. DNA repair *10*, 1213-1222.

Yuan, J., Pu, M., Zhang, Z., and Lou, Z. (2009). Histone H3-K56 acetylation is important for genomic stability in mammals. Cell cycle *8*, 1747-1753.

Zhang, L., Freitas, M.A., Wickham, J., Parthun, M.R., Klisovic, M.I., Marcucci, G., and Byrd, J.C. (2004). Differential expression of histone post-translational modifications in acute myeloid and chronic lymphocytic leukemia determined by high-pressure liquid chromatography and mass spectrometry. Journal of the American Society for Mass Spectrometry *15*, 77-86.

Zhang, X.Y., and Horz, W. (1982). Analysis of highly purified satellite DNA containing chromatin from the mouse. Nucleic acids research *10*, 1481-1494.

Zhou, B.B., and Elledge, S.J. (2000). The DNA damage response: putting checkpoints in perspective. Nature *408*, 433-439.

Zhu, B., Zheng, Y., Pham, A.D., Mandal, S.S., Erdjument-Bromage, H., Tempst, P., and Reinberg, D. (2005). Monoubiquitination of human histone H2B: the factors involved and their roles in HOX gene regulation. Molecular cell *20*, 601-611.

Zhu, Y., Dong, A., Meyer, D., Pichon, O., Renou, J.P., Cao, K., and Shen, W.H. (2006). Arabidopsis NRP1 and NRP2 encode histone chaperones and are required for maintaining postembryonic root growth. The Plant cell *18*, 2879-2892.

Zhu, Z., Chung, W.H., Shim, E.Y., Lee, S.E., and Ira, G. (2008). Sgs1 helicase and two nucleases Dna2 and Exo1 resect DNA double-strand break ends. Cell *134*, 981-994.

Zou, L., and Elledge, S.J. (2003). Sensing DNA damage through ATRIP recognition of RPA-ssDNA complexes. Science *300*, 1542-1548.

Vita

Pingping Wang was born in Shangzhi, Heilongjiang Province, China on June 14th, 1986, the daughter of Yongsheng Wang and Fengzhu Yu. After graduating from Daqing Tieren High School in Daqing, Heilongjiang Province in 2005, she attended Peking University Health Science Center in Beijing, China and earned her Bachelor's degree with a major in Basic Medical Science in 2010. In the end of August of 2010, she started to pursue her doctoral education majored in Biomedical Sciences in The University of Texas MD Anderson Cancer Center UT Health Graduate School of Biomedical Sciences. She joined the Genes and Development Graduate Program in May 2011. Supervised by Dr. Jessica Tyler, she did her dissertation research in the field of DNA double- strand break repair in *Saccharomyces cerevisiae*.